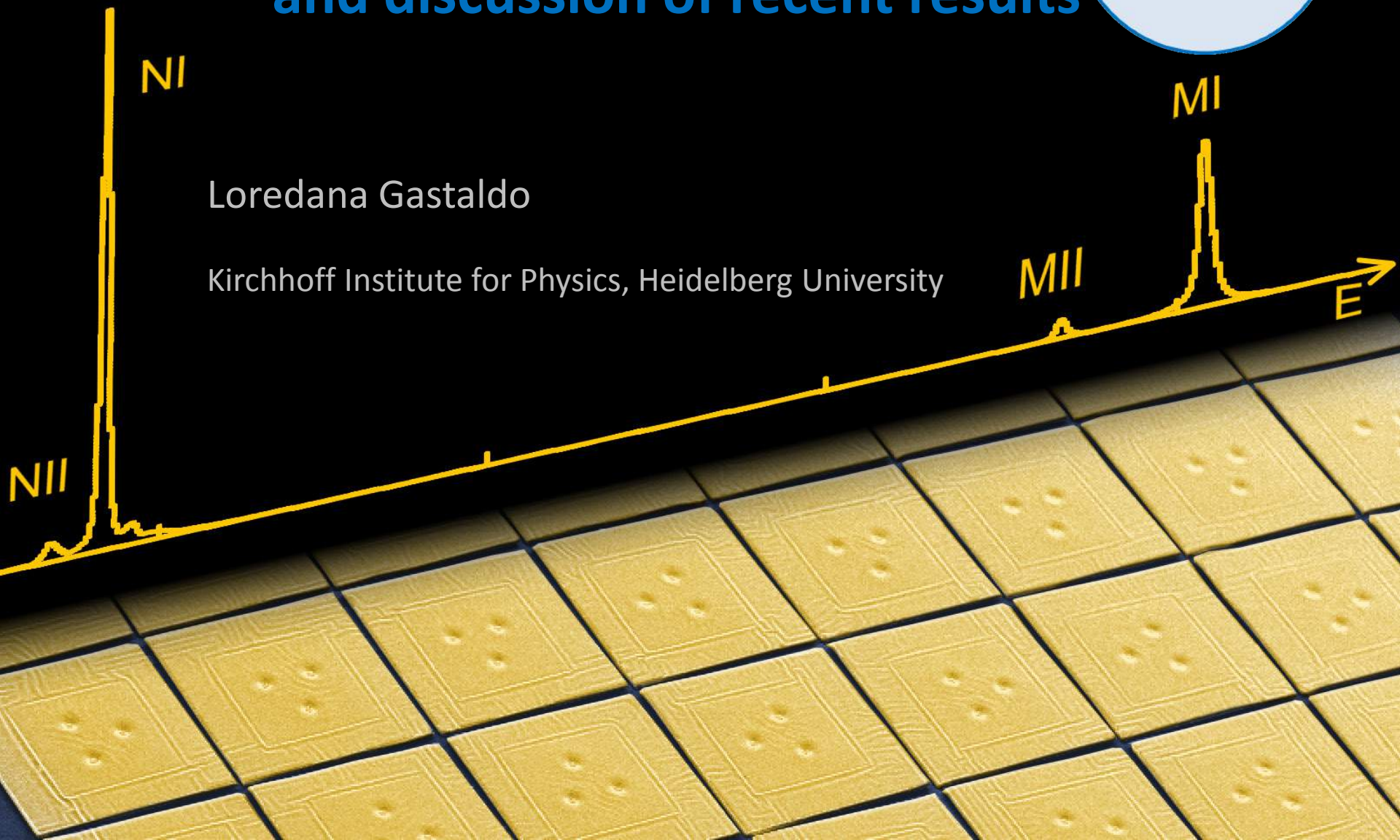


Electron Capture in ^{163}Ho experiment – ECHo and discussion of recent results

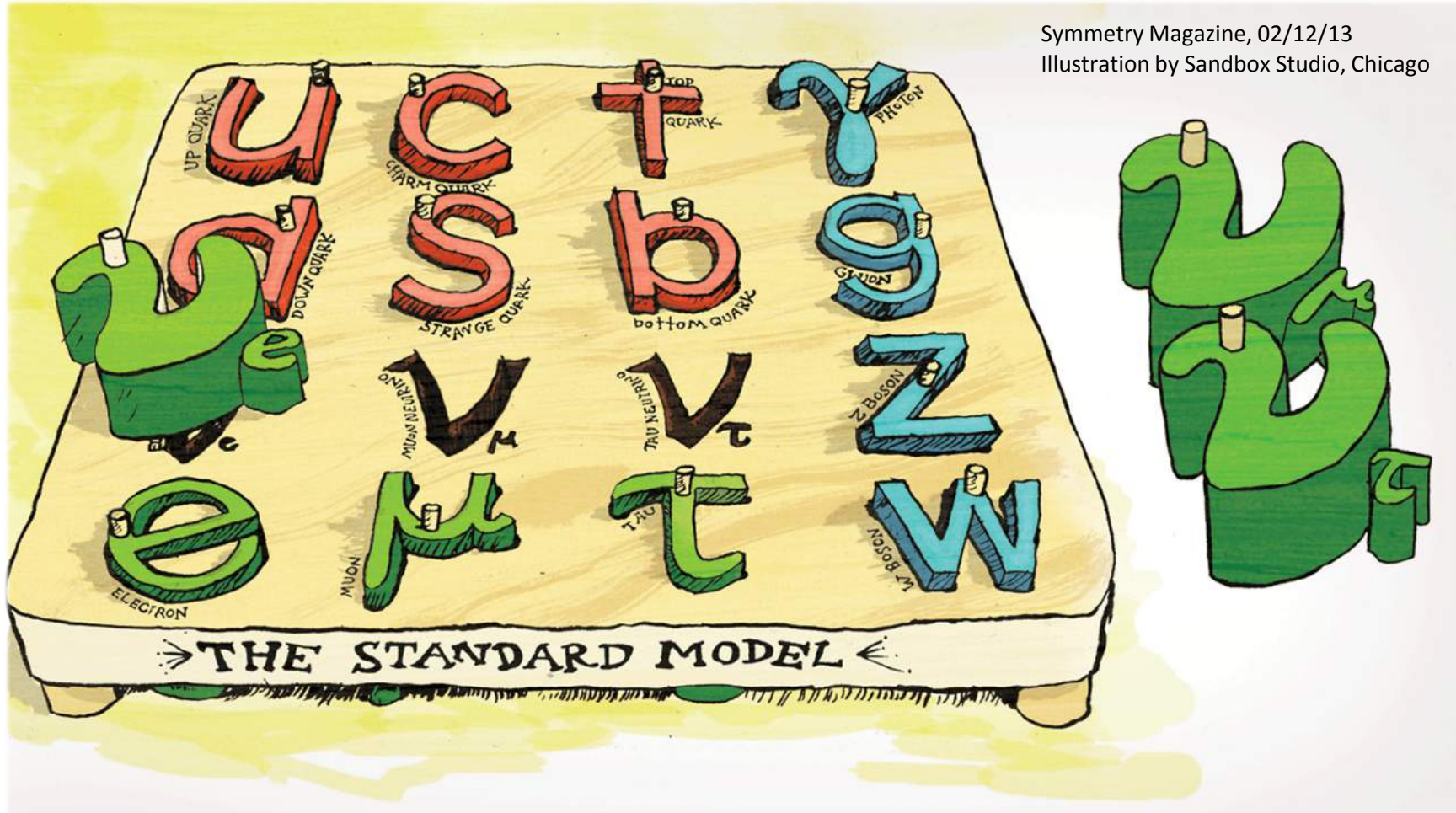


Outline

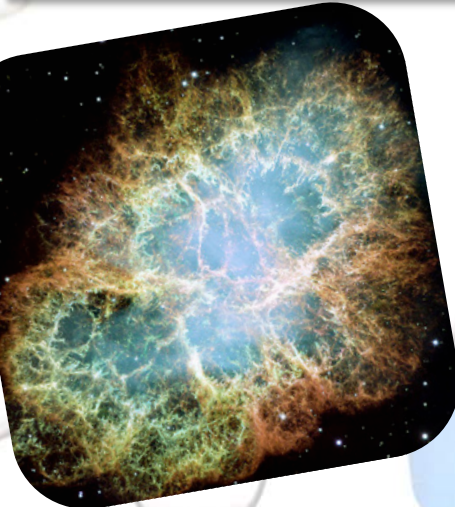
- Introduction
- Electron capture in ^{163}Ho and neutrino mass
- Requirements to achieve sub-eV sensitivity on the electron neutrino mass
- ^{163}Ho -based experiments
- Conclusions and outlook



Massive Neutrinos

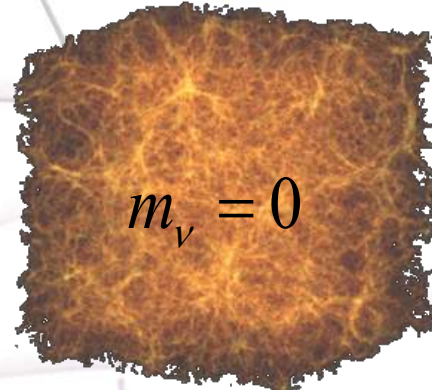


Knowing neutrino mass scale....

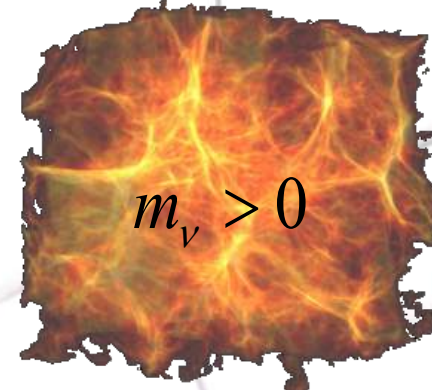


Astrophysics

Supernova neutrinos



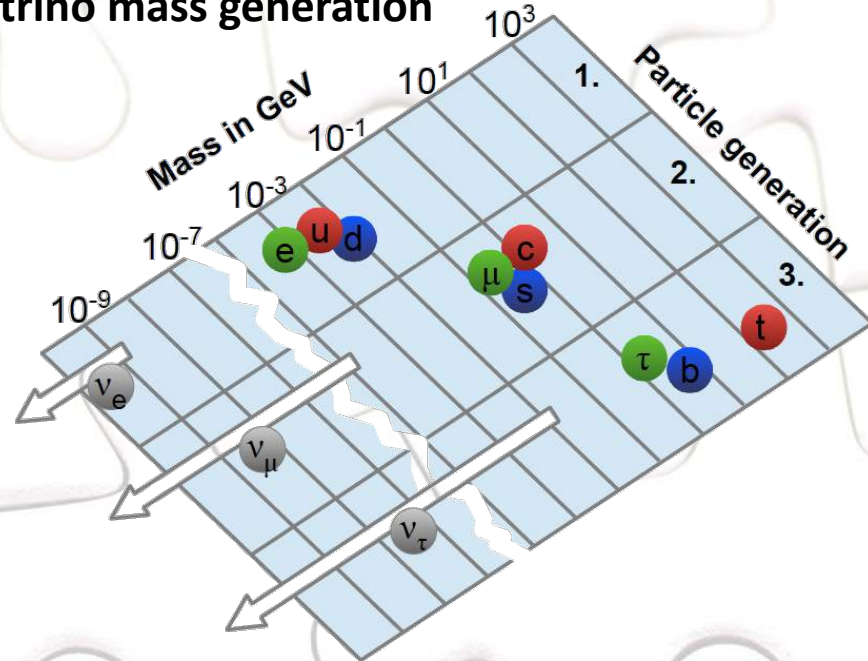
$$m_\nu = 0$$



$$m_\nu > 0$$

Particle Physics

Neutrino mass generation



Cosmology

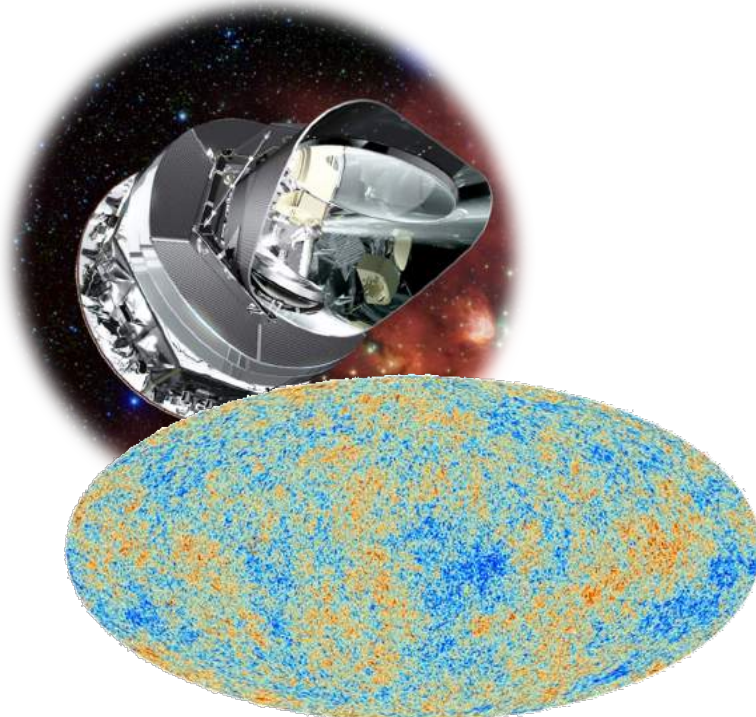
Matter distribution
in the Universe

Neutrino mass determination

Cosmology

$$M_\nu = \sum m_i$$

- Model dependent
- Need of satellites
- Present limit 0.12 – 1 eV
- **Next future 15-50 meV**

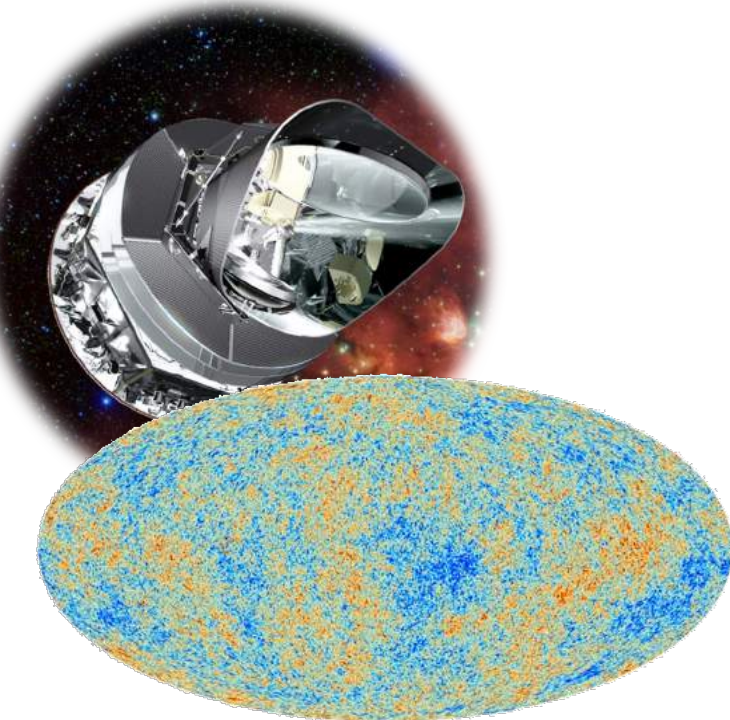


Neutrino mass determination

Cosmology

$$M_\nu = \sum m_i$$

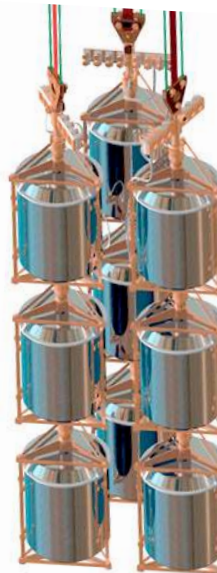
- Model dependent
- Need of satellites
- Present limit 0.12 – 1 eV
- **Next future 15-50 meV**



Neutrinoless Double beta decay

$$m_{\beta\beta} = \left| \sum_i U_{ei}^2 m_i \right|$$

- Model dependent
- Laboratory experiments
- Present limit 0.1 – 0.4 eV
- **Next future 15-50 meV**

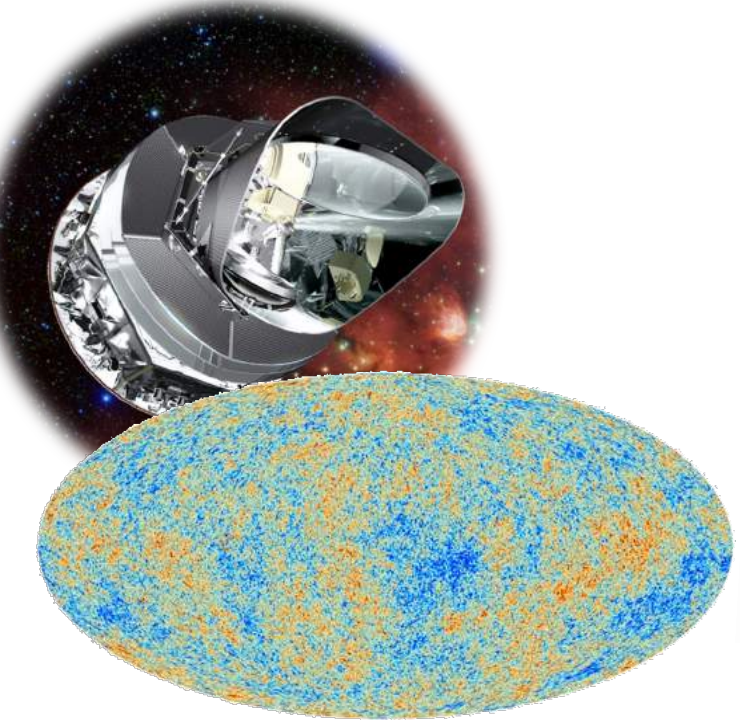


Neutrino mass determination

Cosmology

$$M_\nu = \sum m_i$$

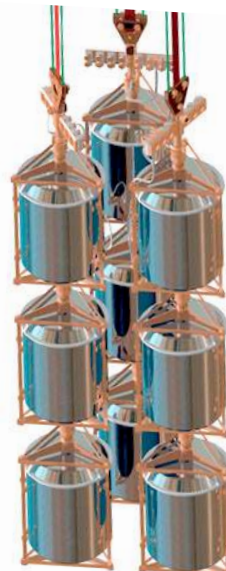
- Model dependent
- Need of satellites
- Present limit 0.12 – 1 eV
- **Next future 15-50 meV**



Neutrinoless Double beta decay

$$m_{\beta\beta} = \left| \sum_i U_{ei}^2 m_i \right|$$

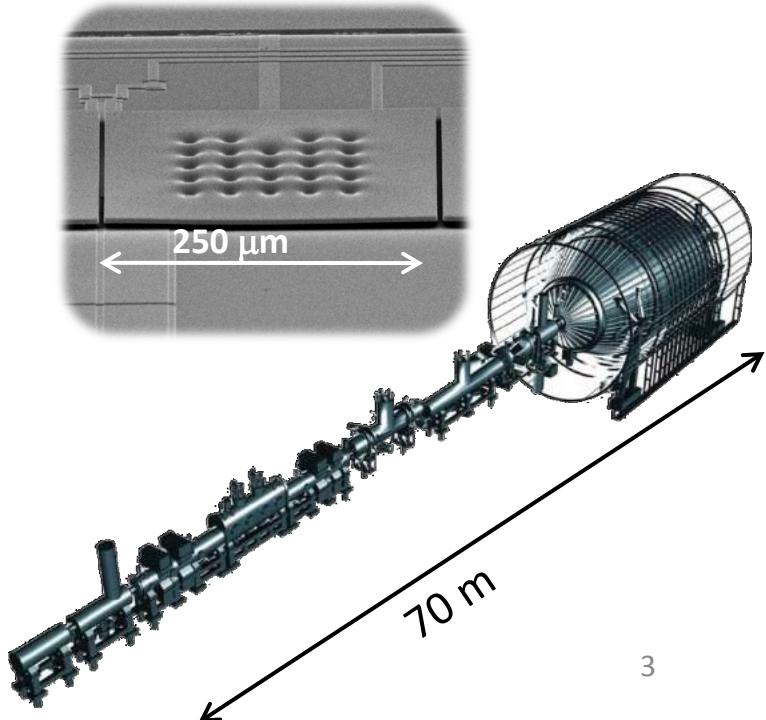
- Model dependent
- Laboratory experiments
- Present limit 0.1 – 0.4 eV
- **Next future 15-50 meV**



Kinematics of β -decay and electron capture

$$m^2(\nu_e) = \sum_i |U_{ei}|^2 m_i^2$$

- Model independent
- Laboratory experiments
- Present limit 2 eV
- **Next future 200 meV**

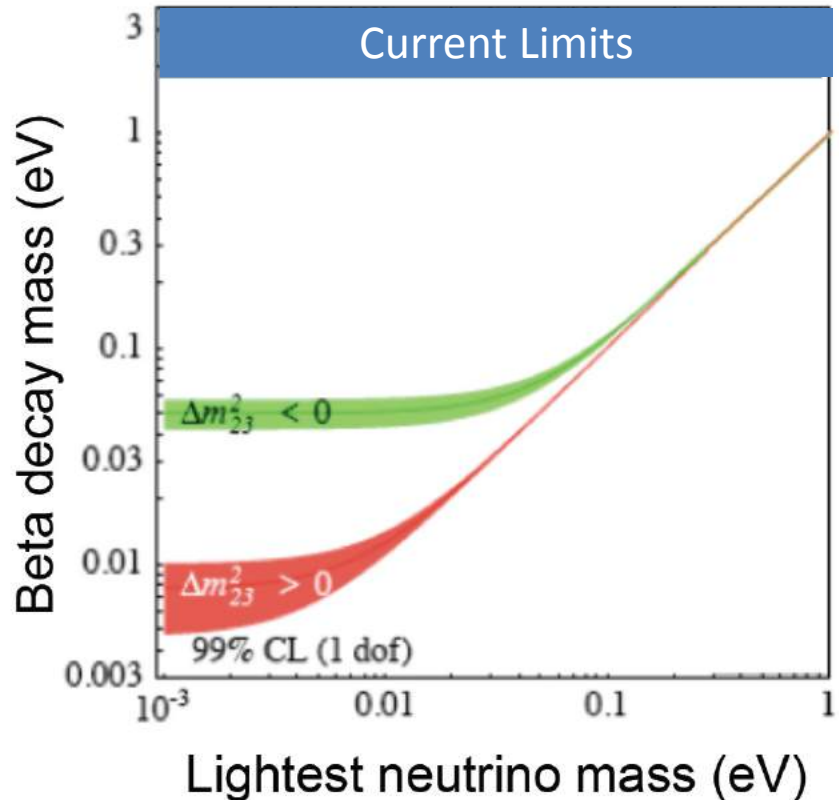


Direct neutrino mass determination

Kinematics of beta decay

$$m^2(\nu_e) = \sum_i |U_{ei}|^2 m_i^2$$

- Model independent
- Laboratory experiments



(1) Ch. Kraus *et al.*, Eur. Phys. J. C **40** (2005) 447
N. Aseev *et al.*, Phys. Rev D **84** (2011) 112003

Direct neutrino mass determination

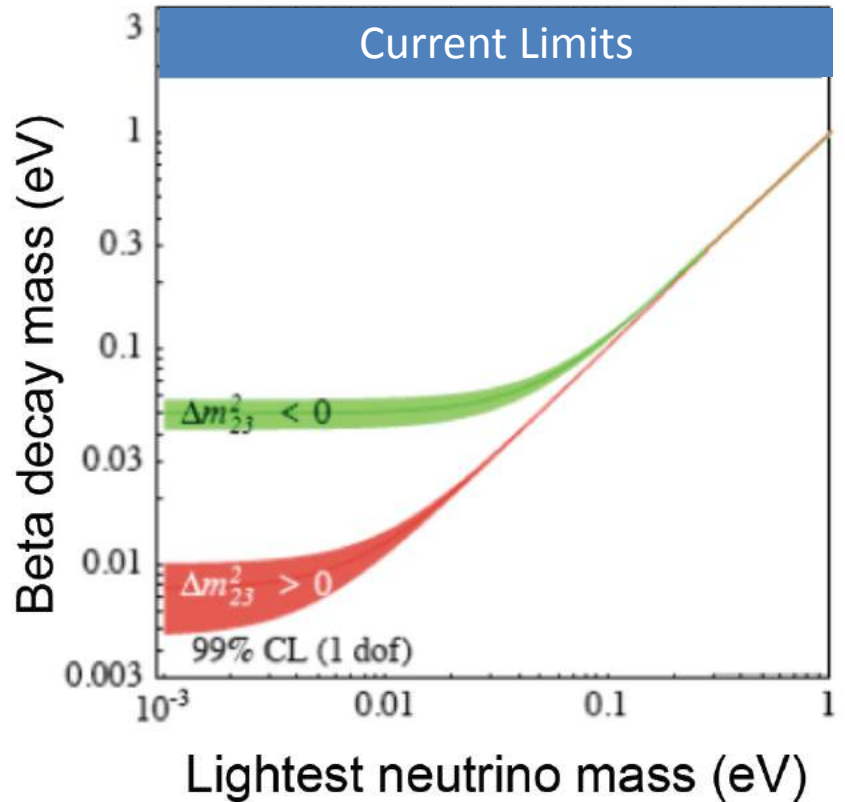
Kinematics of beta decay

$$m^2(\nu_e) = \sum_i |U_{ei}|^2 m_i^2$$

- Model independent
- Laboratory experiments

$$m(\bar{\nu}_e) < 2 \text{ eV} \quad {}^3\text{H} \quad (1)$$

$$m(\nu_e) < 225 \text{ eV} \quad {}^{163}\text{Ho} \quad (2)$$



(1) Ch. Kraus *et al.*, Eur. Phys. J. C **40** (2005) 447
N. Aseev *et al.*, Phys. Rev D **84** (2011) 112003

(2) P. T. Springer, C. L. Bennett, and P. A. Baisden Phys. Rev. A 35 (1987) 679⁴

Direct neutrino mass determination

Kinematics of beta decay

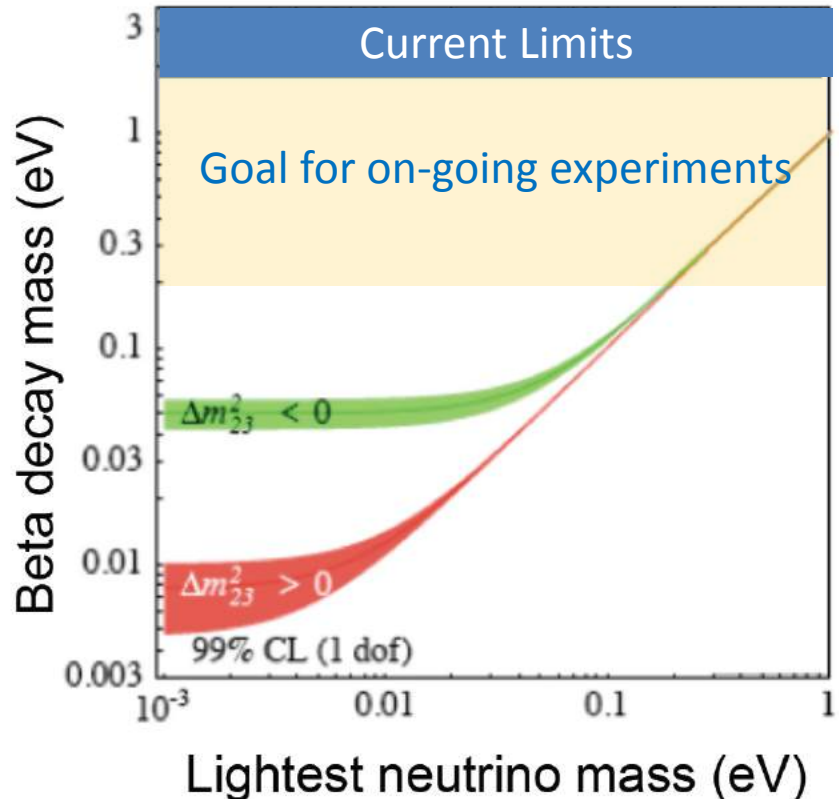
$$m^2(\nu_e) = \sum_i |U_{ei}|^2 m_i^2$$

- Model independent
- Laboratory experiments

$$m(\bar{\nu}_e) < 2 \text{ eV} \quad {}^3\text{H} \quad (1)$$

$$m(\nu_e) < 225 \text{ eV} \quad {}^{163}\text{Ho} \quad (2)$$

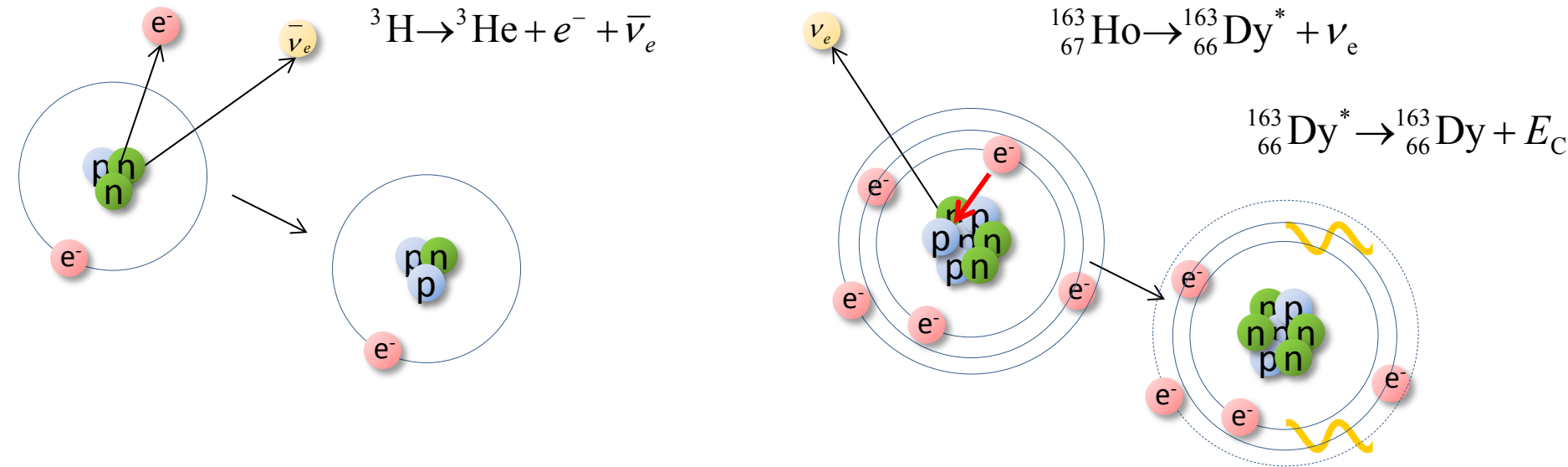
- Next future 200 meV



(1) Ch. Kraus *et al.*, Eur. Phys. J. C **40** (2005) 447
N. Aseev *et al.*, Phys. Rev D **84** (2011) 112003

(2) P. T. Springer, C. L. Bennett, and P. A. Baisden Phys. Rev. A 35 (1987) 679⁴

Beta decay and electron capture



$$\bullet \tau_{1/2} \approx 12.3 \text{ years} \quad (4 \cdot 10^8 \text{ atoms for } 1 \text{ Bq})$$

$$\bullet Q_\beta = 18\,592.01(7) \text{ eV}$$

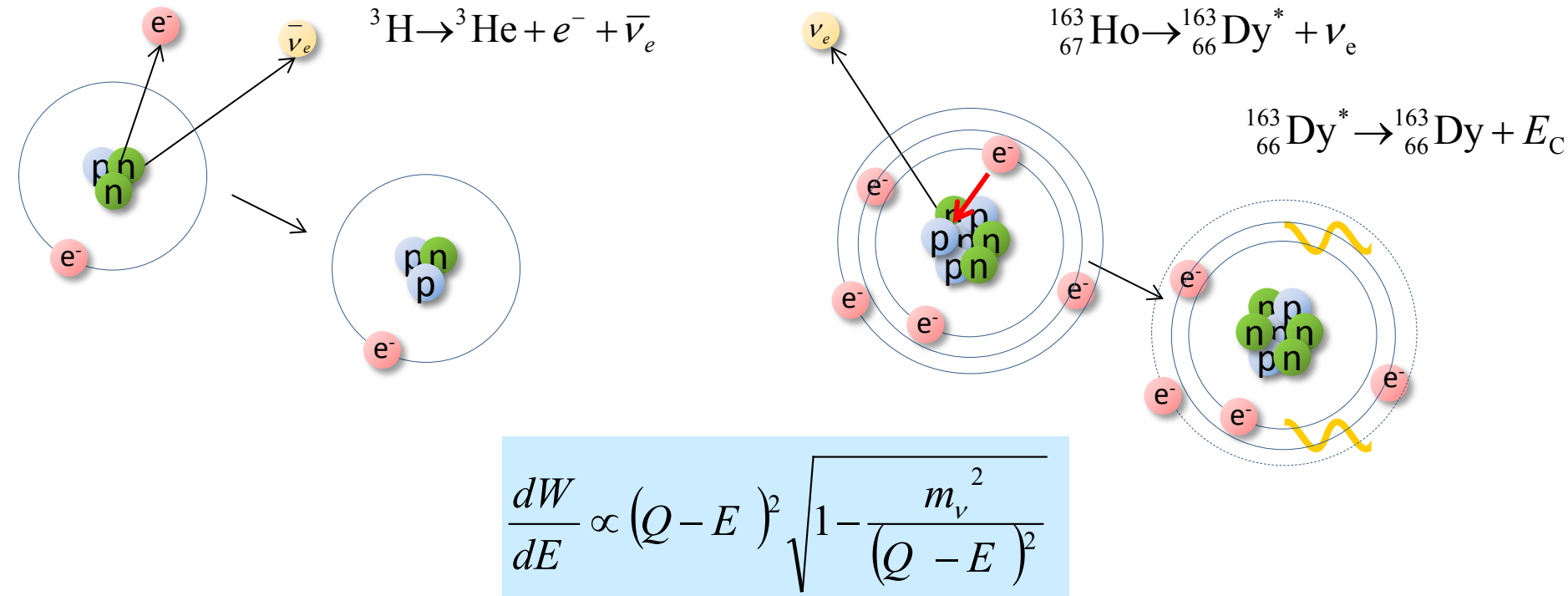
E.G. Myers et al., *Phys. Rev. Lett.* **114** (2015) 013003

$$\bullet \tau_{1/2} \approx 4570 \text{ years} \quad (2 \cdot 10^{11} \text{ atoms for } 1 \text{ Bq})$$

$$\bullet Q_{EC} = (2.833 \pm 0.030^{\text{stat}} \pm 0.015^{\text{syst}}) \text{ keV}$$

S. Eliseev et al., *Phys. Rev. Lett.* **115** (2015) 062501

Beta decay and electron capture



- $\tau_{1/2} \approx 12.3$ years (4*10⁸ atoms for 1 Bq)

- $Q_\beta = 18\,592.01(7)$ eV

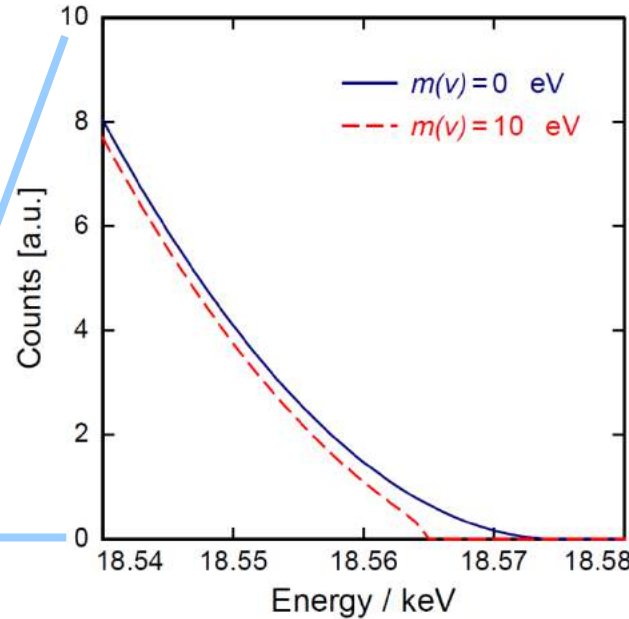
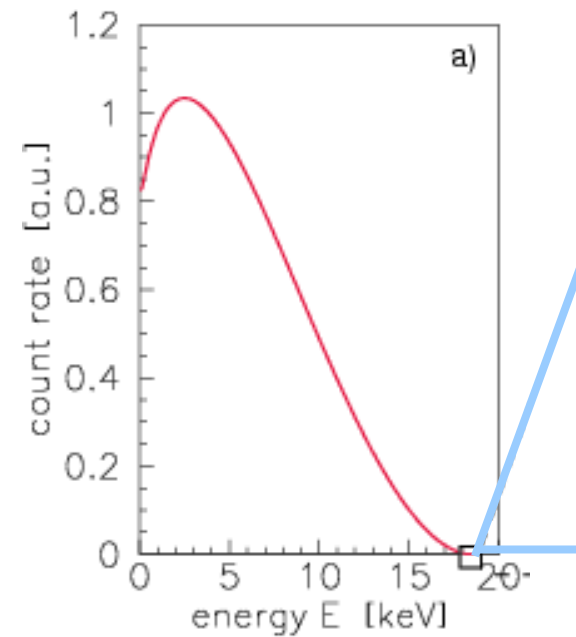
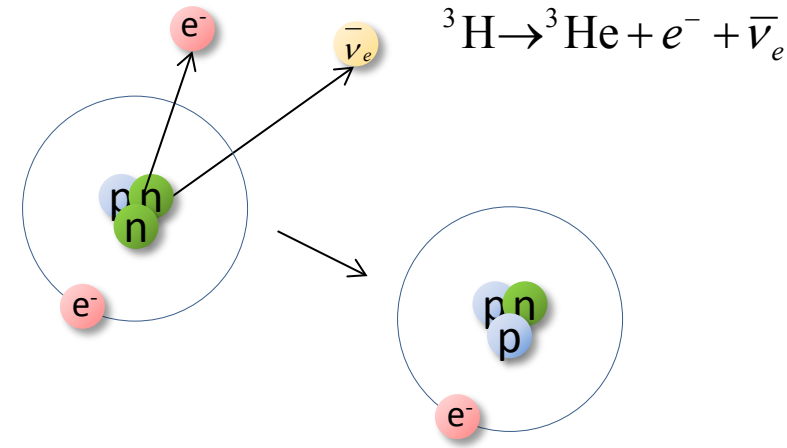
E.G. Myers et al., *Phys. Rev. Lett.* **114** (2015) 013003

- $\tau_{1/2} \approx 4570$ years (2*10¹¹ atoms for 1 Bq)

- $Q_{EC} = (2.833 \pm 0.030^{\text{stat}} \pm 0.015^{\text{syst}})$ keV

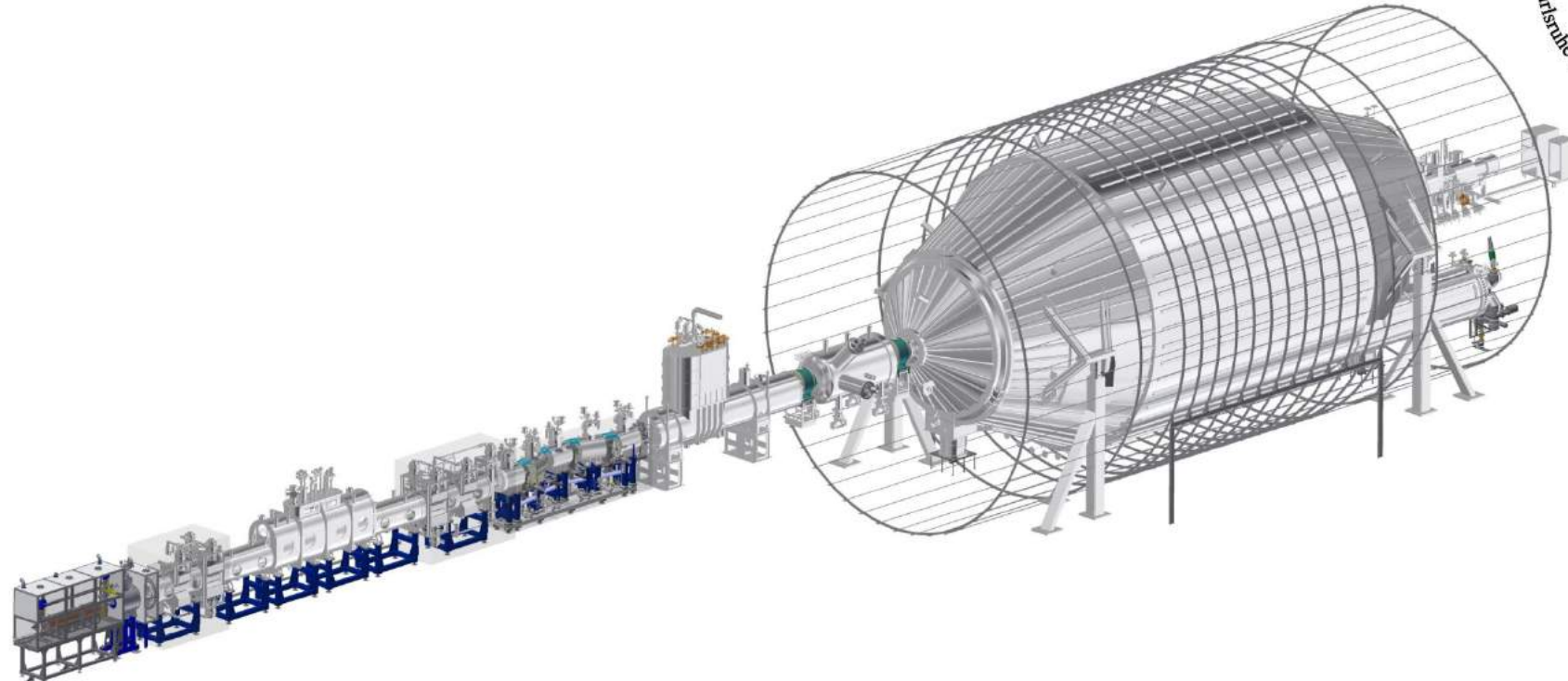
S. Eliseev et al., *Phys. Rev. Lett.* **115** (2015) 062501

Beta decay of ${}^3\text{H}$



The KATRIN experiment

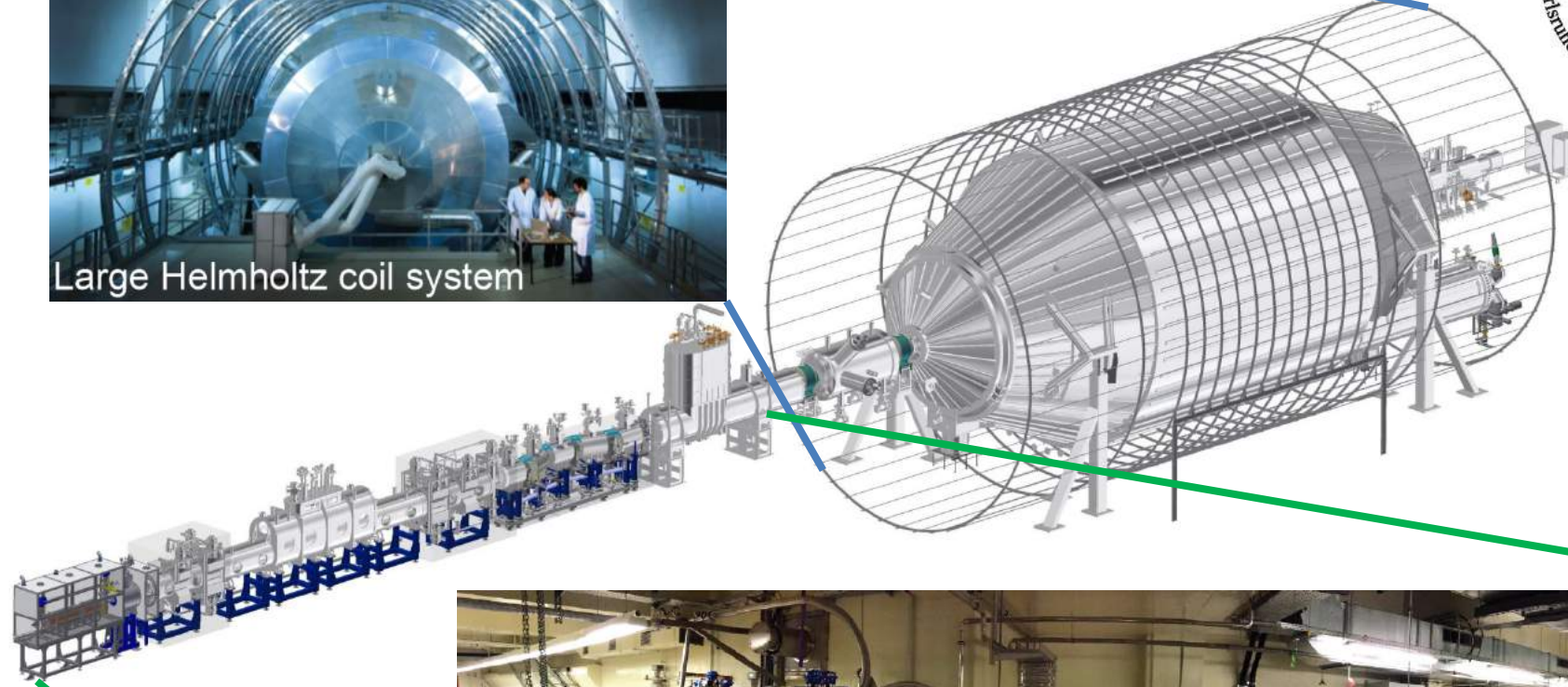
❖ KATRIN - Karlsruhe Tritium Neutrino Experiment



Main ideas:

- high activity source 10^{11} e⁻/s
- high resolution MAC-E* filter to select electrons close to the end point
- count electrons as function of retarding potential
→ integral spectrum

The KATRIN experiment: present status



The KATRIN experiment: present status



Large Helm



Photo Patrick Langer



Photo K. Valerius

^3H based experiments



❖ KATRIN - Karlsruhe Tritium Neutrino Experiment

Main ideas:

- high activity source: $10^{11} \text{ e}^-/\text{s}$
- high resolution MAC-E filter to select electrons close to the end point
- count electrons as function of retarding potential
→ integral spectrum

❖ Project8

Main ideas:

- Source = detector: $10^{11} - 10^{13} \text{ }^3\text{H}_2$ molecules /cm³
- Use cyclotron frequency to extract electron energy
- Differential spectrum



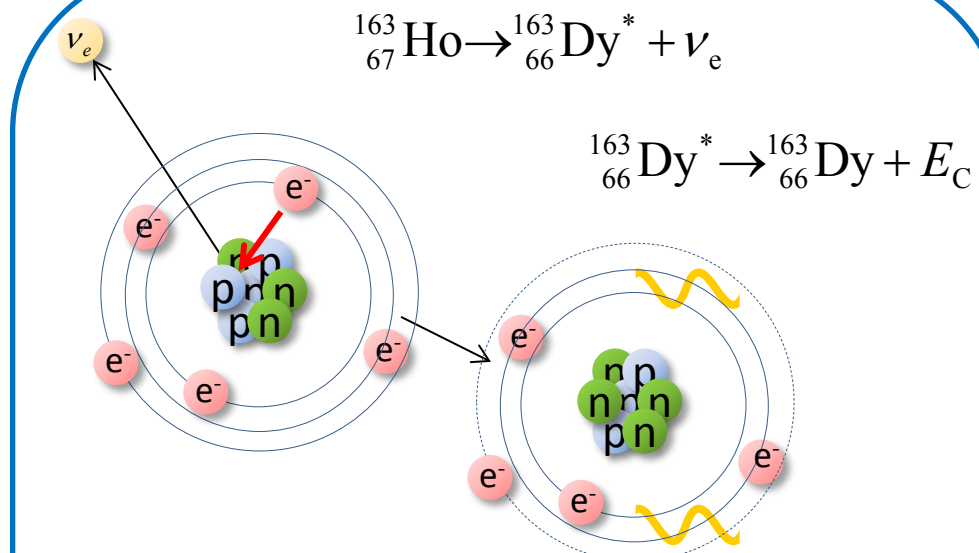
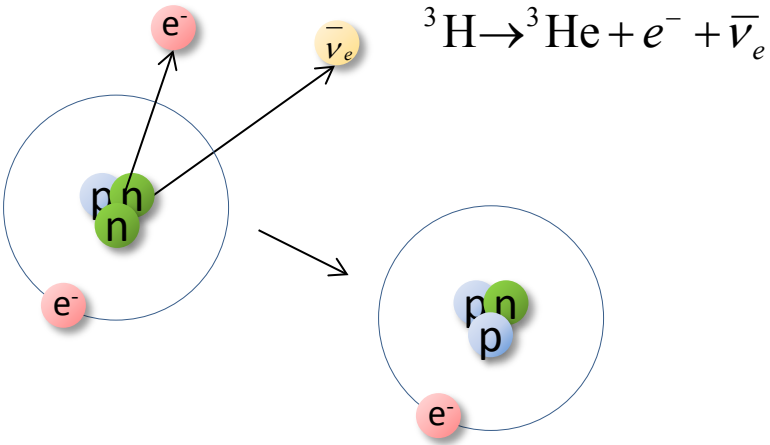
❖ PTOLEMY - Princeton Tritium Observatory for Light, Early-Universe, Massive-Neutrino Yield

Main ideas:

- large area tritium source: 100 g atomic ^3H
- MAC-E Iter to select electrons close to the end point
- RF tracking and time-of-flight systems
- cryogenic calorimetry → differential spectrum



Beta decay and electron capture



- $\tau_{1/2} \approx 12.3 \text{ years}$ (4×10^8 atoms for 1 Bq)

- $Q_{EC} = 18\,592.01(7) \text{ eV}$

E.G. Myers et al., *Phys. Rev. Lett.* **114** (2015) 013003

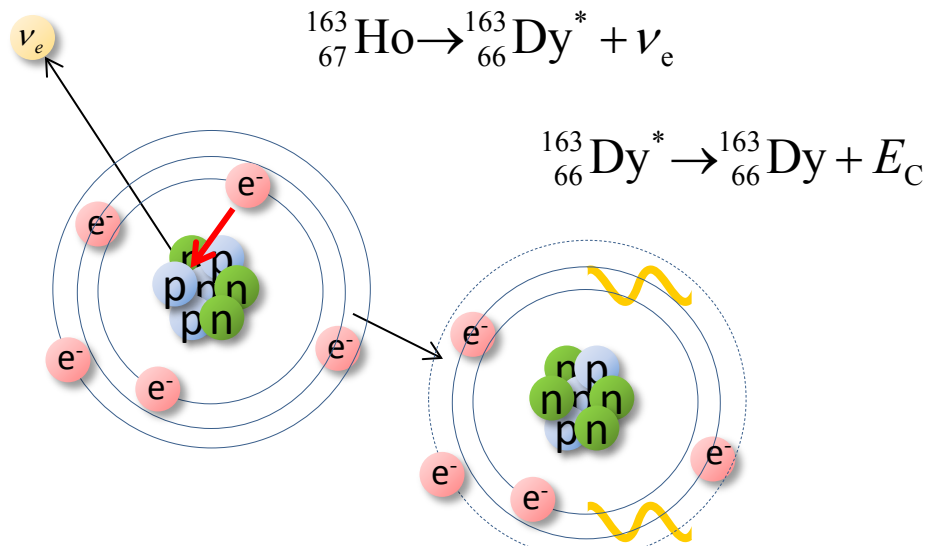
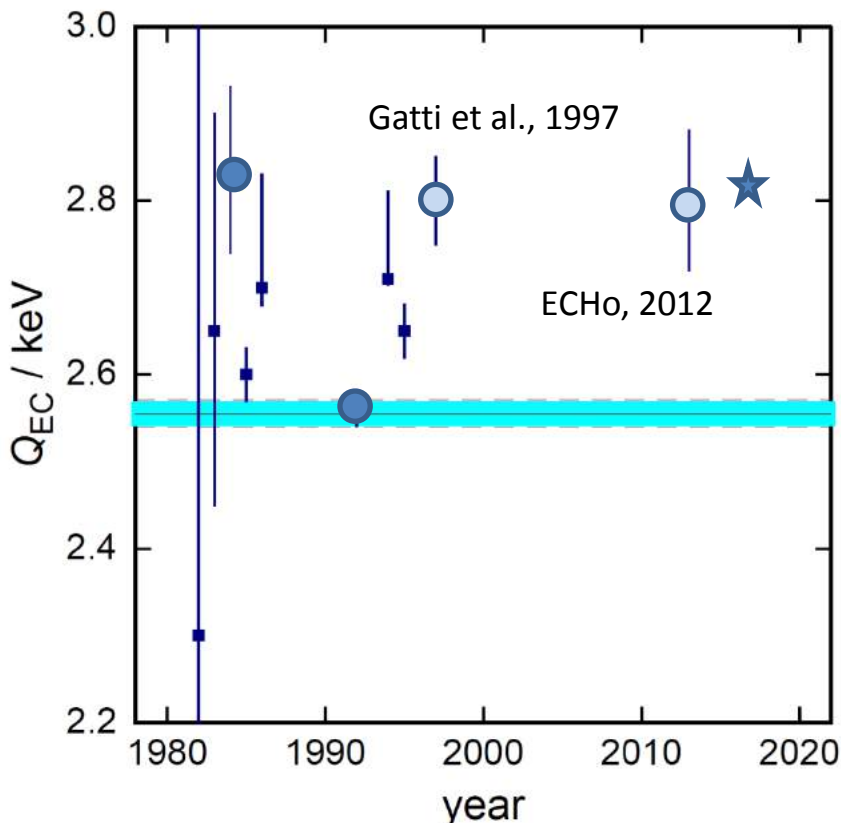
- $\tau_{1/2} \approx 4570 \text{ years}$ (2×10^{11} atoms for 1 Bq)

- $Q_{EC} = (2.833 \pm 0.030^{\text{stat}} \pm 0.015^{\text{syst}}) \text{ keV}$

S. Eliseev et al., *Phys. Rev. Lett.* **115** (2015) 062501

Electron capture in ^{163}Ho : Q_{EC} determination

- Calorimetric measurements
- Measurements of x-rays
- ★ $Q_{\text{EC}} = m(^{163}\text{Ho}) - m(^{163}\text{Dy})$



- $\tau_{1/2} \approx 4570$ years (2* 10^{11} atoms for 1 Bq)
- $Q_{\text{EC}} = (2.833 \pm 0.030^{\text{stat}} \pm 0.015^{\text{syst}}) \text{ keV}$

S. Eliseev et al., *Phys. Rev. Lett.* **115** (2015) 062501

Electron capture in ^{163}Ho : Q_{EC} determination

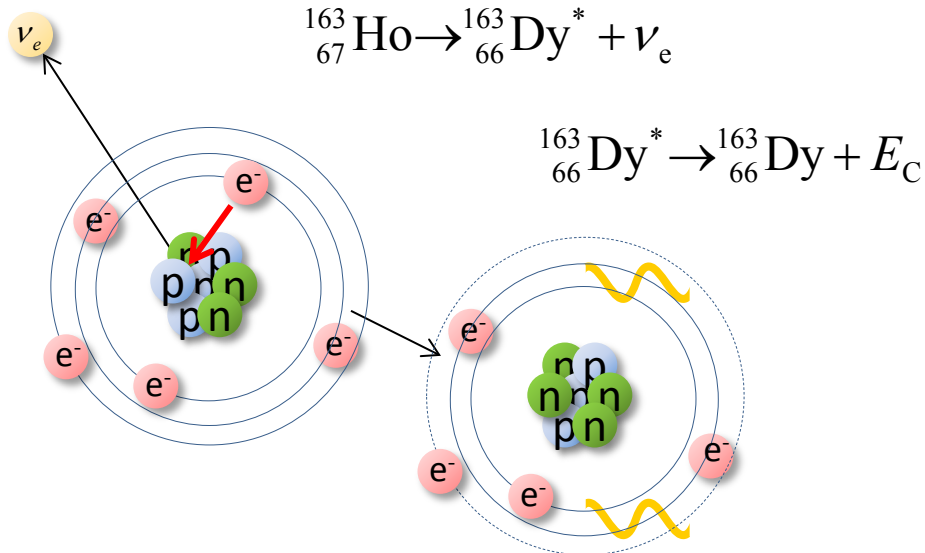
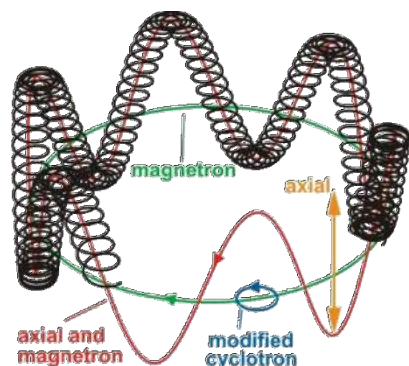
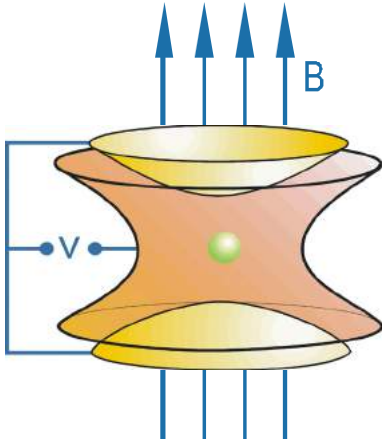
- Calorimetric measurements
- Measurements of x-rays
- $Q_{\text{EC}} = m(^{163}\text{Ho}) - m(^{163}\text{Dy})$

Penning Trap Mass Spectroscopy

@TRIGA TRAP (Uni-Mainz) (*)

@SHIPTRAP (GSI – Darmstadt) (**)

$$\nu_c = \frac{qB}{m}$$



• $\tau_{1/2} \approx 4570$ years (2*10¹¹ atoms for 1 Bq)

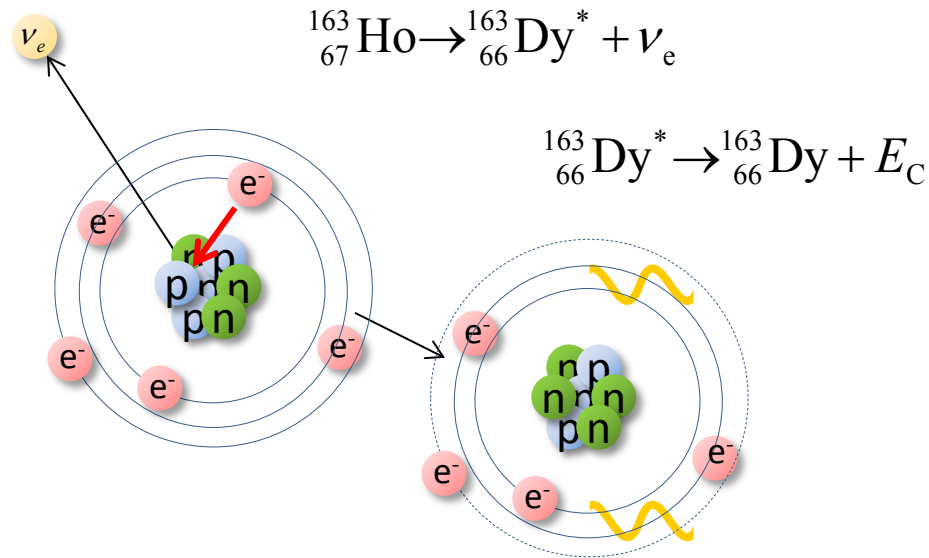
• $Q_{\text{EC}} = (2.833 \pm 0.030^{\text{stat}} \pm 0.015^{\text{syst}}) \text{ keV}$

S. Eliseev et al., *Phys. Rev. Lett.* **115** (2015) 062501 (**)
F. Schneider et al., *Eur. Phys. J. A* **51** (2015) 89 (*)

Electron capture in ^{163}Ho : spectrum

Atomic de-excitation:

- X-ray emission
- Auger electrons
- Coster-Kronig transitions



• $\tau_{1/2} \approx 4570$ years (2*10¹¹ atoms for 1 Bq)

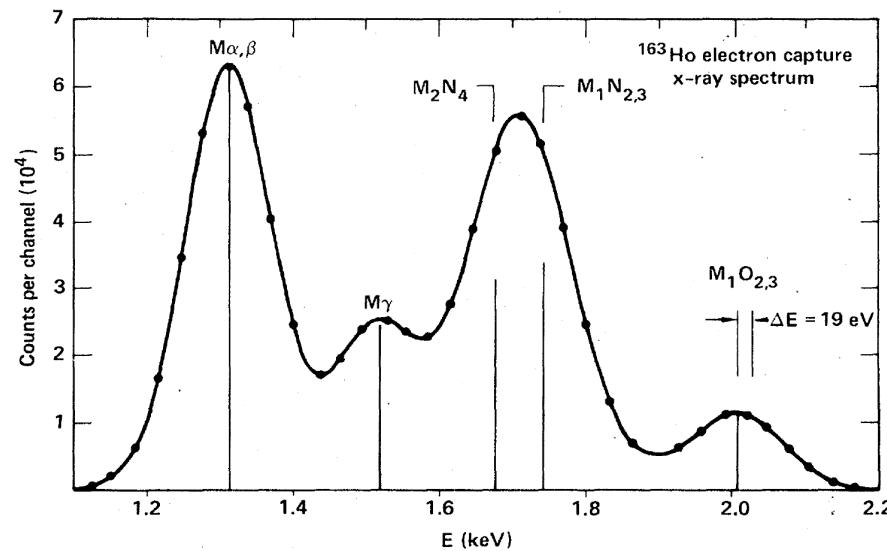
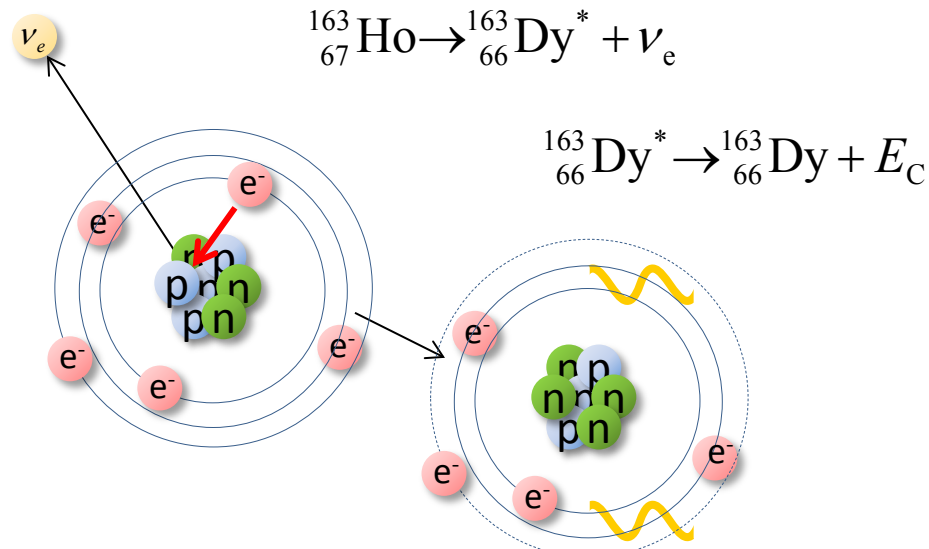
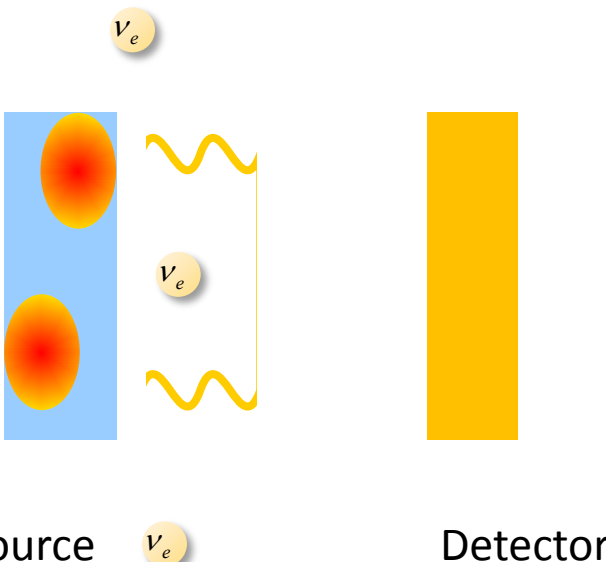
• $Q_{EC} = (2.833 \pm 0.030^{\text{stat}} \pm 0.015^{\text{syst}})$ keV

S. Eliseev et al., *Phys. Rev. Lett.* **115** (2015) 062501

Electron capture in ^{163}Ho : spectrum

Atomic de-excitation:

- X-ray emission
- Auger electrons
- Coster-Kronig transitions

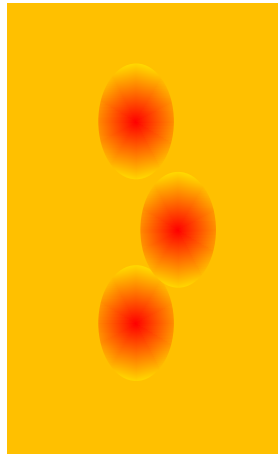
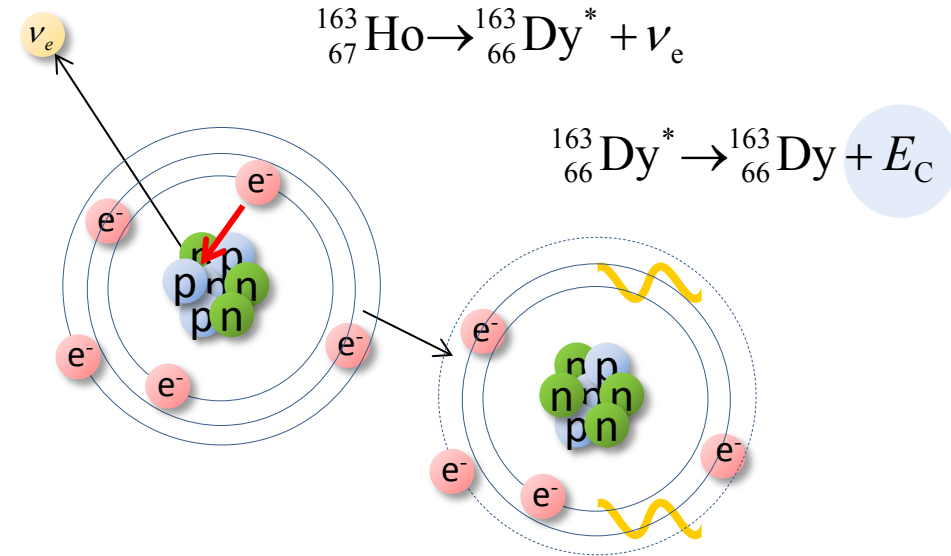


Electron capture in ^{163}Ho : spectrum

Atomic de-excitation:

- X-ray emission
- Auger electrons
- Coster-Kronig transitions

Calorimetric measurement



Source = Detector

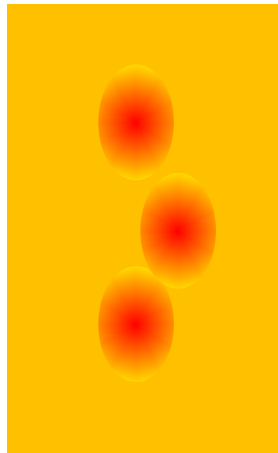
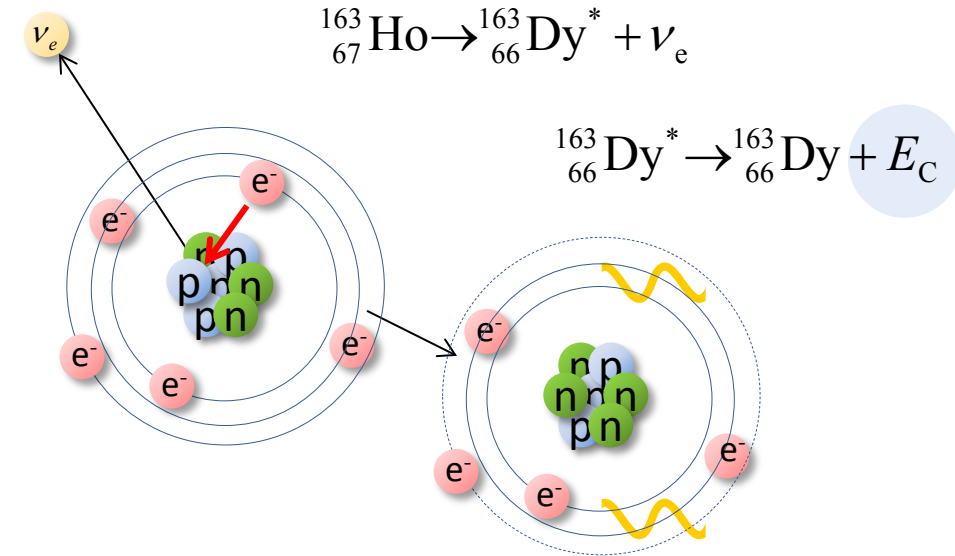
ν_e

Electron capture in ^{163}Ho : spectrum

Atomic de-excitation:

- X-ray emission
- Auger electrons
- Coster-Kronig transitions

Calorimetric measurement



Source = Detector

ν_e

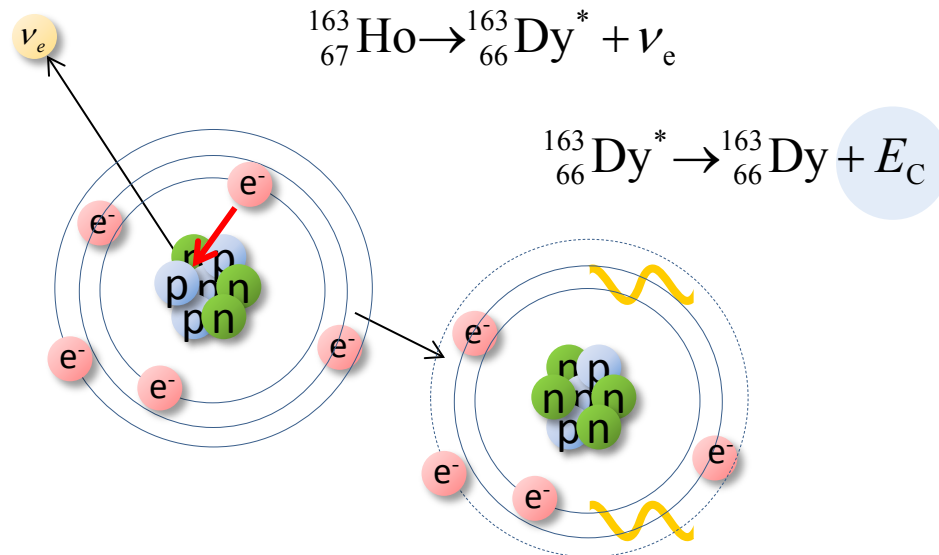


Electron capture in ^{163}Ho : spectrum

Atomic de-excitation:

- X-ray emission
- Auger electrons
- Coster-Kronig transitions

Calorimetric measurement



Volume 118B, number 4, 5, 6

PHYSICS LETTERS

9 December 1982

CALORIMETRIC MEASUREMENTS OF ^{163}HO DECAY AS TOOLS TO DETERMINE THE ELECTRON NEUTRINO MASS

A. DE RÚJULA and M. LUSIGNOLI ¹

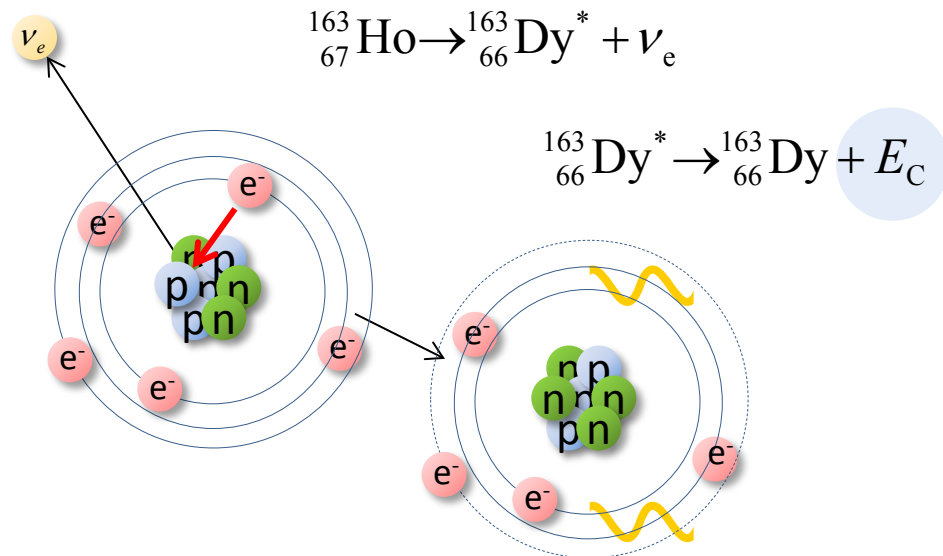
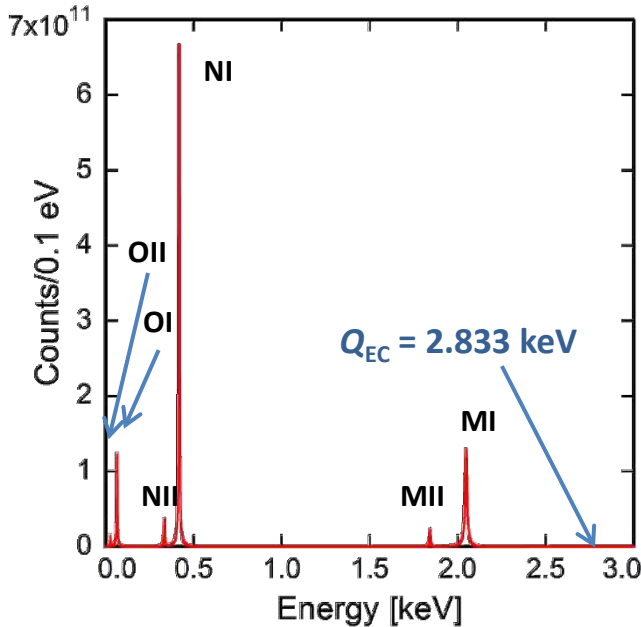
CERN, Geneva, Switzerland

Electron capture in ^{163}Ho : spectrum

Atomic de-excitation:

- X-ray emission
- Auger electrons
- Coster-Kronig transitions

Calorimetric measurement



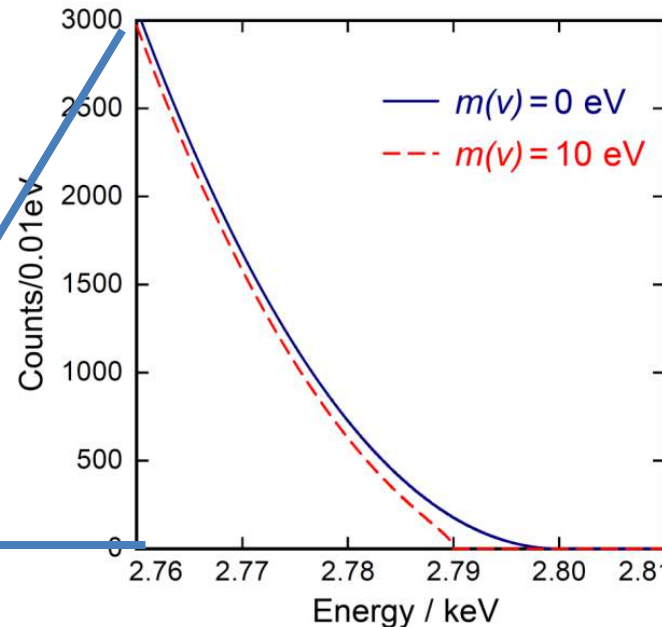
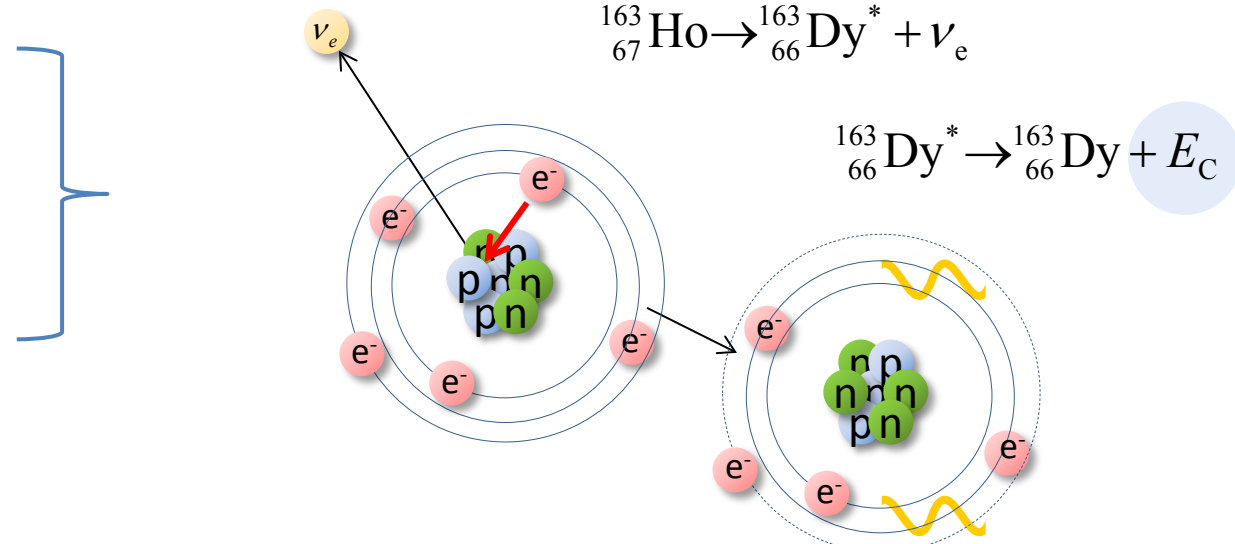
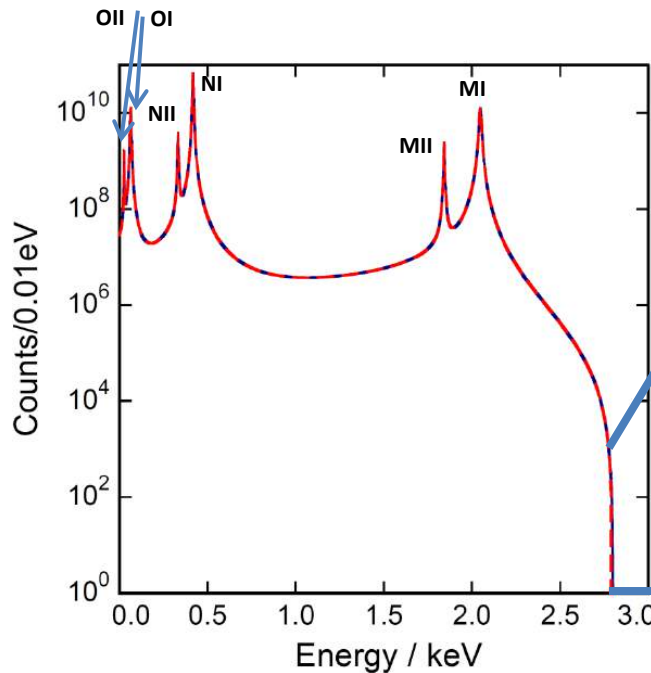
$$\frac{dW}{dE_C} = A(Q_{\text{EC}} - E_C)^2 \sqrt{1 - \frac{m_\nu^2}{(Q_{\text{EC}} - E_C)^2}} \sum_H B_H \varphi_H^2(0) \frac{\frac{\Gamma_H}{2\pi}}{(E_C - E_H)^2 + \frac{\Gamma_H^2}{4}}$$

Electron capture in ^{163}Ho : spectrum

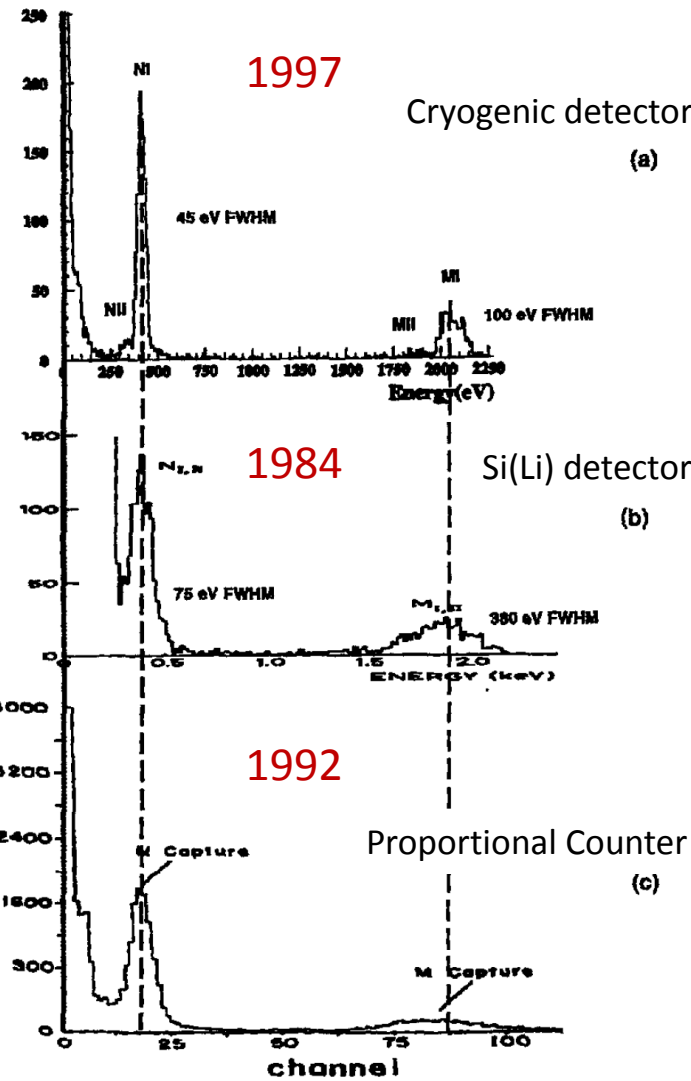
Atomic de-excitation:

- X-ray emission
- Auger electrons
- Coster-Kronig transitions

Calorimetric measurement



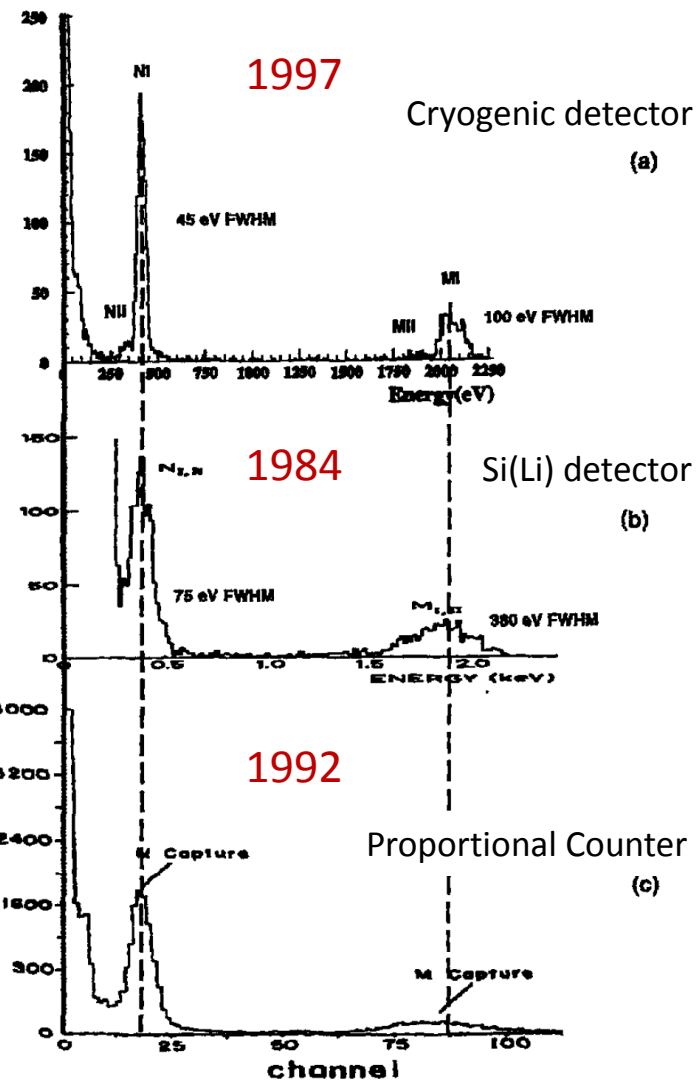
Electron capture in ^{163}Ho : history



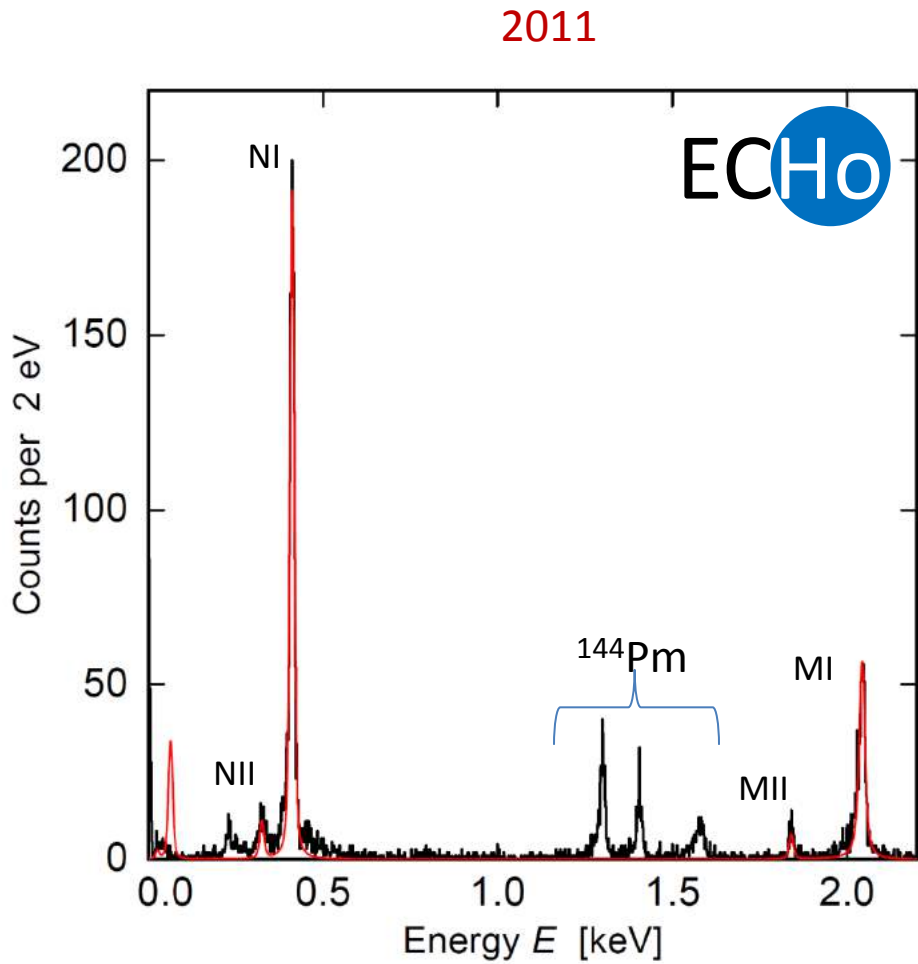
F. Gatti et al., Physics Letters B 398 (1997) 415-419

- (a) F. Gatti et al., Physics Letters B 398 (1997) 415-419
- (b) E. Laesgaard et al., Proceeding of 7th International Conference on Atomic Masses and Fundamental Constants (AMCO-7), (1984).
- (c) F.X. Hartmann and R.A. Naumann, Nucl. Instr. Meth. A 313 (1992) 237.

Electron capture in ^{163}Ho : history

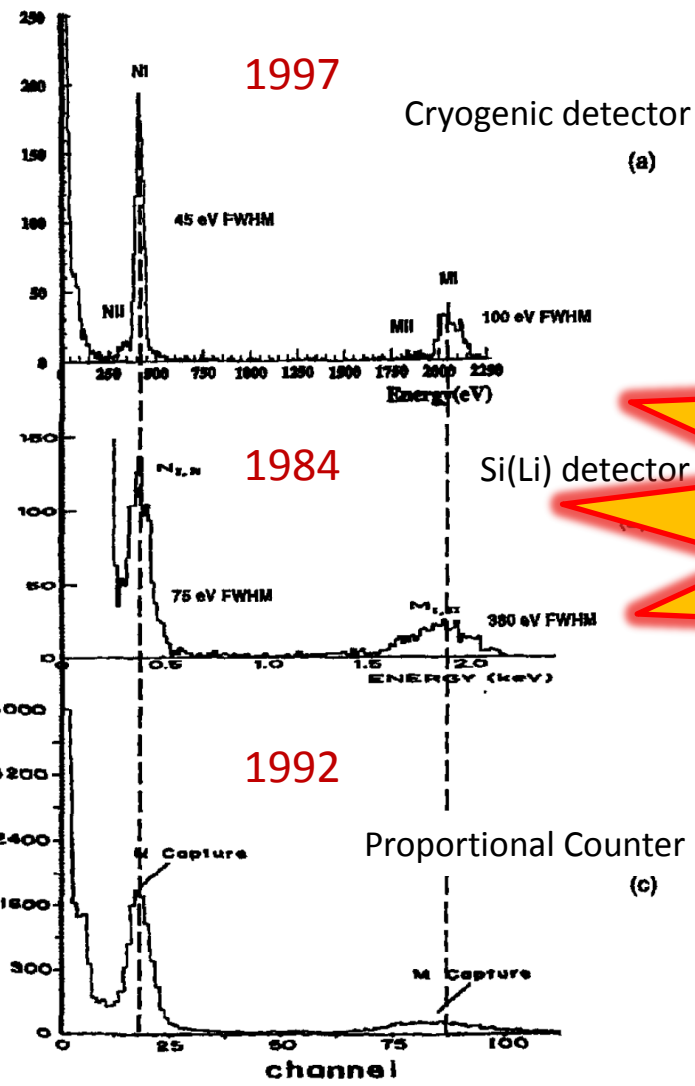


F. Gatti et al., Physics Letters B 398 (1997) 415-419

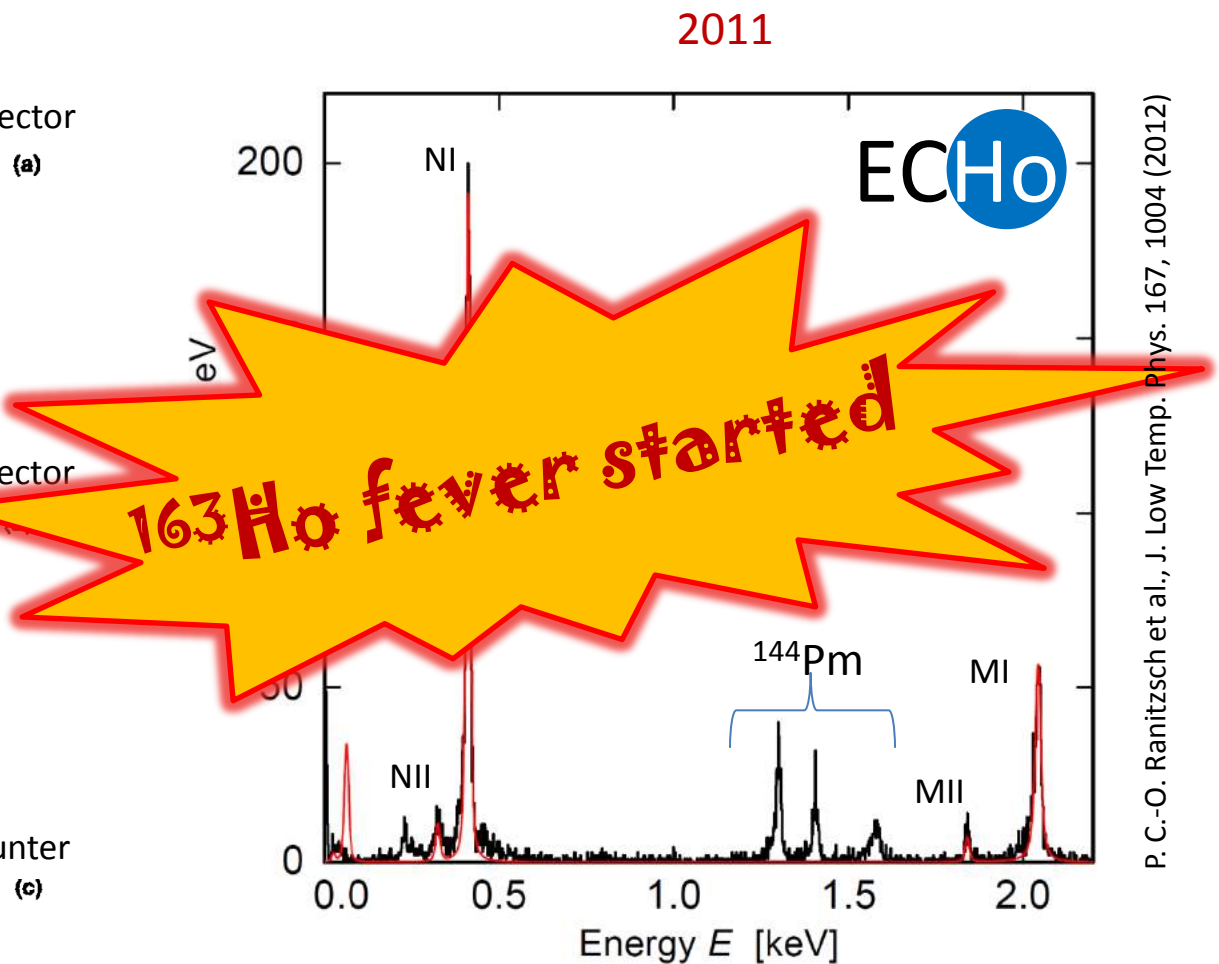


- (a) F. Gatti et al., Physics Letters B 398 (1997) 415-419
(b) E. Laesgaard et al., Proceeding of 7th International Conference on Atomic Masses and Fundamental Constants (AMCO-7), (1984).
(c) F.X. Hartmann and R.A. Naumann, Nucl. Instr. Meth. A 3 13 (1992) 237.

Electron capture in ^{163}Ho : history



F. Gatti et al., Physics Letters B 398 (1997) 415-419



- (a) F. Gatti et al., Physics Letters B 398 (1997) 415-419
- (b) E. Laesgaard et al., Proceeding of 7th International Conference on Atomic Masses and Fundamental Constants (AMCO-7), (1984).
- (c) F.X. Hartmann and R.A. Naumann, Nucl. Instr. Meth. A 313 (1992) 237.

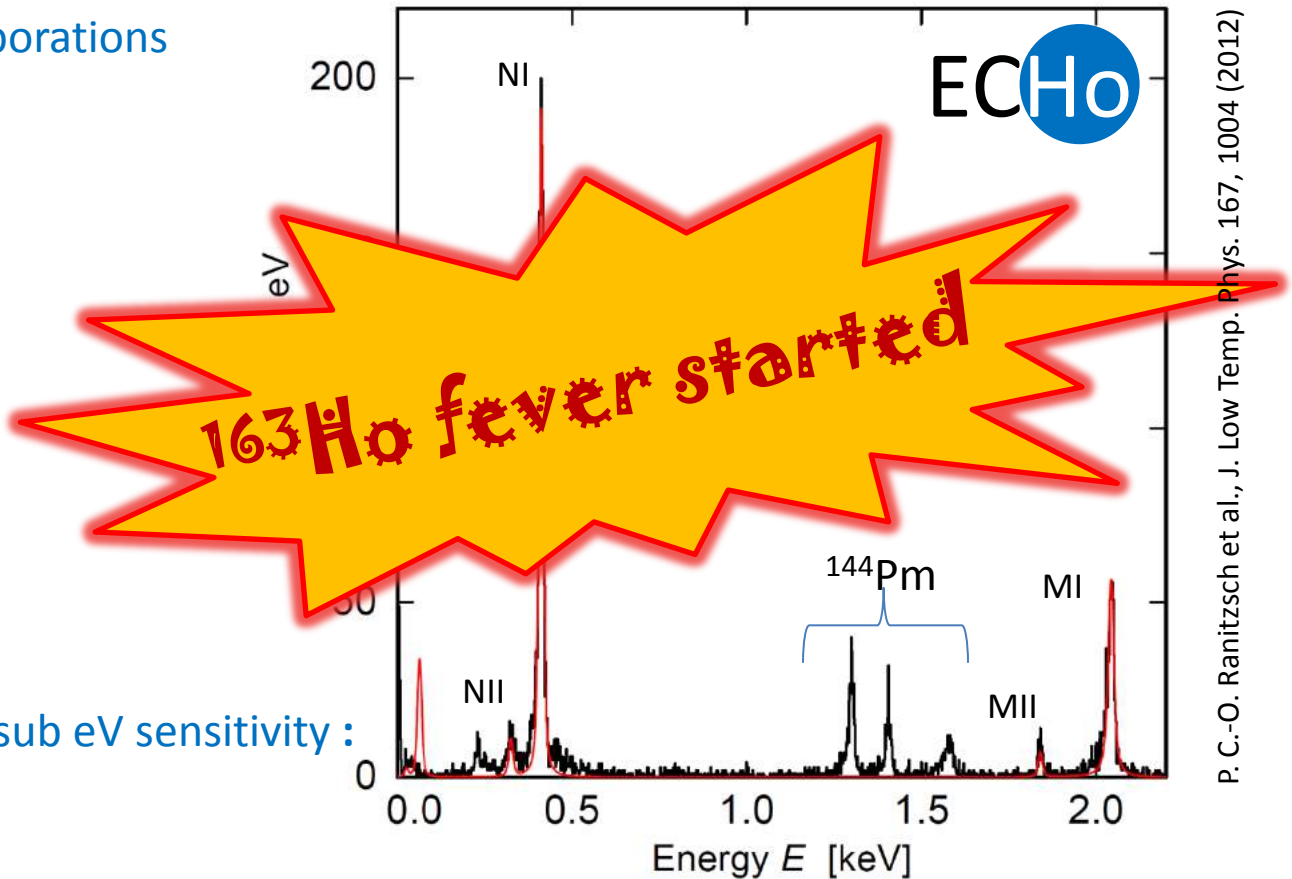
Electron capture in ^{163}Ho : present

- Calorimetric measurement of the ^{163}Ho spectrum
- Three international collaborations

ECHO (1)

HOLMES (2)

NuMECS (3)



P. C.-O. Ranitzsch et al., J. Low Temp. Phys. 167, 1004 (2012)

Common challenges to reach sub eV sensitivity :

- Detector performance
- High purity ^{163}Ho source
- Background reduction
- Description of the ^{163}Ho EC spectrum

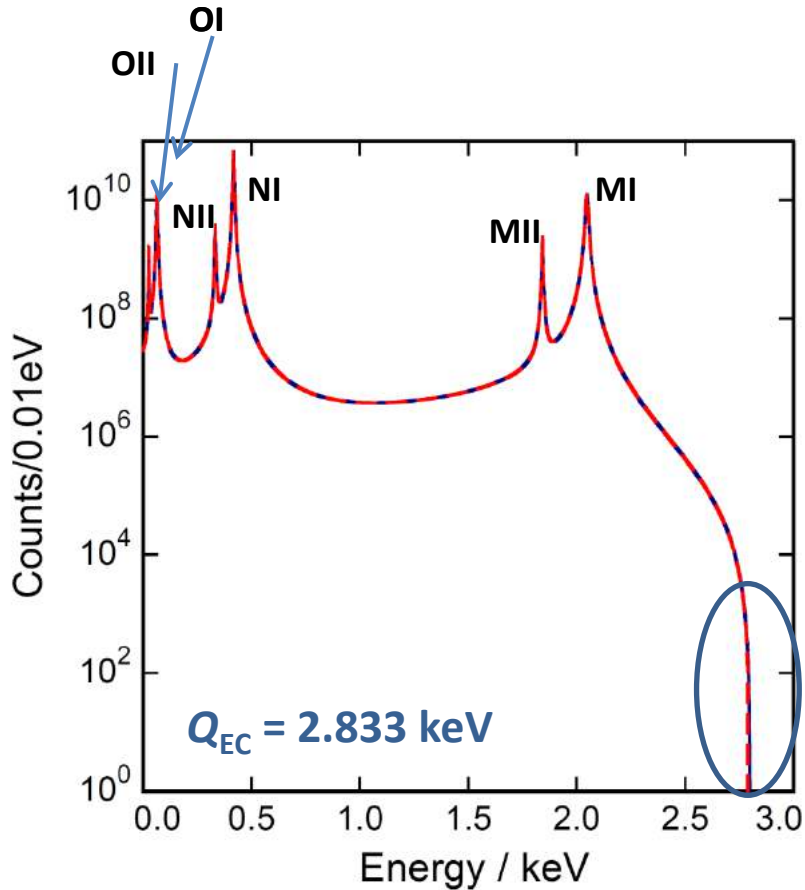
- (1) The ECHO Collaboration EPJ-ST 226 8 (2017) 1623
(2) B. Alpert et al, Eur. Phys. J. C (2015) 75:112
(3) M. Croce et al., arXiv:1510.03874

Requirements for sub-eV sensitivity in ECHo

Requirements for sub-eV sensitivity in ECHo

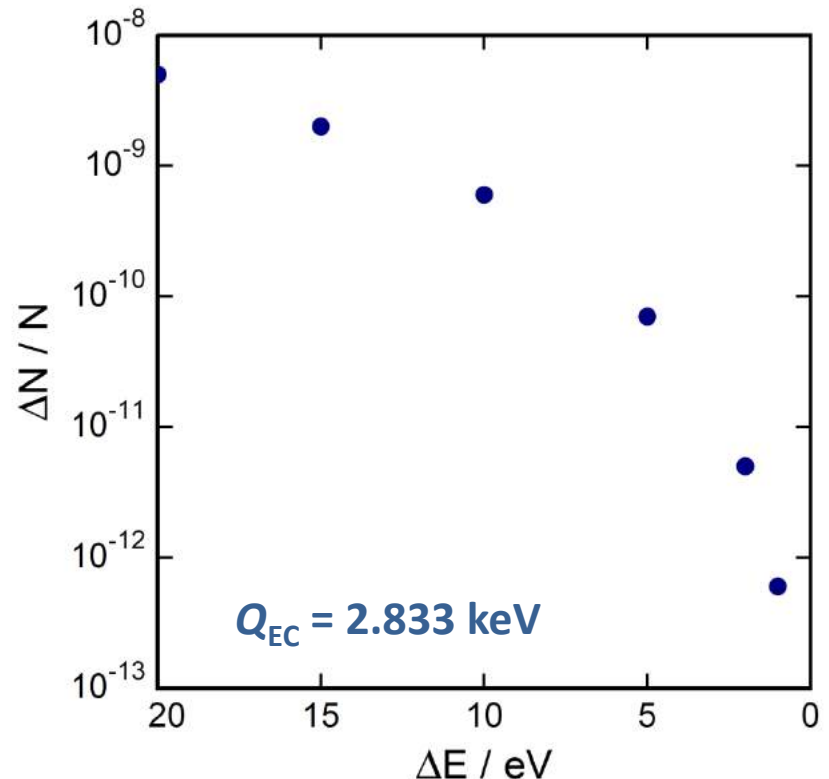
Statistics in the end point region

- $N_{ev} > 10^{14}$ $\rightarrow A \approx 1 \text{ MBq}$



Fraction of events at endpoint regions

- In the interval 2.832 - 2.833 keV
only 6×10^{-13}



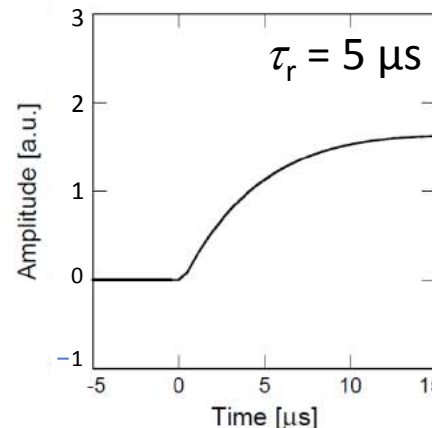
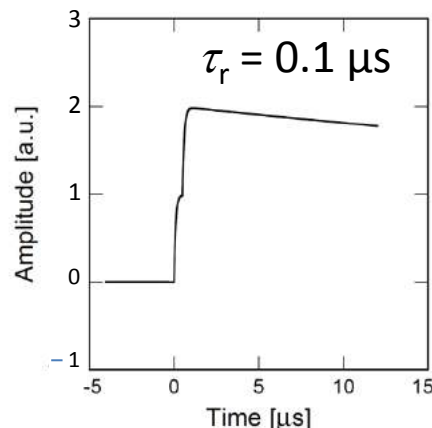
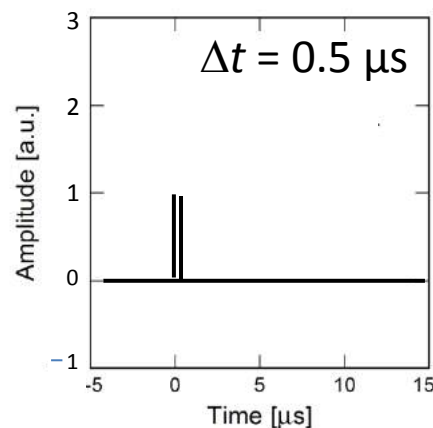
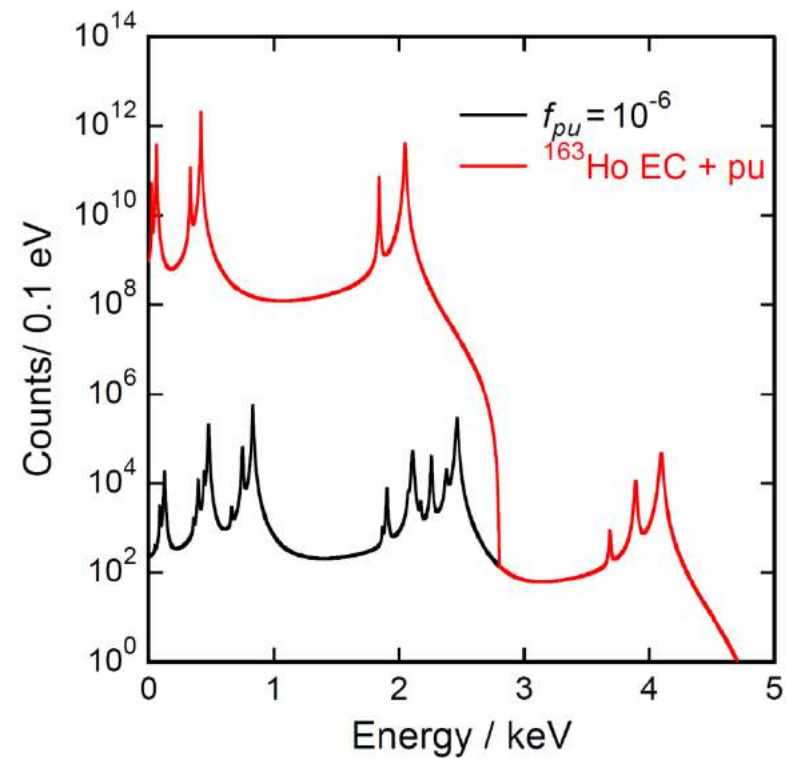
Requirements for sub-eV sensitivity in ECHo

Statistics in the end point region

- $N_{\text{ev}} > 10^{14} \rightarrow A \approx 1 \text{ MBq}$

Unresolved pile-up ($f_{\text{pu}} \sim a \cdot \tau_r$)

- $f_{\text{pu}} < 10^{-5}$
- $\tau_r < 1 \mu\text{s} \rightarrow a \sim 10 \text{ Bq}$
- 10^5 pixels



Requirements for sub-eV sensitivity in ECHo

Statistics in the end point region

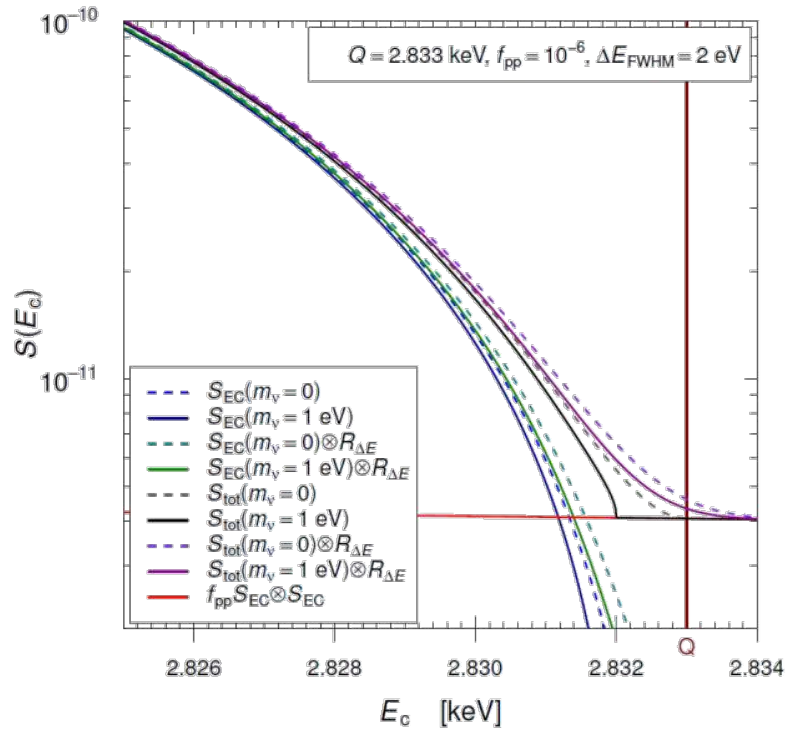
- $N_{\text{ev}} > 10^{14} \rightarrow A \approx 1 \text{ MBq}$

Unresolved pile-up ($f_{\text{pu}} \sim a \cdot \tau_r$)

- $f_{\text{pu}} < 10^{-5}$
- $\tau_r < 1 \mu\text{s} \rightarrow a \sim 10 \text{ Bq}$
- 10^5 pixels

Precision characterization of the endpoint region

- $\Delta E_{\text{FWHM}} < 3 \text{ eV}$



Requirements for sub-eV sensitivity in ECHo

Statistics in the end point region

- $N_{ev} > 10^{14}$ $\rightarrow A \approx 1 \text{ MBq}$

Unresolved pile-up ($f_{pu} \sim a \cdot \tau_r$)

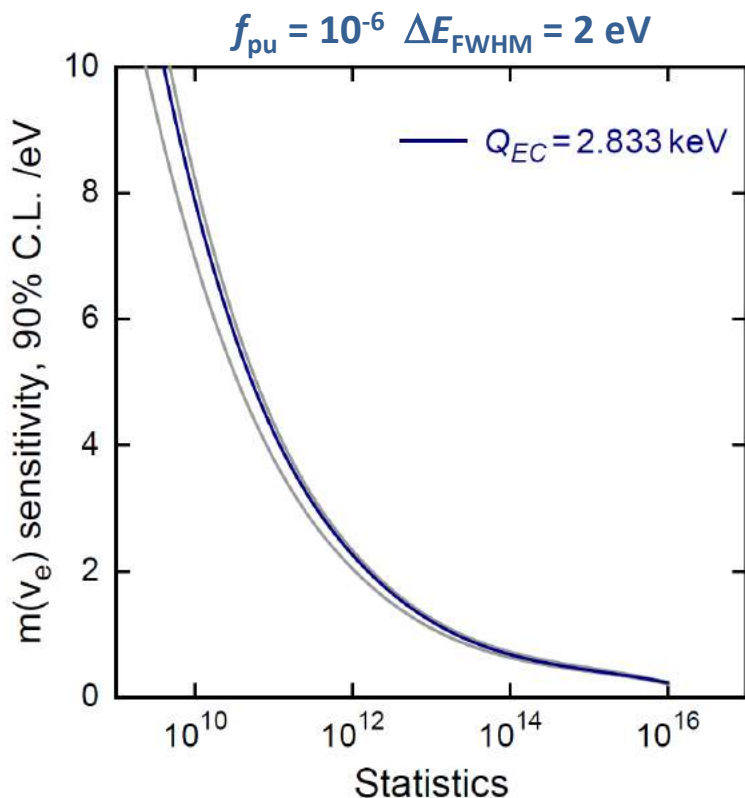
- $f_{pu} < 10^{-5}$
- $\tau_r < 1 \mu\text{s} \rightarrow a \sim 10 \text{ Bq}$
- 10^5 pixels

Precision characterization of the endpoint region

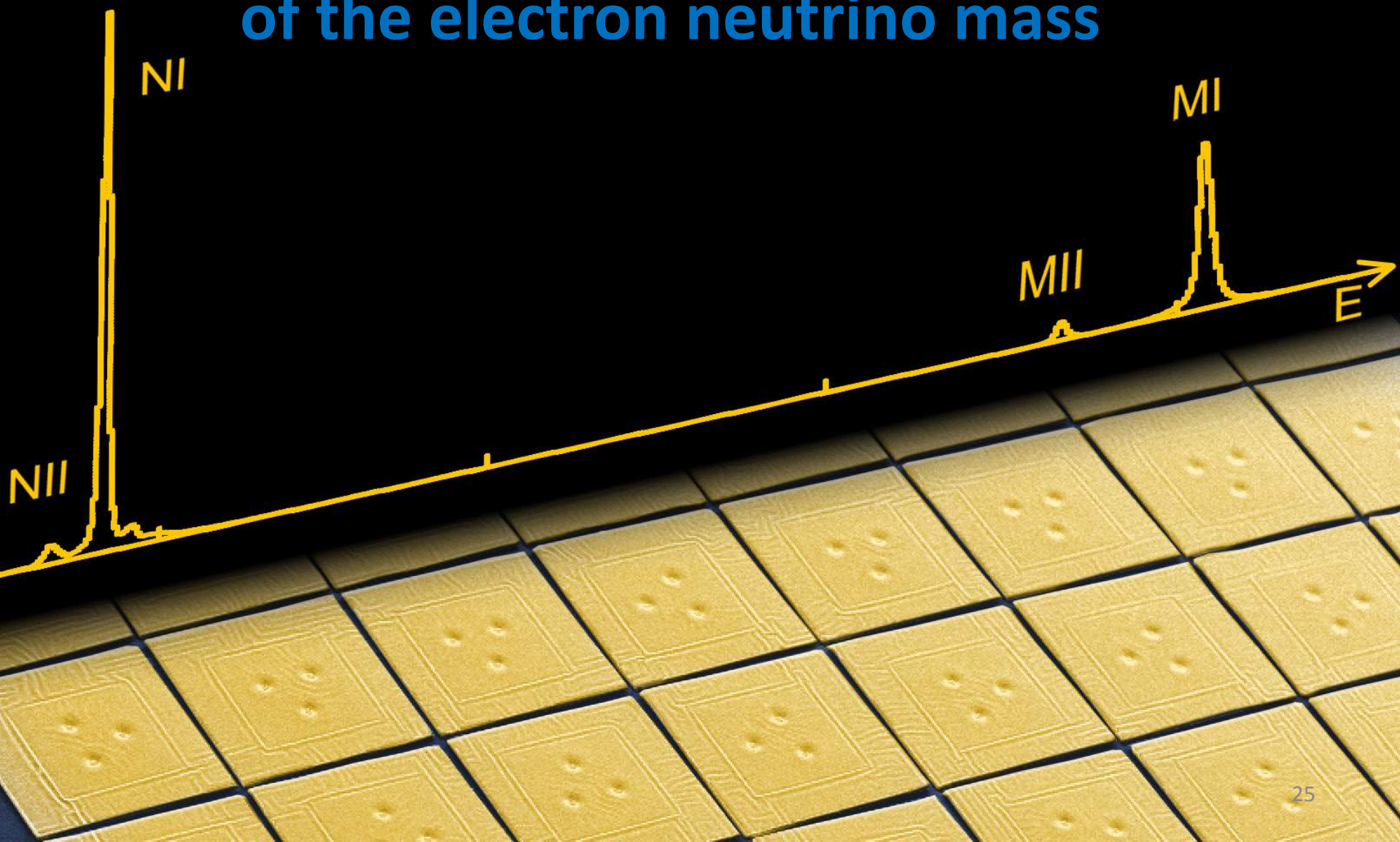
- $\Delta E_{FWHM} < 3 \text{ eV}$

Background level

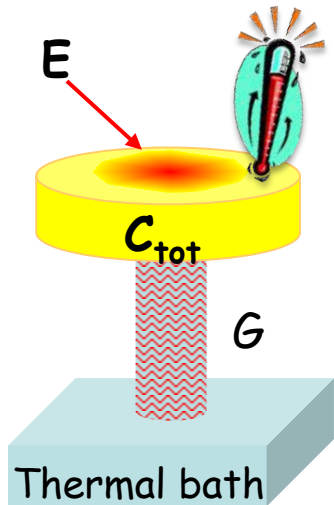
- $< 10^{-6} \text{ events/eV/det/day}$



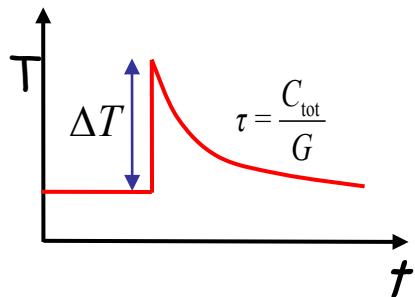
Low temperature detectors for direct determination of the electron neutrino mass



Low temperature micro-calorimeters



$$\Delta T \cong \frac{E}{C_{\text{tot}}}$$

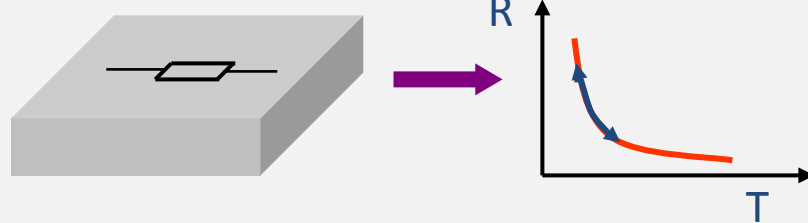


$$\left. \begin{array}{l} E = 10 \text{ keV} \\ C_{\text{tot}} = 1 \text{ pJ/K} \end{array} \right\} \rightarrow \sim 1 \text{ mK}$$

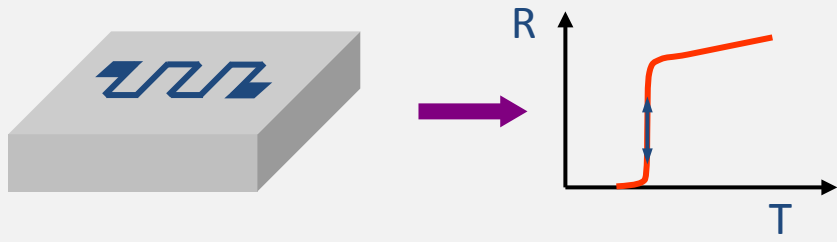
- Very small volume
- Working temperature below 100 mK
 - small specific heat
 - small thermal noise
- Very sensitive temperature sensor

Temperature sensors

Resistance of highly doped semiconductors



Resistance at superconducting transition, TES

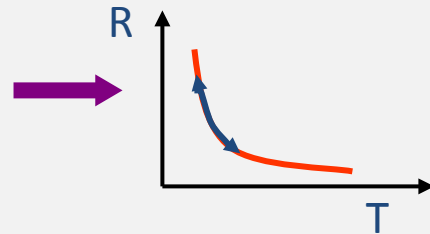
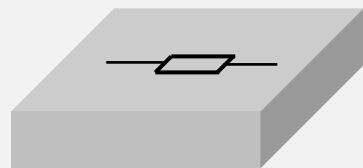


Magnetization of paramagnetic material, MMC

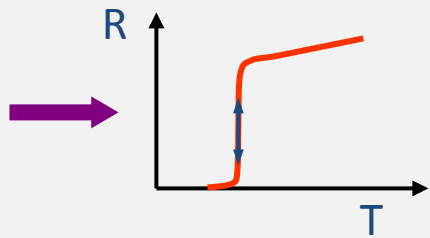


Temperature sensors

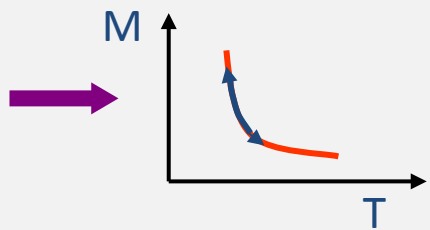
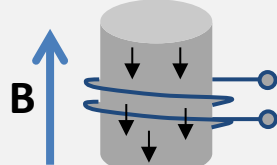
Resistance of highly doped semiconductors



Resistance at superconducting transition, TES



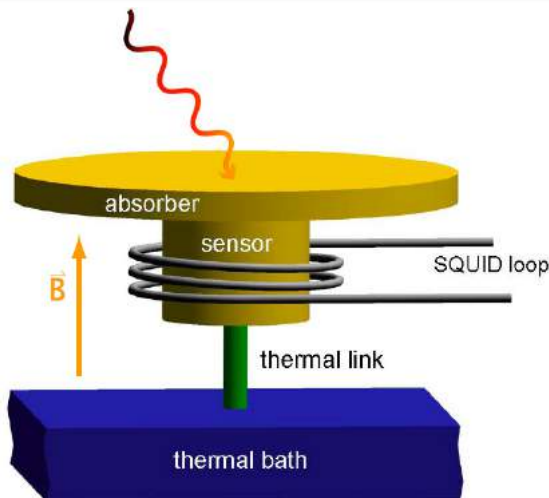
Magnetization of paramagnetic material, MMC



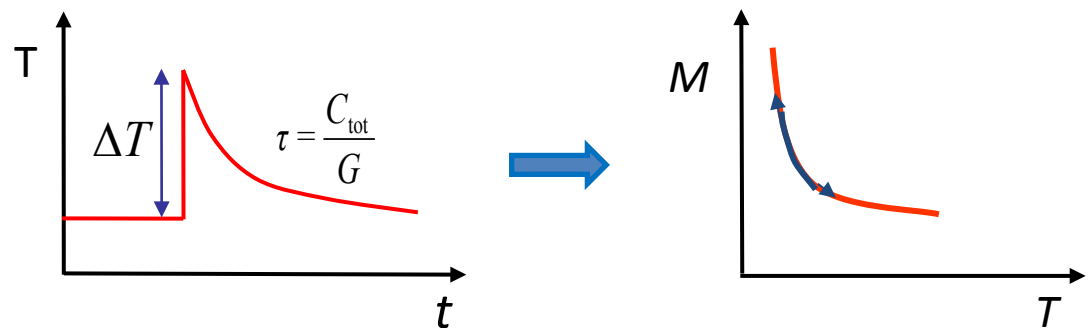
HOLMES
NuMECS

ECHO

Metallic magnetic calorimeters (MMCs)



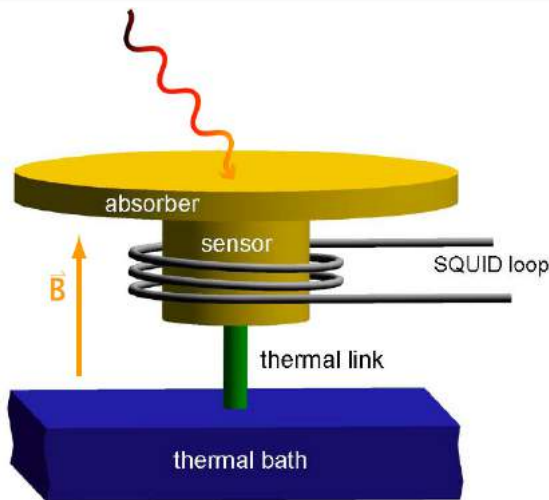
A. Fleischmann et al.,
AIP Conf. Proc. **1185**, 571, (2009)



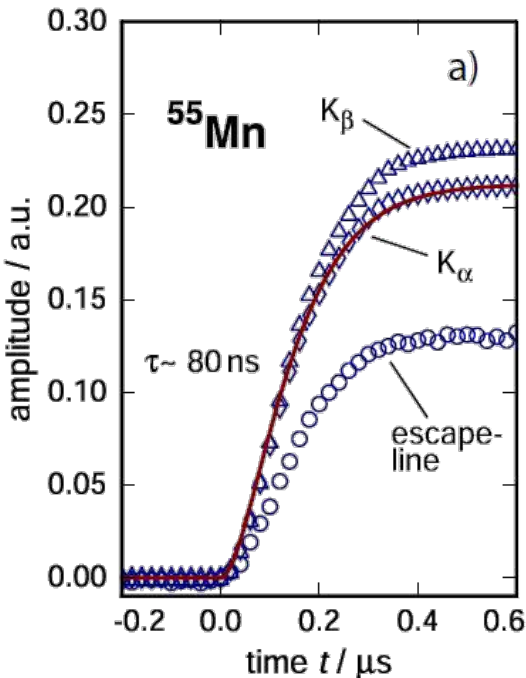
- Paramagnetic Au:Er sensor
Ag:Er

$$\Delta\Phi_s \propto \frac{\partial M}{\partial T} \Delta T \rightarrow \Delta\Phi_s \propto \frac{\partial M}{\partial T} \frac{E}{C_{\text{sens}} + C_{\text{abs}}}$$

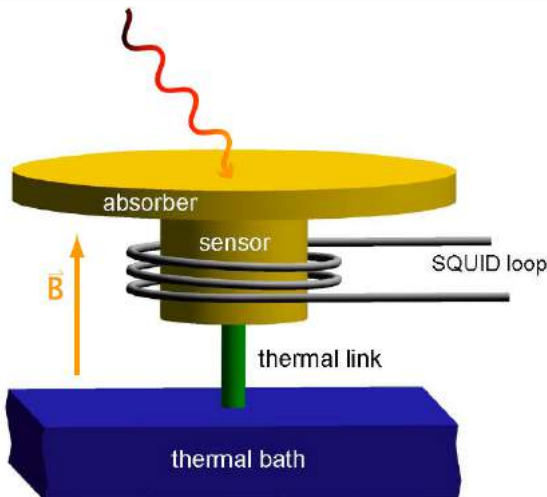
Metallic magnetic calorimeters (MMCs)



Fast risetime
→ Reduction un-resolved pile-up

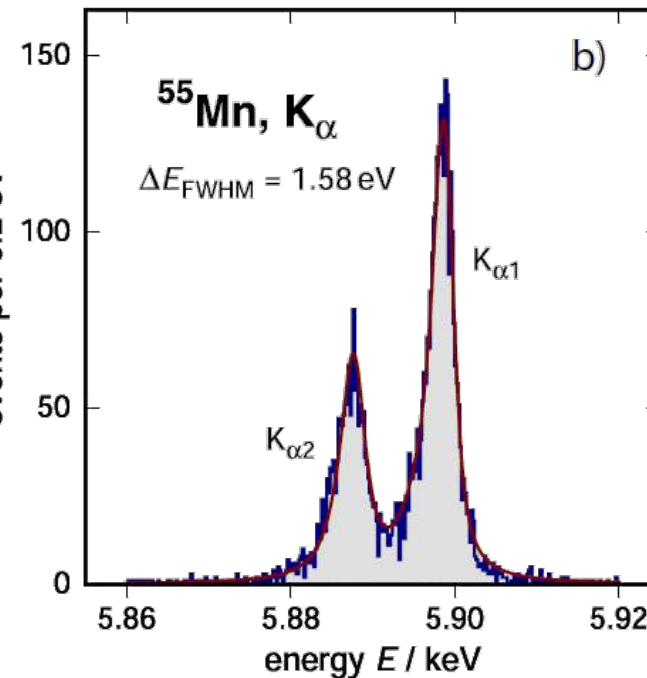
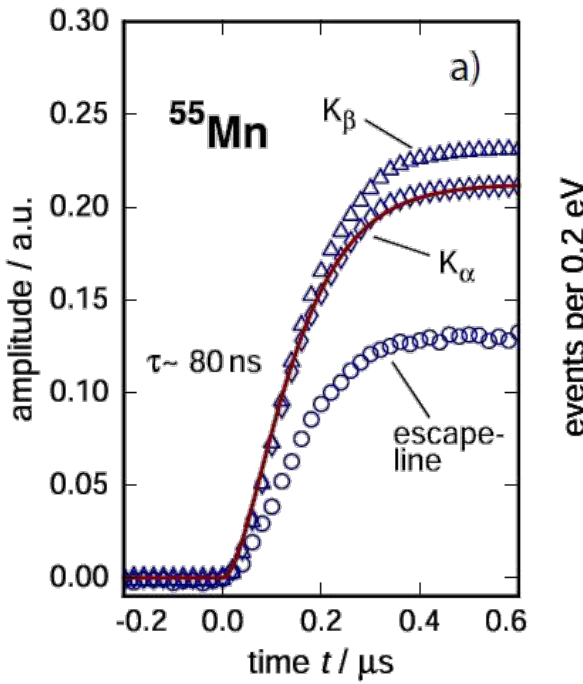


Metallic magnetic calorimeters (MMCs)

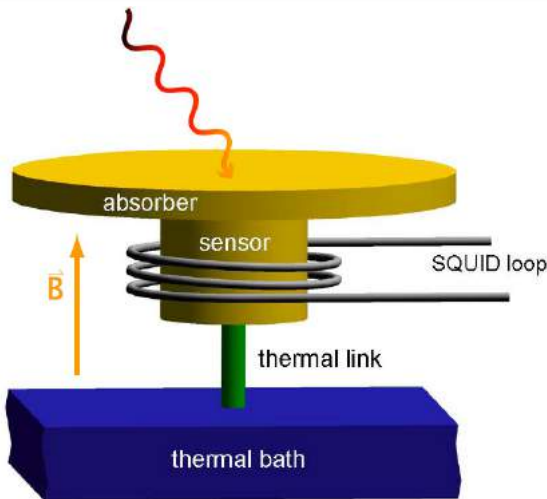


Fast risetime
→ Reduction un-resolved pile-up

Extremely good energy resolution
→ Reduced smearing in the end point region



Metallic magnetic calorimeters (MMCs)



Fast risetime

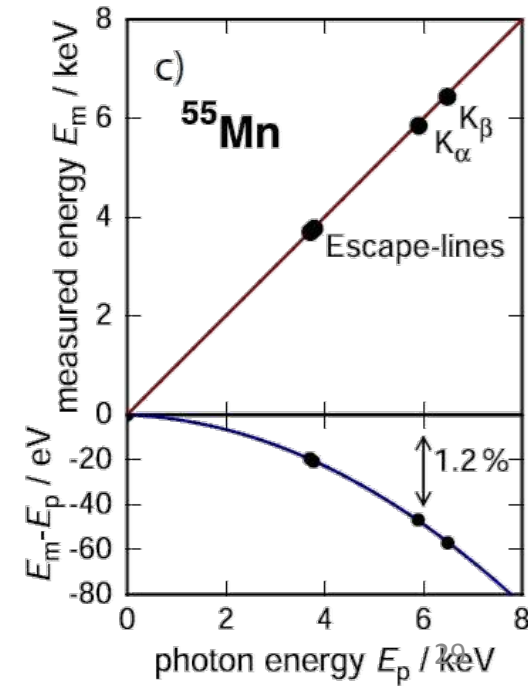
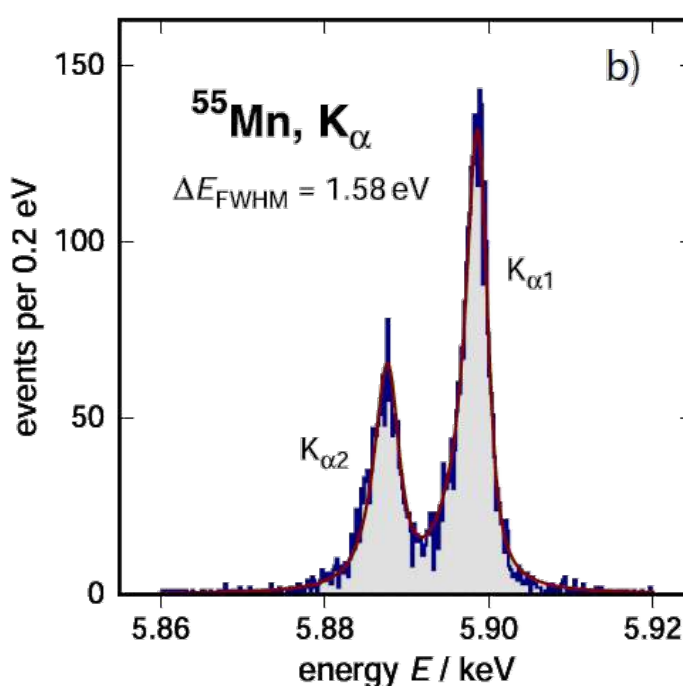
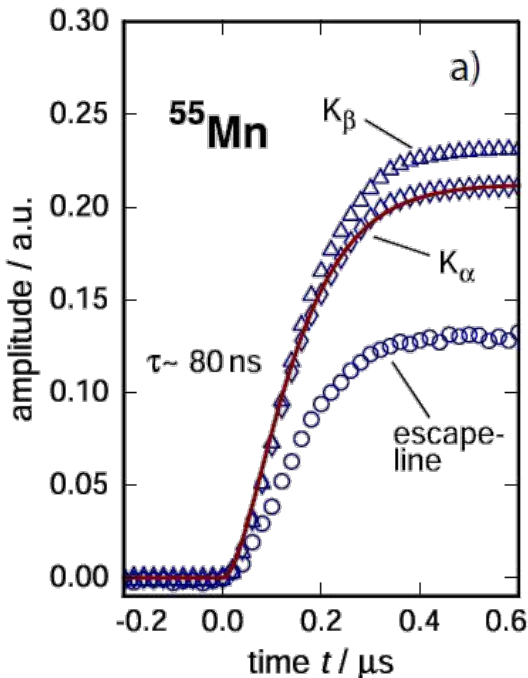
→ Reduction un-resolved pile-up

Extremely good energy resolution

→ Reduced smearing in the end point region

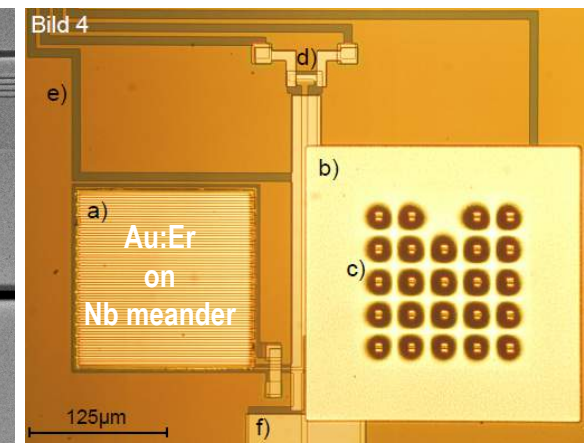
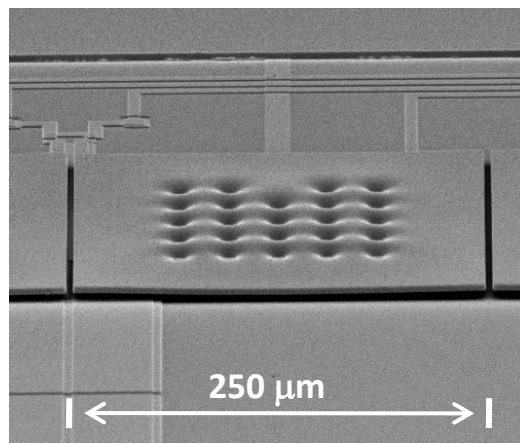
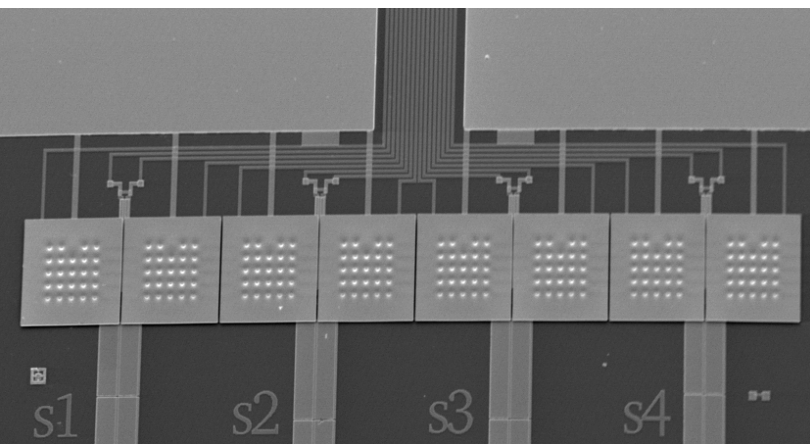
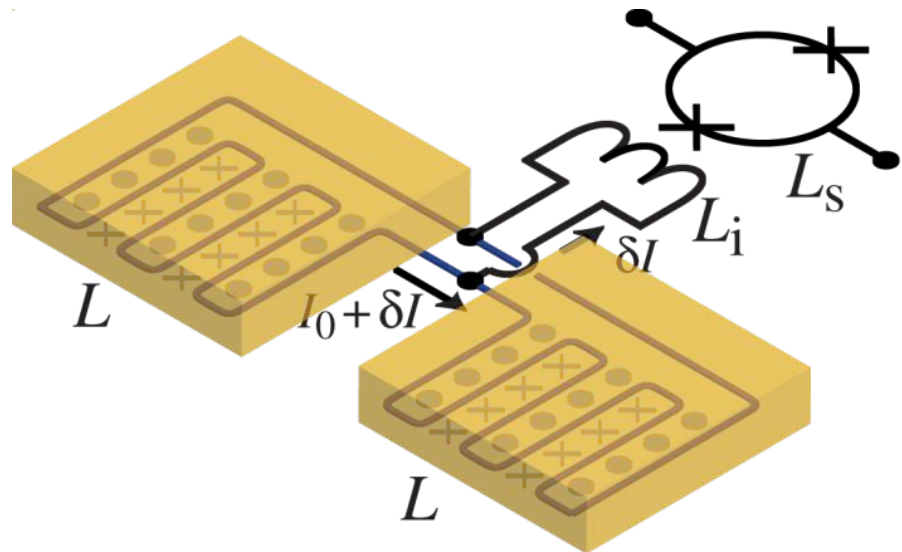
Excellent linearity

→ precise definition of the energy scale



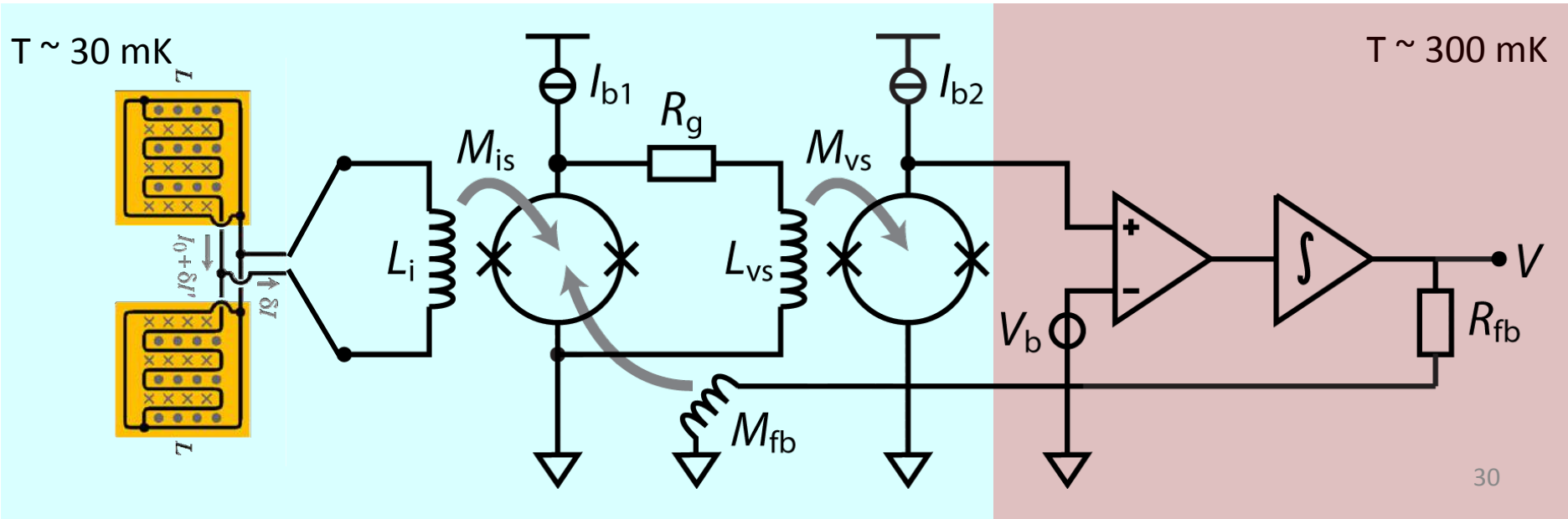
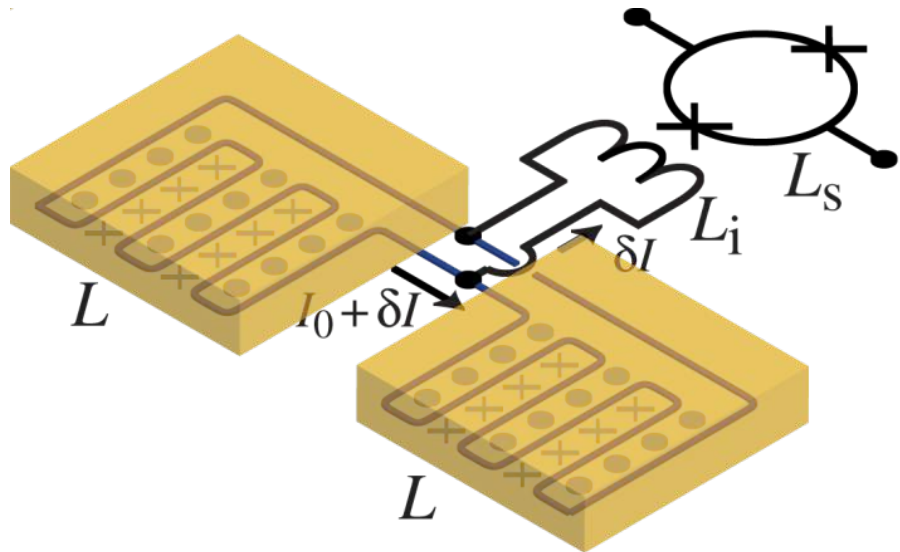
MMC geometry and read-out

- Planar temperature sensor
- B-field generated by persistent current



MMC geometry and read-out

- Planar temperature sensor
 - B-field generated by persistent current
 - transformer coupled to SQUID
-
- Two-stage SQUID read-out

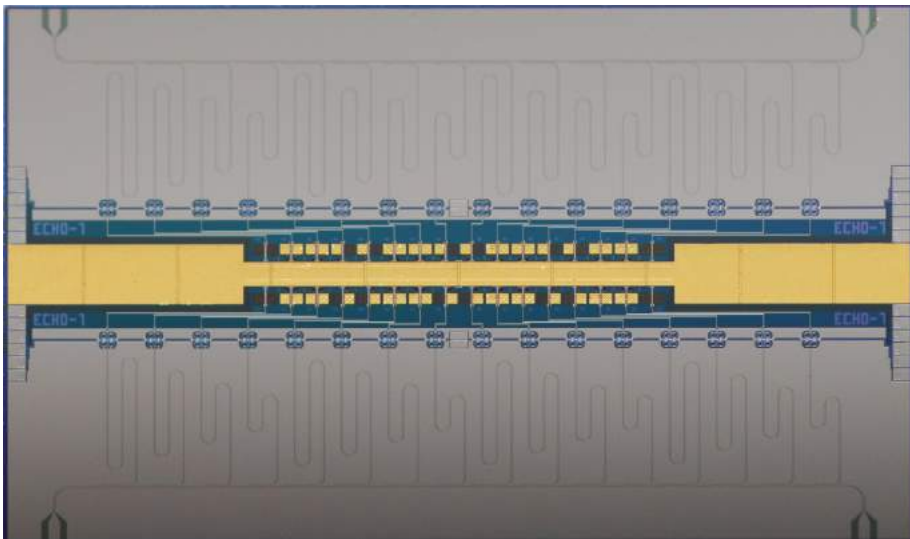


Multiplexing readout

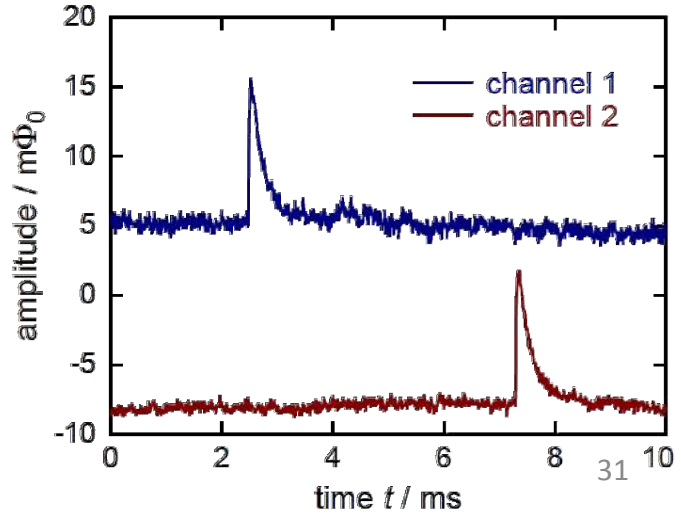
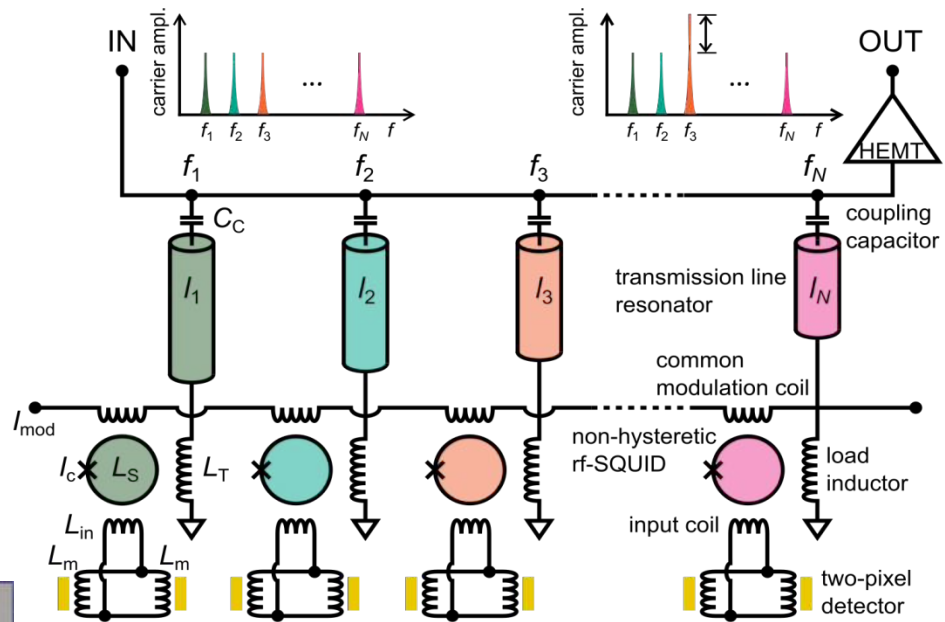
Microwave SQUID multiplexing

Single HEMT amplifier and 2 coaxes
to read out **100 - 1000** detectors

- Reliable fabrication of **64-pixel array**
- Successful characterization of first prototypes
→ optimization of design parameters

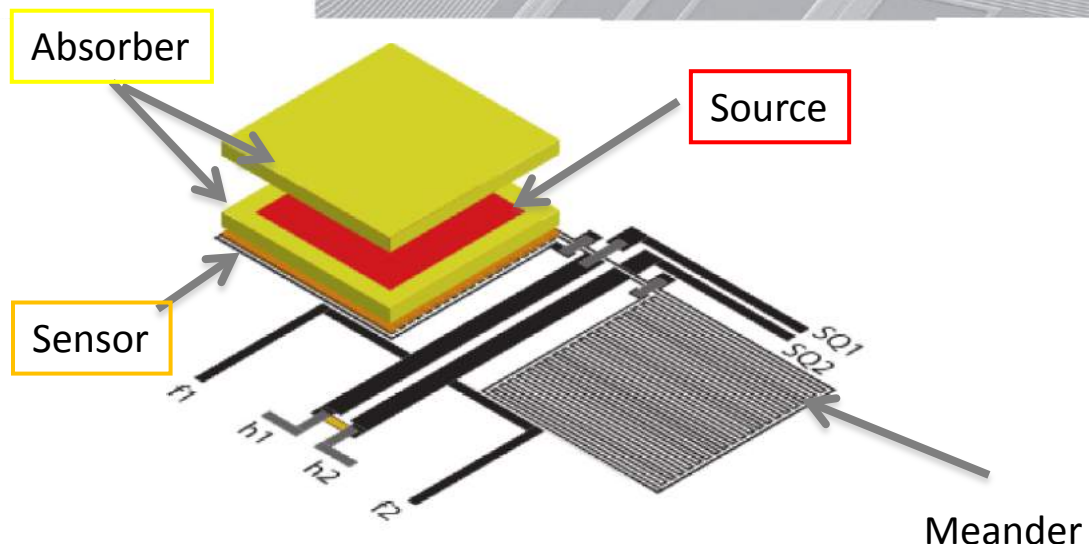
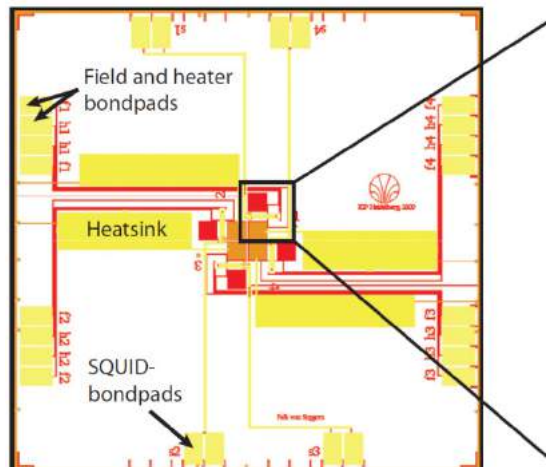
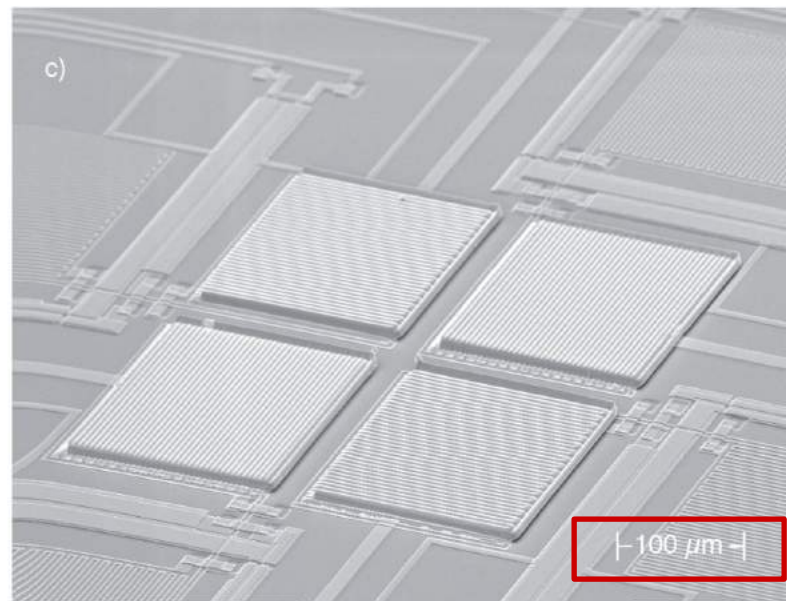


Microwave SQUID Multiplexer for the Readout of Metallic Magnetic Calorimeters
S.Kempf et al., J. Low. Temp. Phys. 175 (2014) 850-860



First detector prototype for ^{163}Ho – ECHo-0

- Absorber for calorimetric measurement
→ ion implantation @ ISOLDE-CERN in 2009
on-line process
- About 0.01 Bq per pixel
- Operated over more than 4 years

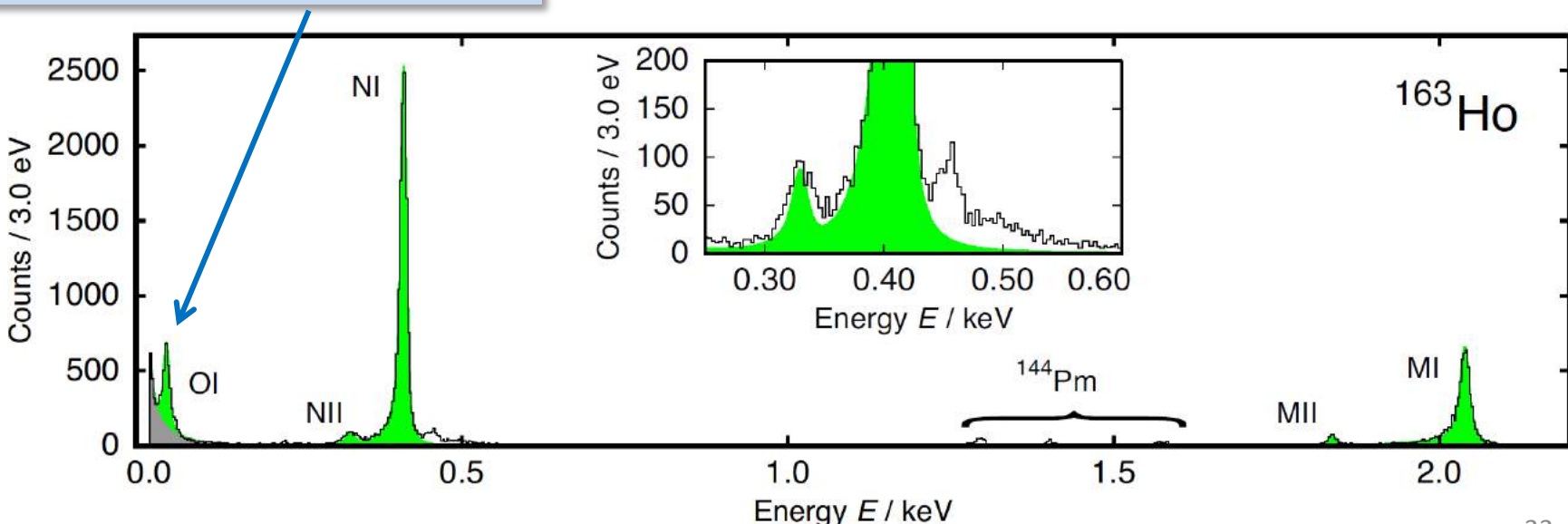


Calorimetric spectrum

- Rise Time ~ 130 ns
- $\Delta E_{\text{FWHM}} = 7.6$ eV @ 6 keV (2013)
- Non-Linearity < 1% @ 6keV

	E_{H} bind.	E_{H} exp.	Γ_{H} lit.	Γ_{H} exp
MI	2.047	2.040	13.2	13.7
MII	1.845	1.836	6.0	7.2
NI	0.420	0.411	5.4	5.3
NII	0.340	0.333	5.3	8.0
OI	0.050	0.048	5.0	4.3

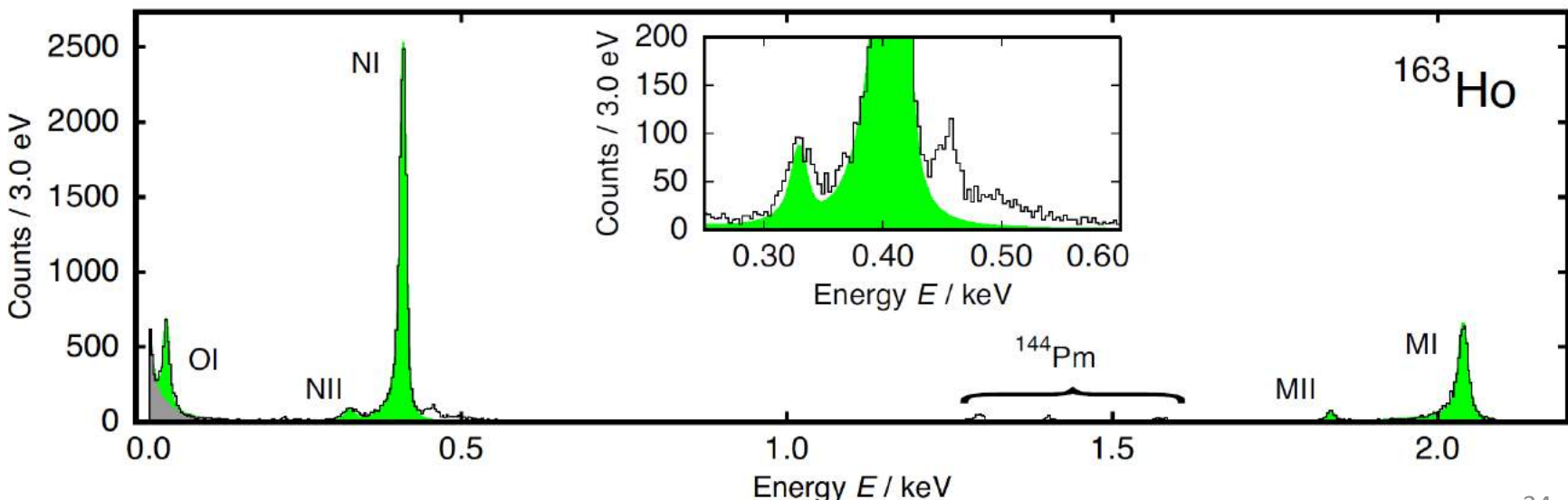
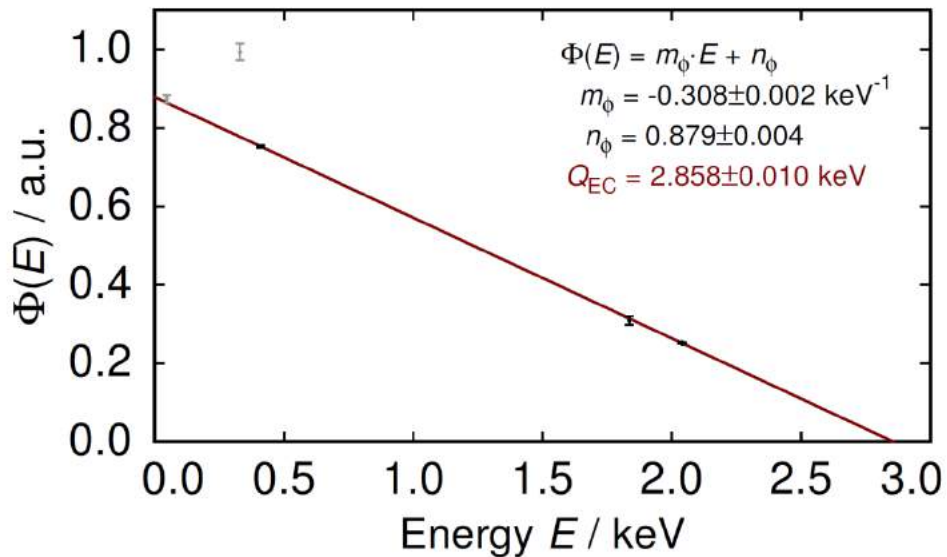
First calorimetric measurement
of the OI-line



Q_{EC} determination

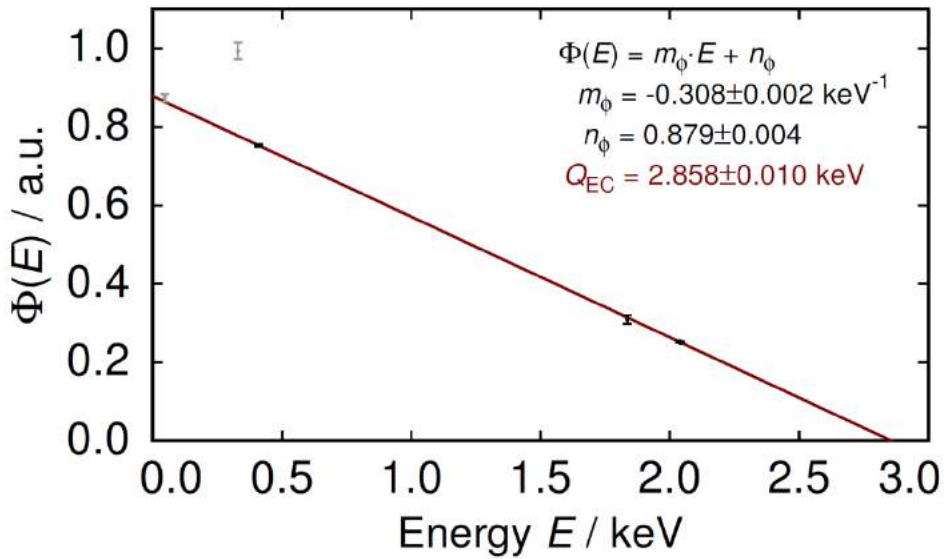
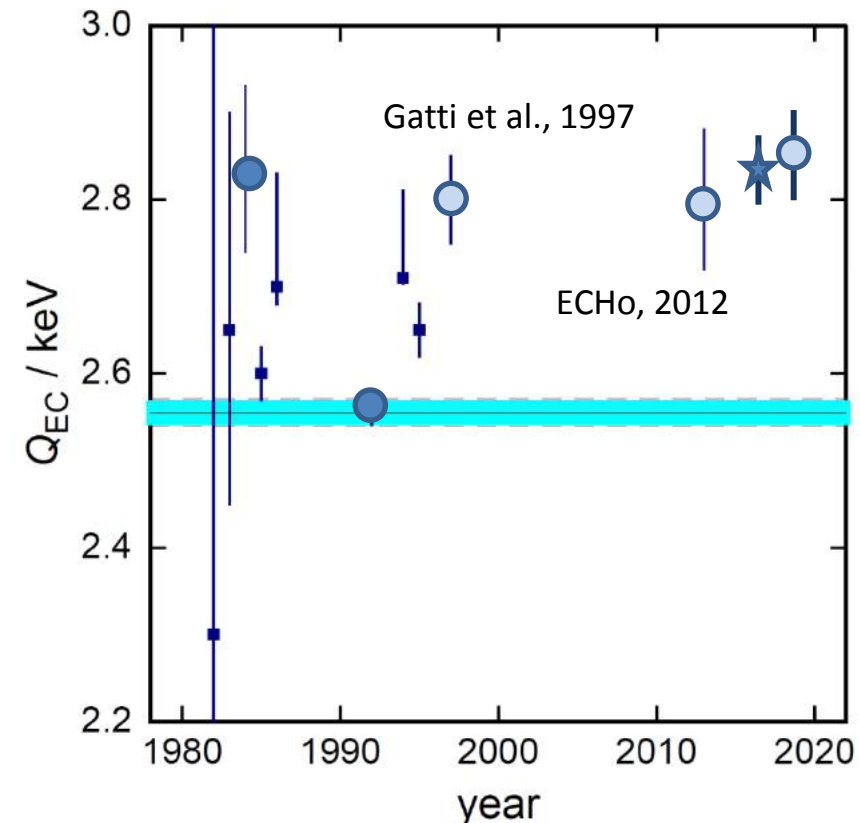
$$\Phi_H(E) = \sqrt{\frac{n_H}{\varphi_H^2(0)B_H}} \propto \sqrt{C}(Q_{EC} - E_H)$$

Line amplitudes are affected by the phase space factor



Q_{EC} determination

$$\Phi_H(E) = \sqrt{\frac{n_H}{\varphi_H^2(0)B_H}} \propto \sqrt{C}(Q_{EC} - E_H)$$



Our result:

$$Q_{EC} = (2.858 \pm 0.010^{\text{stat}} \pm 0.05^{\text{syst}}) \text{ keV}$$

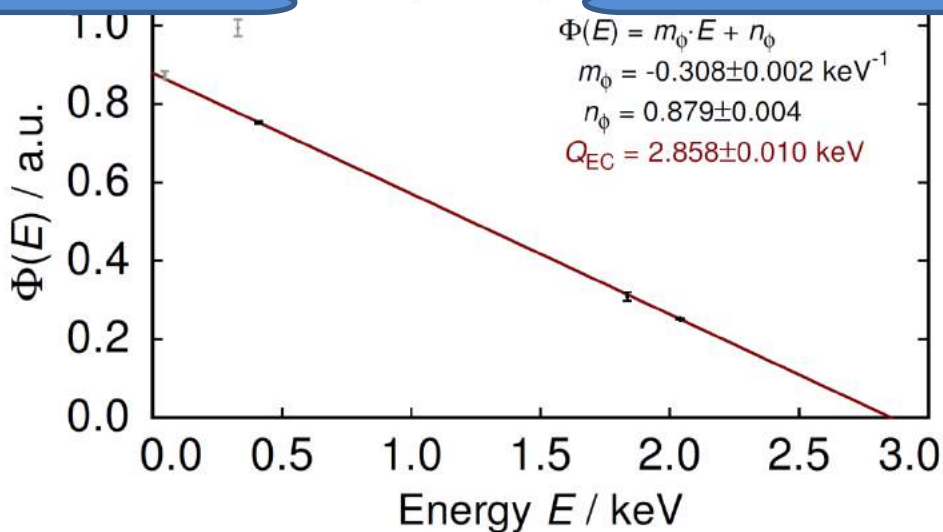
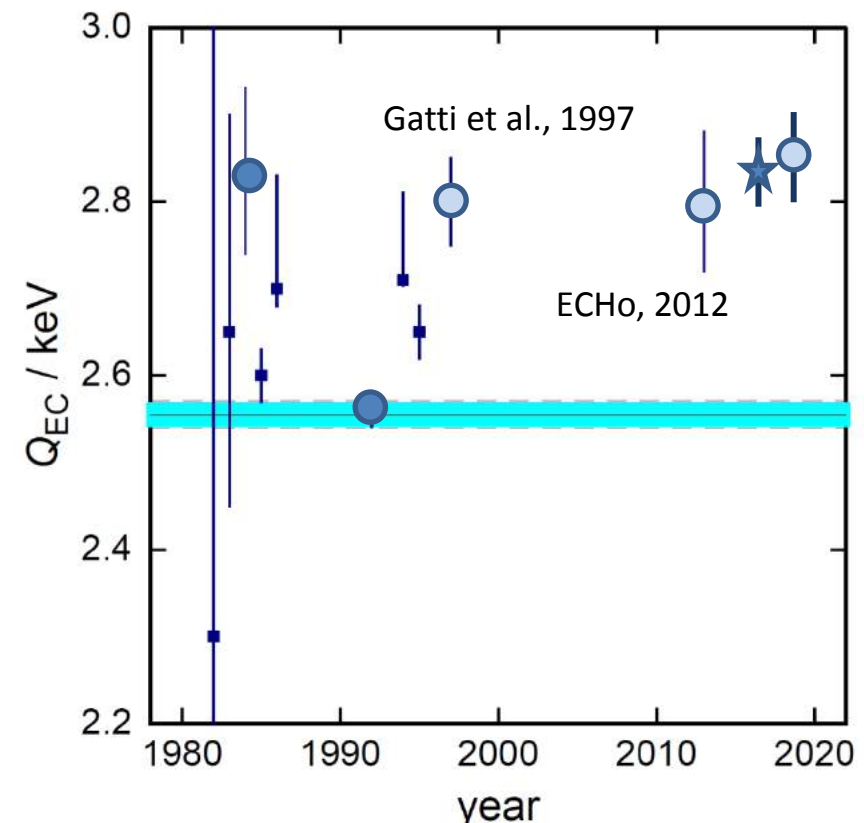
Penning Trap Mass Spectrometry result:

$$Q_{EC} = (2.833 \pm 0.030^{\text{stat}} \pm 0.015^{\text{syst}}) \text{ keV}$$

Q_{EC} determination

$$\Phi_H(E) = \sqrt{\frac{n_H}{\varphi_H^2(0)B_H}} \propto \sqrt{C}(Q_{EC} - E_H)$$

Good agreement between
the two measurements



Our result:

$$Q_{EC} = (2.858 \pm 0.010^{\text{stat}} \pm 0.05^{\text{syst}}) \text{ keV}$$

Penning Trap Mass Spectrometry result:

$$Q_{EC} = (2.833 \pm 0.030^{\text{stat}} \pm 0.015^{\text{syst}}) \text{ keV}$$



Scaling up

ECHo-1k (2015 - 2018)

^{163}Ho activity: $A_t = 1 \text{ kBq}$

Detectors: Metallic Magnetic Calorimeters

→ Energy resolution $\Delta E_{\text{FWHM}} \leq 5 \text{ eV}$

→ Time resolution $\tau \leq 1 \mu\text{s}$

Unresolved pile-up fraction $f_{\text{pu}} \leq 10^{-5}$

→ activity per pixel: $A = 10 \text{ Bq}$

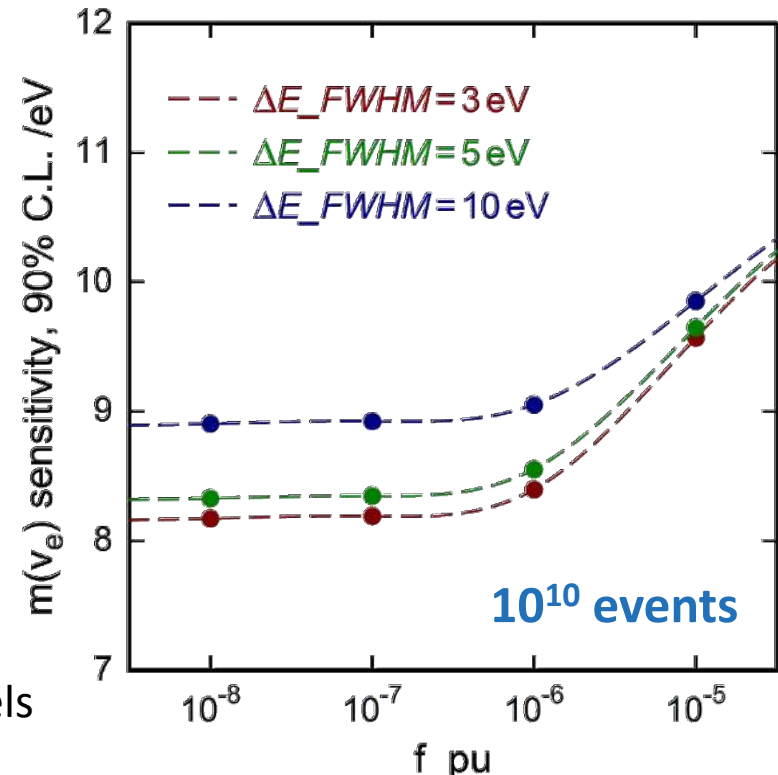
→ number of detectors $N = 100$

Read-out : Parallel read-out: 1 array ~50 single pixels

→ Demonstrate Microwave SQUID Multiplexing

Background $b < 10^{-5} / \text{eV/det/day}$

Measuring time $t = 1 \text{ year}$



$$m(v_e) < 10 \text{ eV} \text{ 90% C.L.}$$

ECHo-1M (next future)

^{163}Ho activity: $A_t = 1 \text{ MBq}$

Detectors: Metallic Magnetic Calorimeters

→ Energy resolution $\Delta E_{\text{FWHM}} \leq 3 \text{ eV}$

→ Time resolution $\tau \leq 0.1 \mu\text{s}$

Unresolved pile-up fraction $f_{\text{pu}} \leq 10^{-6}$

→ activity per pixel: $A = 10 \text{ Bq}$

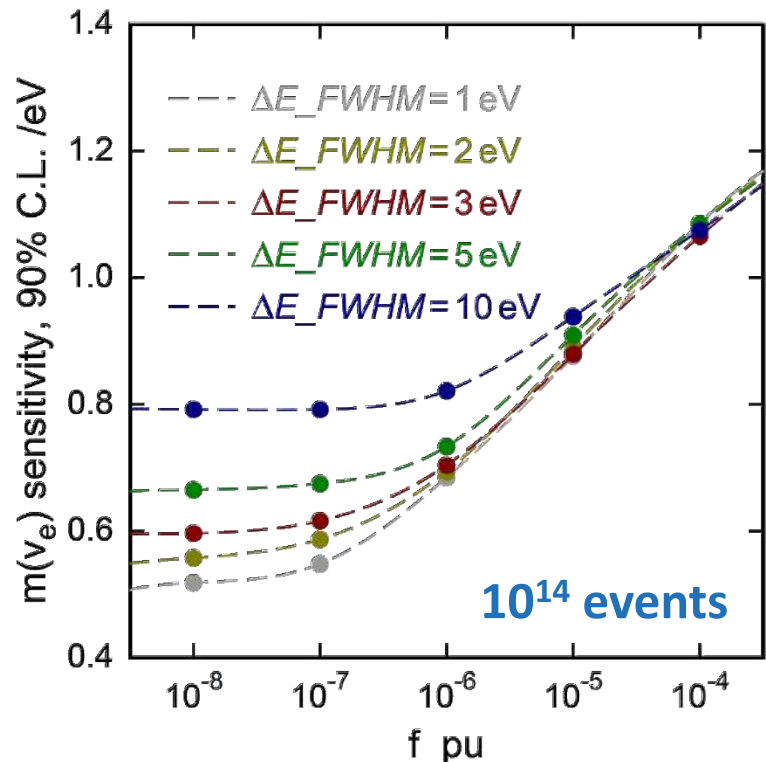
→ number of detectors $N = 10^5$

Read-out : Microwave SQUID Multiplexing

→ 100 arrays with ~1000 single pixels

Background $b < 10^{-6} / \text{eV/det/day}$

Measuring time $t = 1 - 3 \text{ year}$



$m(v_e) < 1 \text{ eV} \text{ 90% C.L.}$

^{163}Ho high purity source

Required activity in the detectors: Final experiment $\rightarrow >10^6 \text{ Bq} \rightarrow >10^{17} \text{ atoms}$

- Neutron irradiation
 (n,γ) -reaction on ^{162}Er

High cross-section



Radioactive contaminants



Er161 3.21 h 3/2-	Er162 0+ EC 0.14	Er163 75.0 m 5/2+ EC	Er164 0+ EC 1.61	Er165 10.36 h 5/2- EC	Er166 0+ 33.6
Ho160 25.6 m 5+ EC *	Ho161 2.48 h 7/2- EC *	Ho162 15.0 m 1+ EC *	Ho163 0.70 y 2- EC *	Ho164 29 m 1+ EC, β^- *	Ho165 7/2- 100
Dy159 144.4 d 3/2- EC	Dy160 0+ 2.34	Dy161 5/2+ 18.9	Dy162 0+ 25.5	Dy163 5/2- 24.9	Dy164 0+ 28.2
Tb158 180 y 3- EC, β^- *	Tb159 3/2+ 100	Tb160 72.3 d 3- β^-	Tb161 6.88 d 3/2+ β^-	Tb162 7.60 m 1- β^-	Tb163 19.5 m 3/2+ β^-

^{163}Ho high purity source

Required activity in the detectors: Final experiment $\rightarrow >10^6 \text{ Bq} \rightarrow >10^{17} \text{ atoms}$

- Neutron irradiation
 (n,γ) -reaction on ^{162}Er

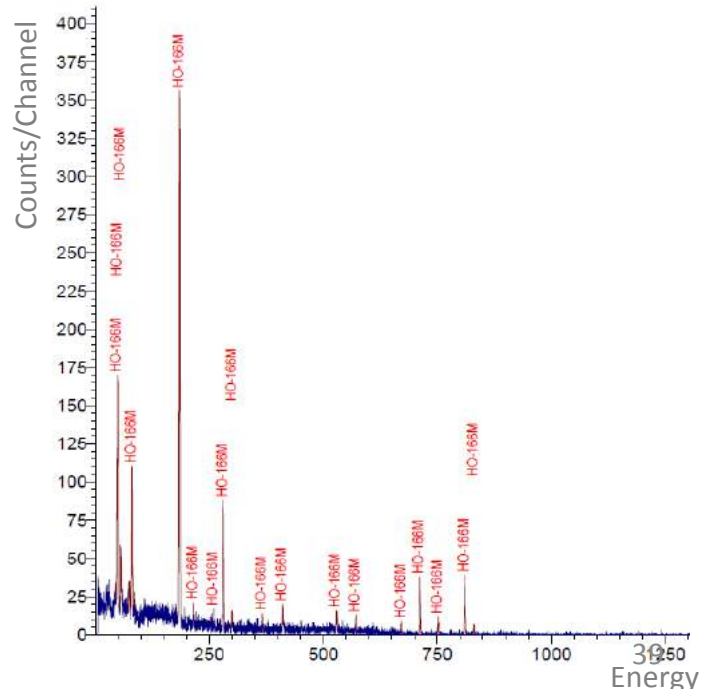
High cross-section

Radioactive contaminants

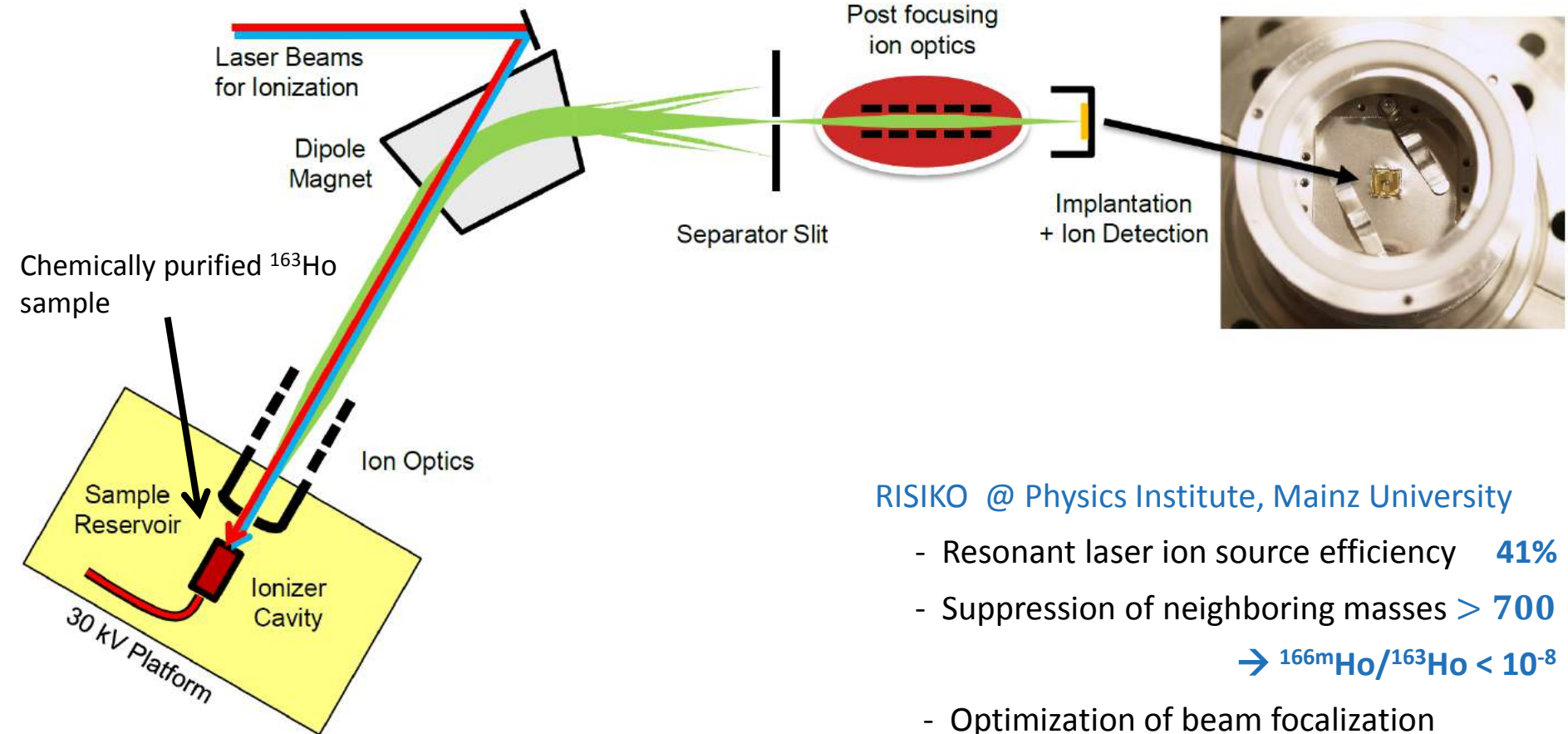


Excellent chemical separation

Er161 3.21 h 3/2-	Er162 0+ EC 0.14	Er163 75.0 m 5/2+ EC	Er164 0+ EC 1.61	Er165 10.36 h 5/2- EC	Er166 0+ 33.6
Ho160 25.6 m 5+ EC *	Ho161 2.48 h 7/2- EC	Ho162 15.0 m 1+ EC *	Ho163 0.70 y 2- EC	Ho164 29 m 1+ EC, β^- *	Ho165 7/2- 100
Dy159 144.4 d 3/2- EC	Dy160 0+ 2.34	Dy161 5/2+ 18.9	Dy162 0+ 25.5	Dy163 5/2- 24.9	Dy164 0+ 28.2
Tb158 180 y 3- EC, β^- 100	Tb159 3/2+ 100	Tb160 72.3 d 3- β^-	Tb161 6.88 d 3/2+ β^-	Tb162 7.60 m 1- β^-	Tb163 19.5 m 3/2+ β^-



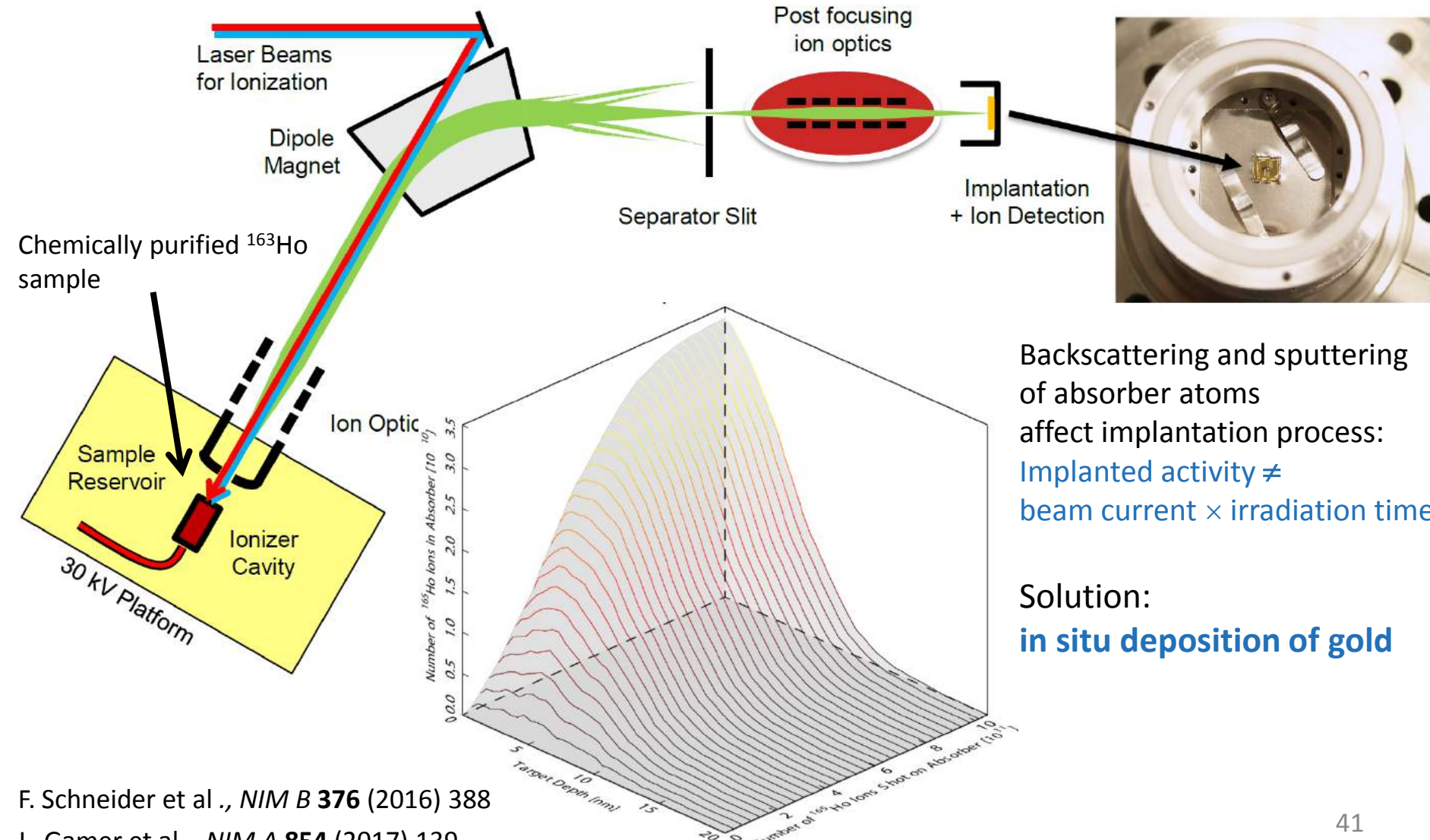
Mass separation and ^{163}Ho ion-implantation



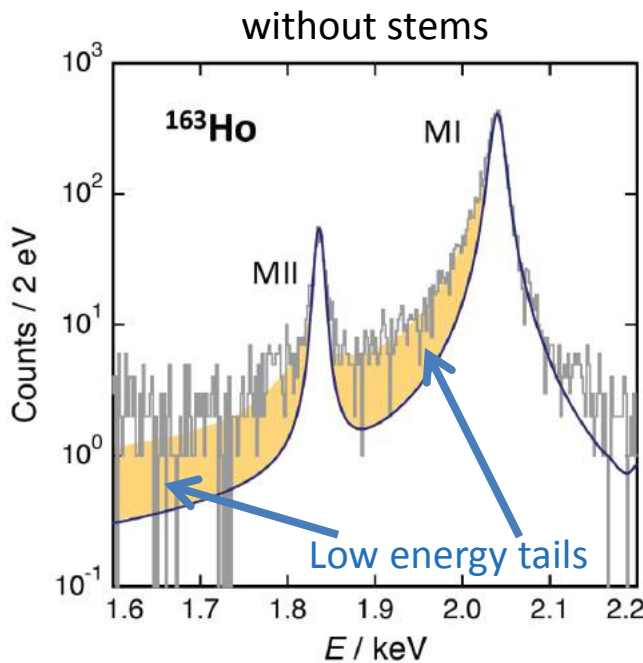
RISIKO @ Physics Institute, Mainz University

- Resonant laser ion source efficiency **41%**
- Suppression of neighboring masses > 700
→ $^{166\text{m}}\text{Ho}/^{163}\text{Ho} < 10^{-8}$
- Optimization of beam focalization

Mass separation and ^{163}Ho ion-implantation

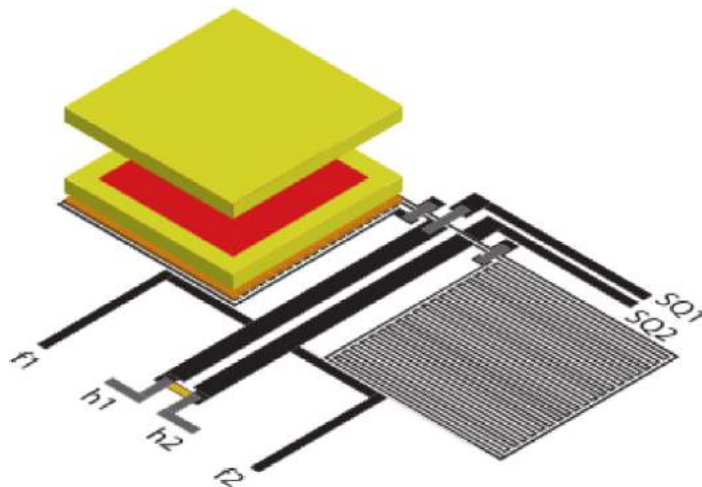


Enclosing ^{163}Ho in MMC absorbers

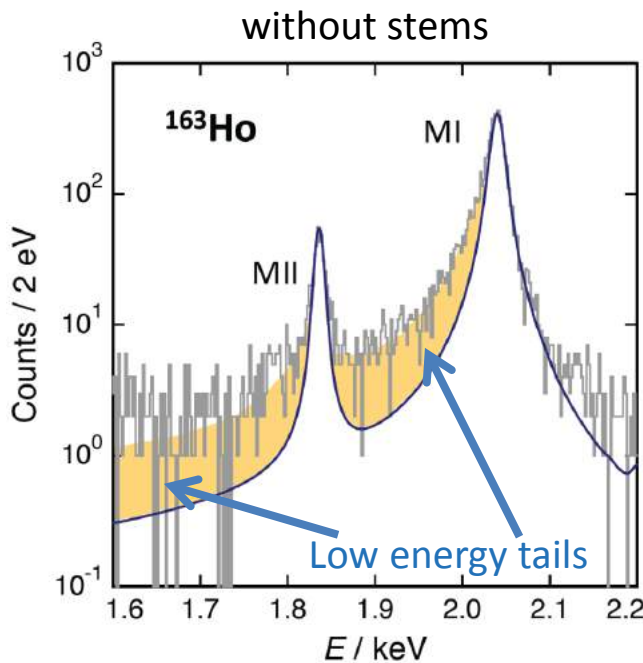


ECHO-0 detector showed [asymmetric detector response](#)

- Loss of high energy phonons to the substrate
- full contact between sensor and absorber



Enclosing ^{163}Ho in MMC absorbers



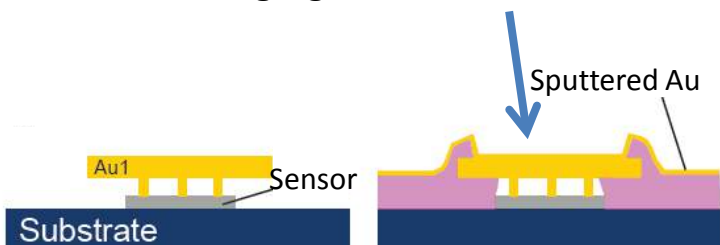
ECHO-0 detector showed **asymmetric detector response**

- Loss of high energy phonons to the substrate
- full contact between sensor and absorber

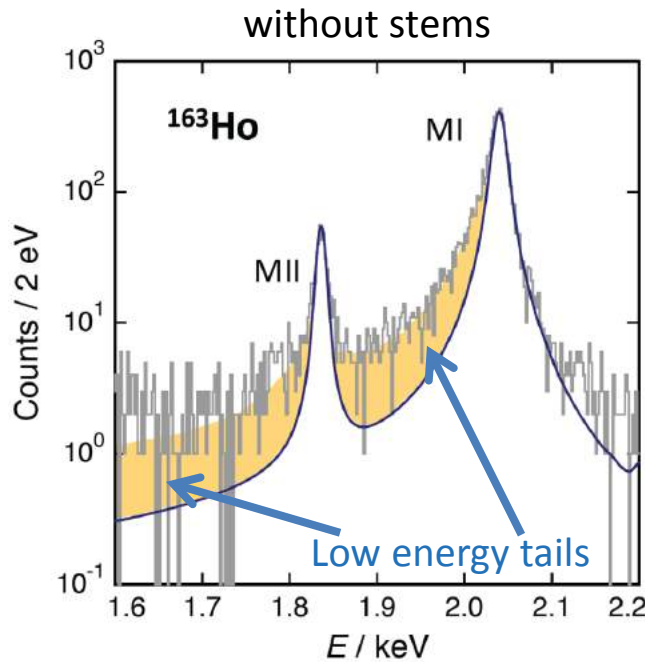
→ **New detector fabrication process**

reduced contact area between absorber and sensor

Definition of the **implantation area** by microstructuring a photoresist layer on overhanging absorbers



Enclosing ^{163}Ho in MMC absorbers

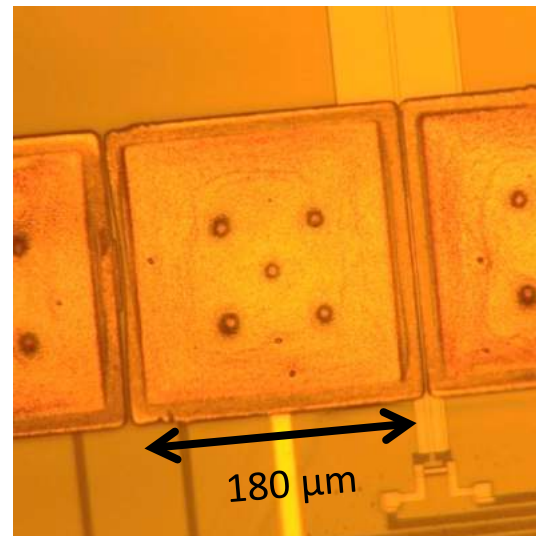
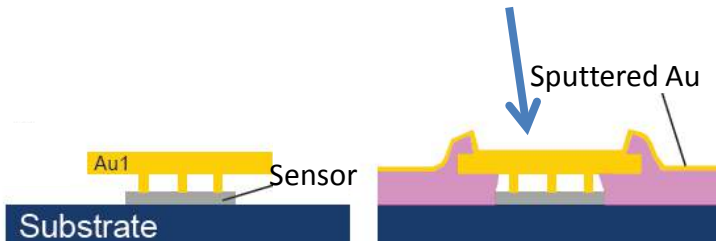


ECHO-0 detector showed asymmetric detector response

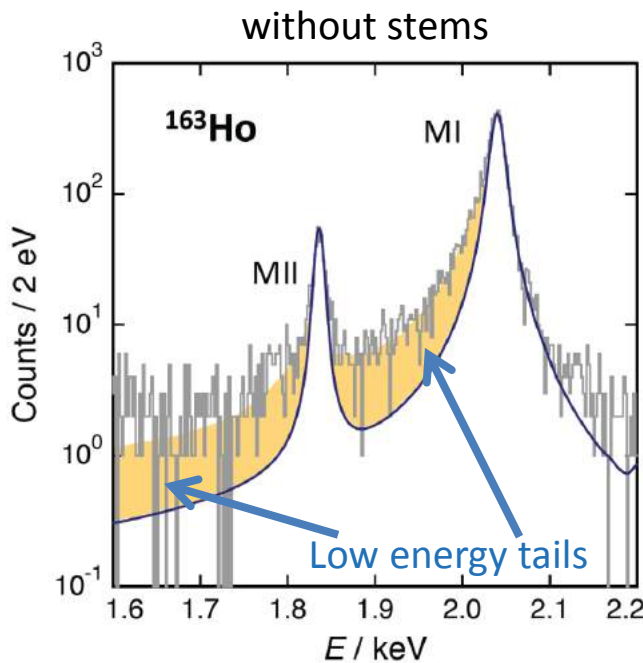
- Loss of high energy phonons to the substrate
- full contact between sensor and absorber

→ New detector fabrication process
reduced contact area between absorber and sensor

Definition of the implantation area by microstructuring a photoresist layer on overhanging absorbers



Enclosing ^{163}Ho in MMC absorbers



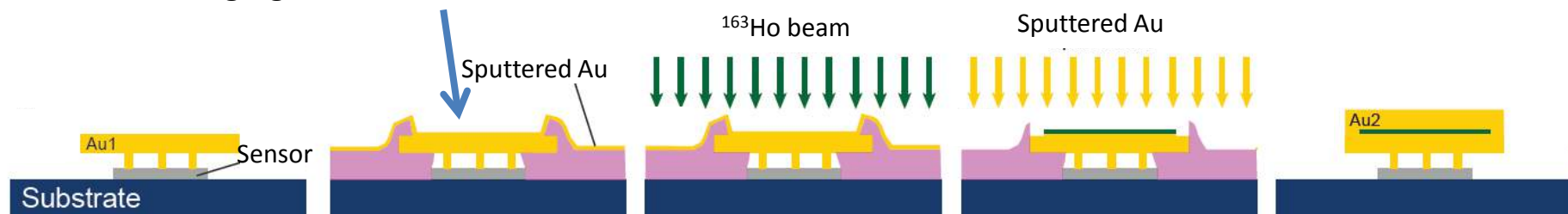
ECHO-0 detector showed asymmetric detector response

- Loss of high energy phonons to the substrate
- full contact between sensor and absorber

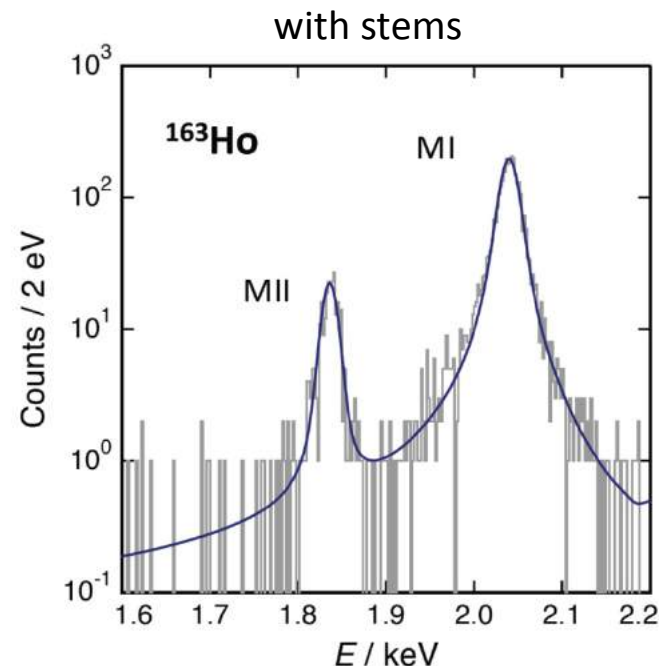
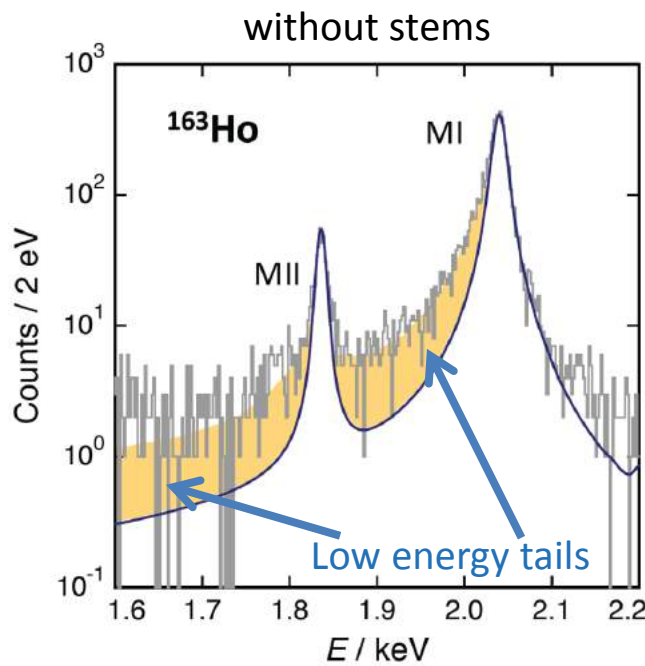
→ New detector fabrication process

reduced contact area between absorber and sensor

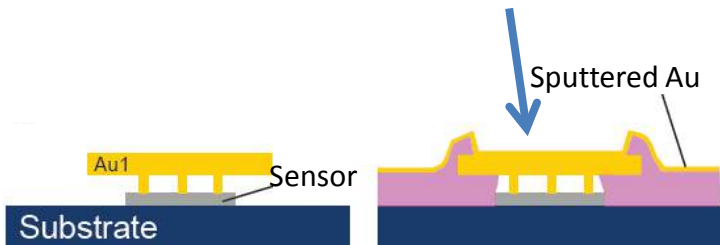
Definition of the implantation area by microstructuring a photoresist layer on overhanging absorbers



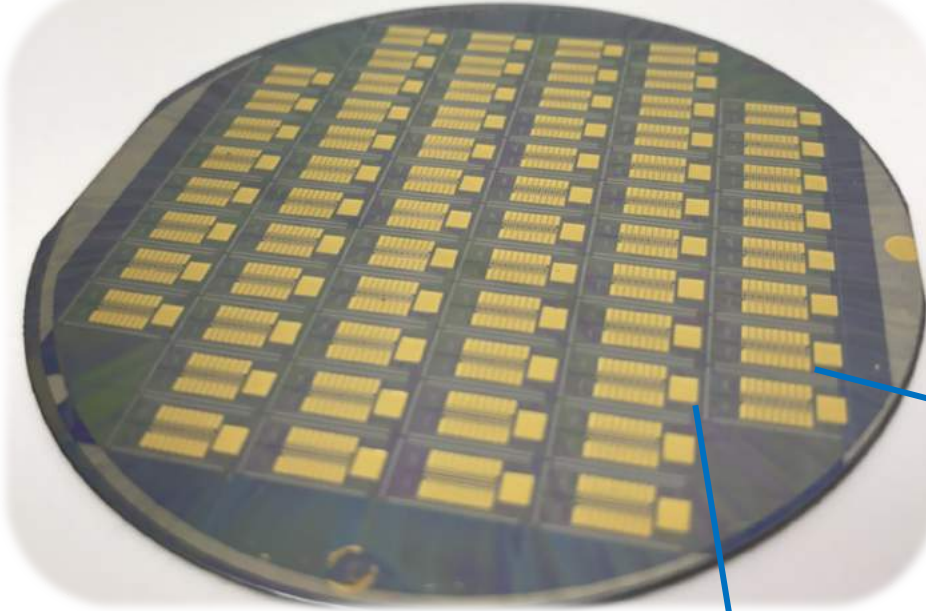
Enclosing ^{163}Ho in MMC absorbers



Definition of the **implantation area** by microstructuring a photoresist layer on overhanging absorbers



ECHO-1k array



3“ wafer with 64 ECHO-1k chip

Suitable for
parallel and multiplexed readout

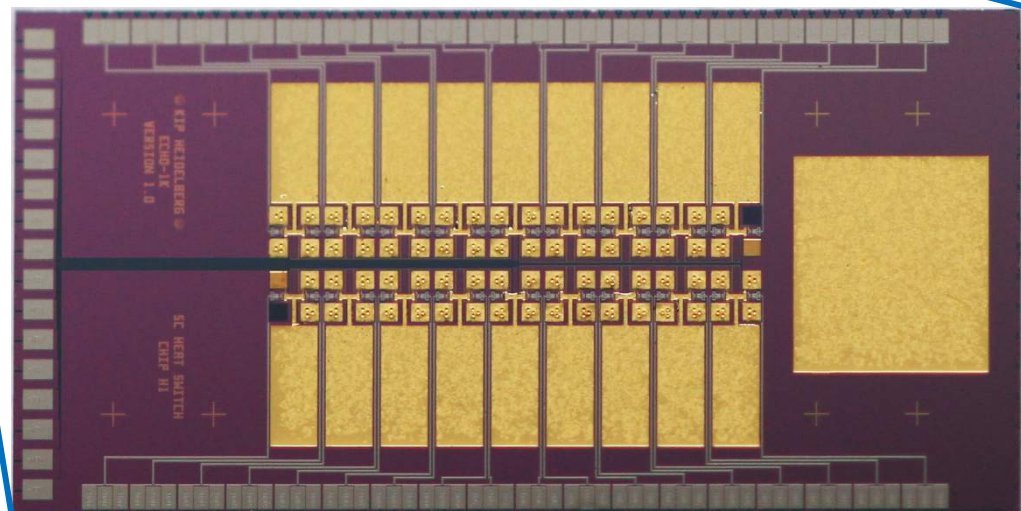
64 pixels which can be loaded with ^{163}Ho
+ 4 detectors for diagnostics

Design performance:

$\Delta E_{\text{FWHM}} \sim 5 \text{ eV}$

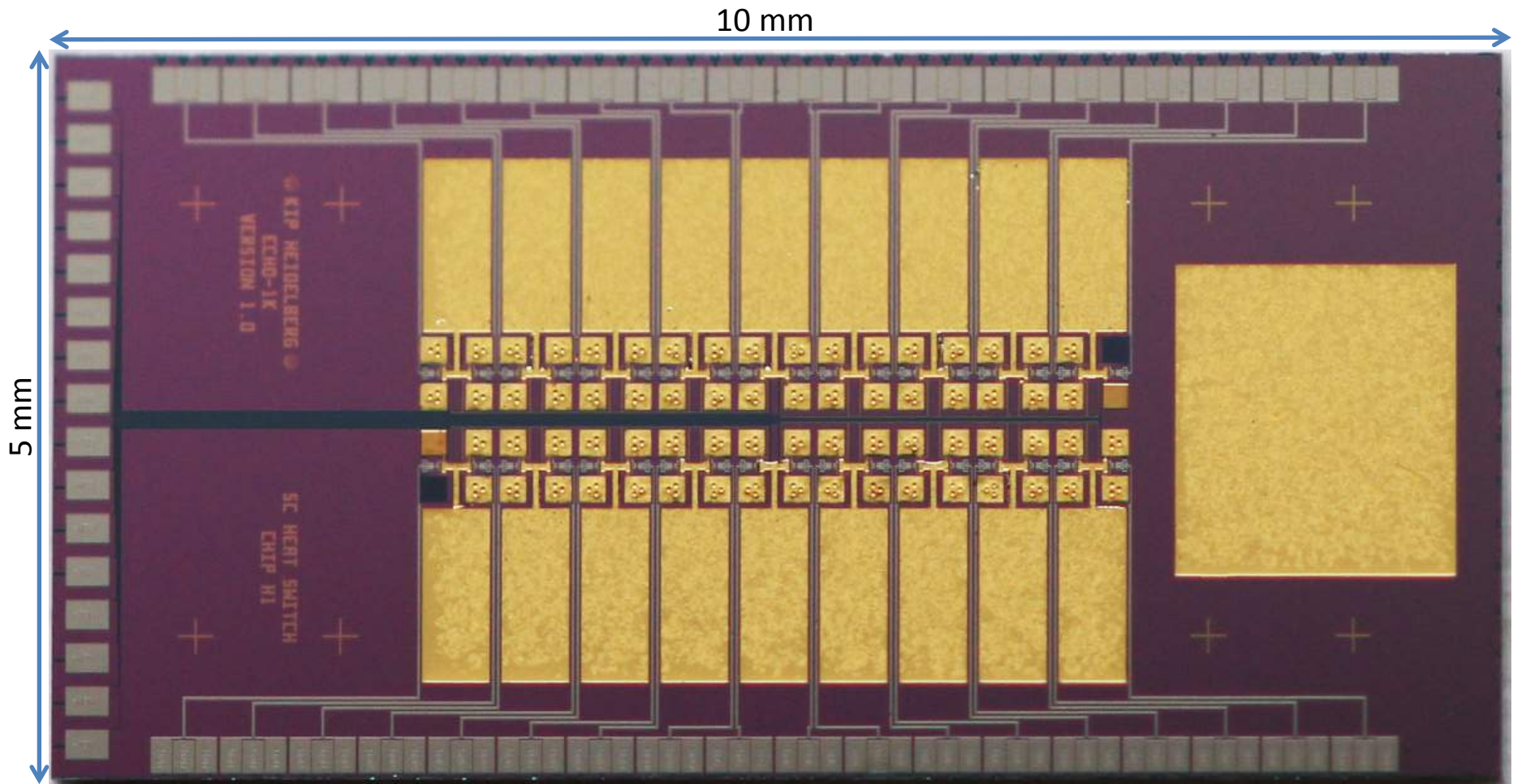
$\tau_r \sim 90 \text{ ns}$ (single channel readout)

$\tau_r \sim 300 \text{ ns}$ (multiplexed read-out)



ECHO-1k array

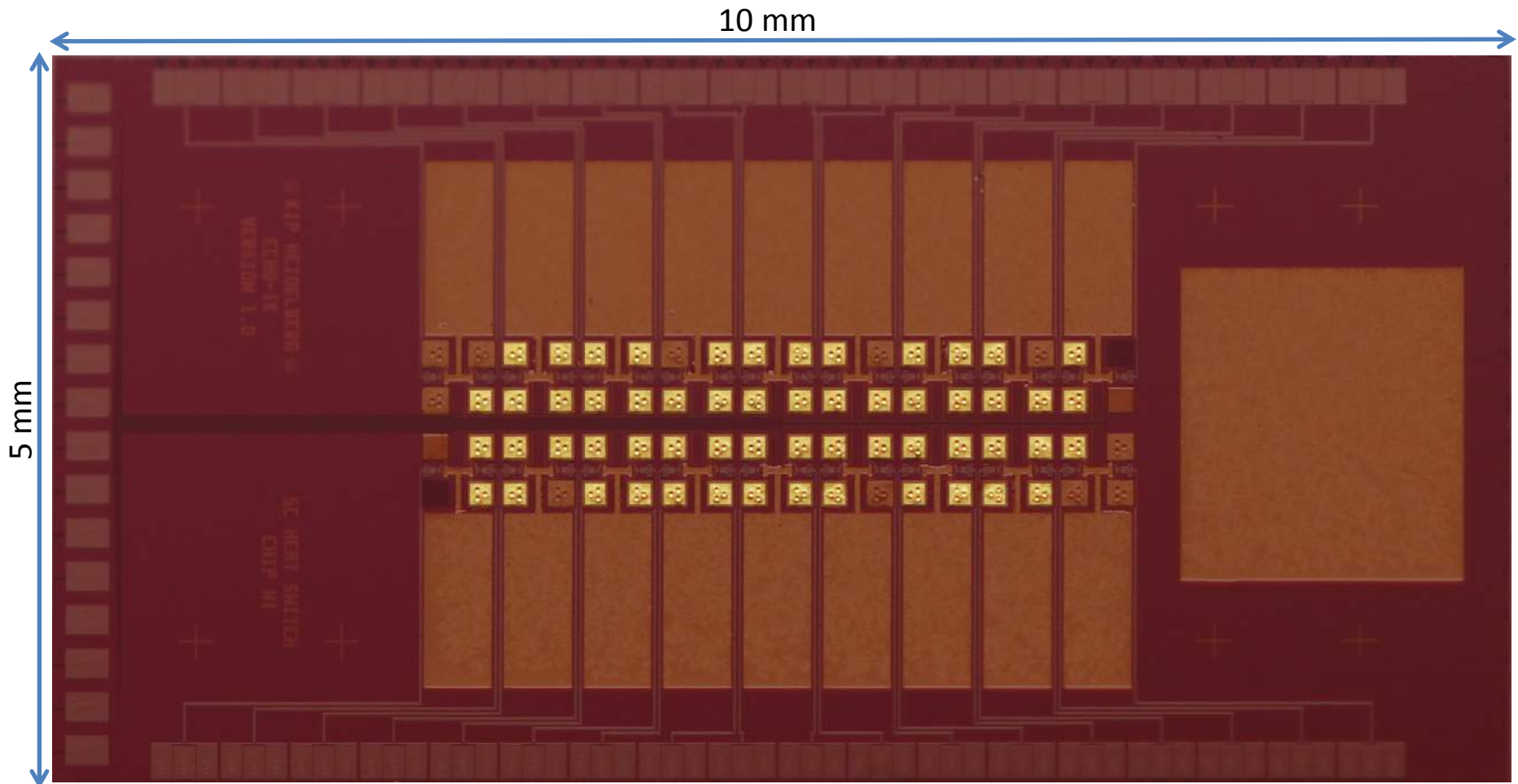
100% of the chips selected at RT have good performance at low temperature



ECHo-1k array

high geometrical efficiency for ^{163}Ho implantation

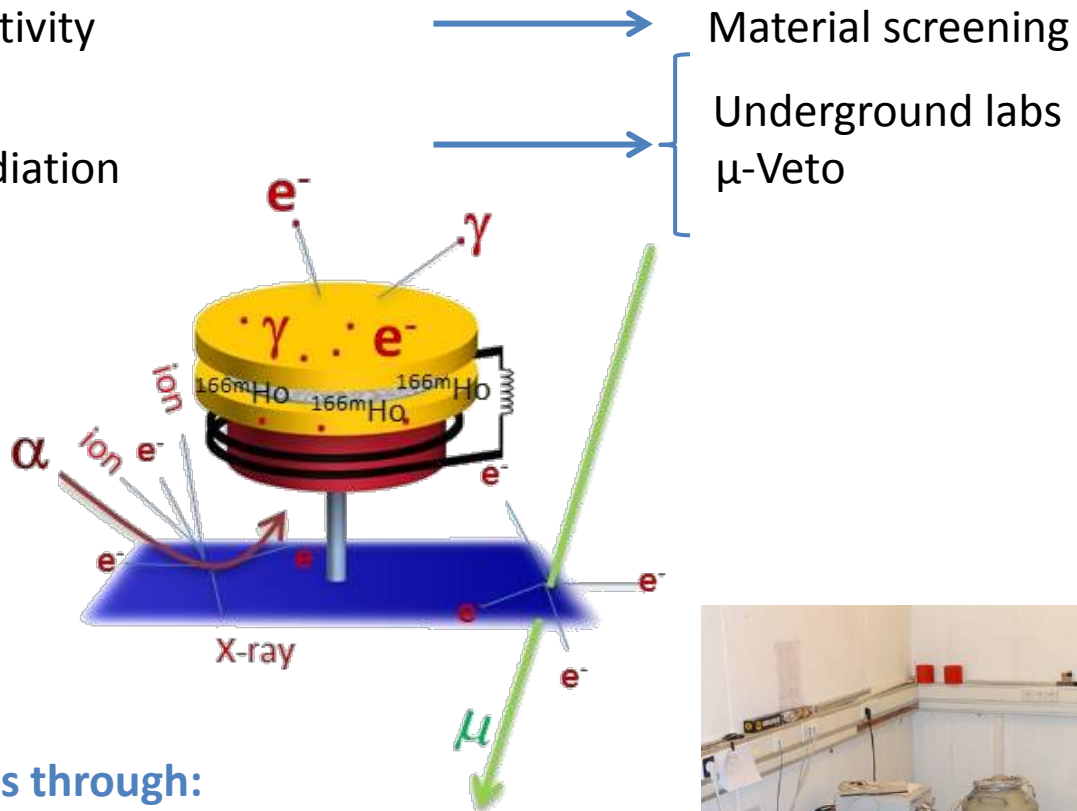
presence of non-implanted chips for in-situ background determination



Background in ECHo

Background sources:

- Radioactivity in the detector
- Environmental radioactivity
- Cosmic rays
- Induced secondary radiation



Study of background sources through:

- Monte Carlo simulations
- Dedicated experiments

Screening facilities

- Uni-Tübingen
- Felsenkeller



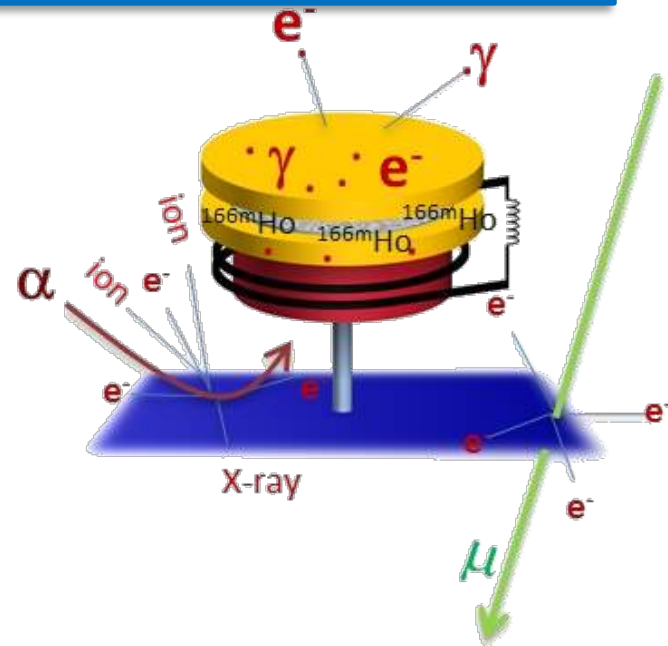
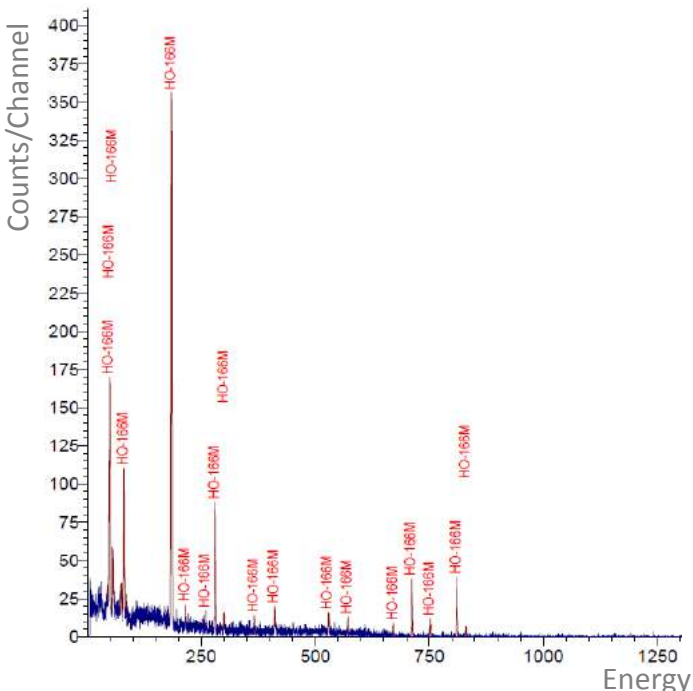
Background in ECHO

Background sources:

- **Radioactivity in the detector**
presence of ^{166m}Ho in Ho samples for implantation

RISIKO @ Physics Institute, Mainz University

$$\rightarrow {}^{166m}\text{Ho}/{}^{163}\text{Ho} < 10^{-8}$$



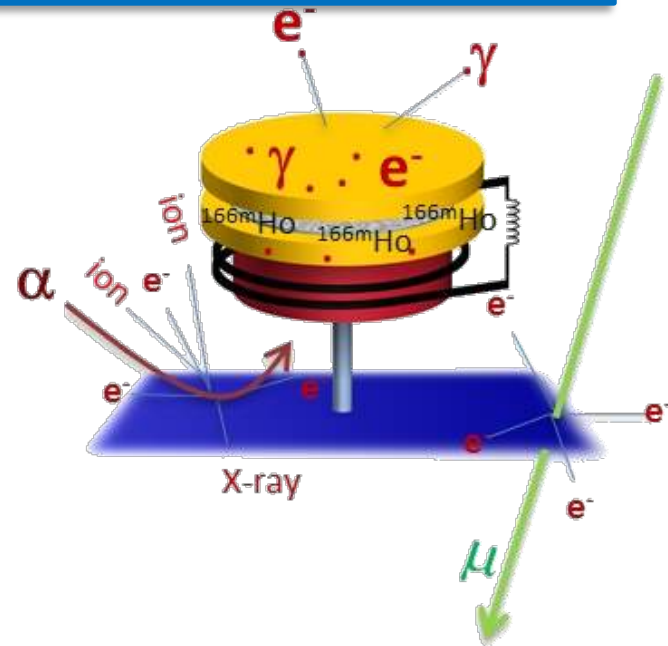
Background in ECHO

Background sources:

- **Radioactivity in the detector**
presence of ^{166m}Ho in Ho samples for implantation

RISIKO @ Physics Institute, Mainz University

$$\rightarrow {}^{166m}\text{Ho}/{}^{163}\text{Ho} < 10^{-8}$$



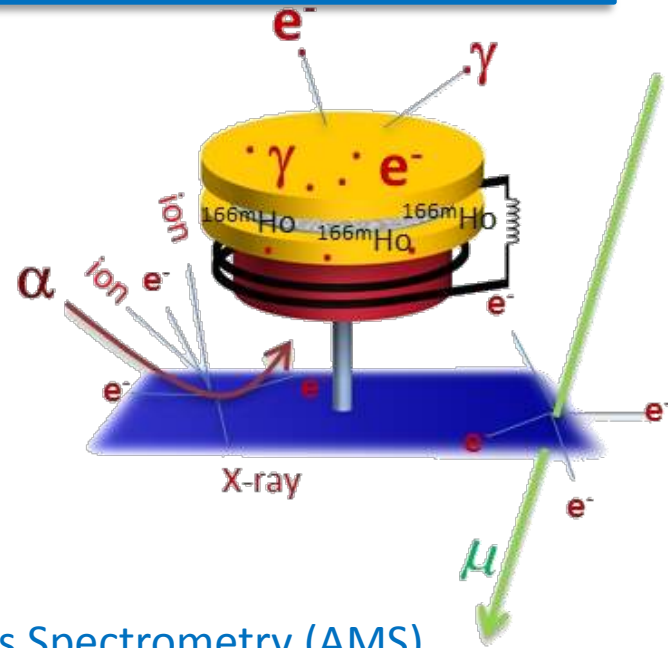
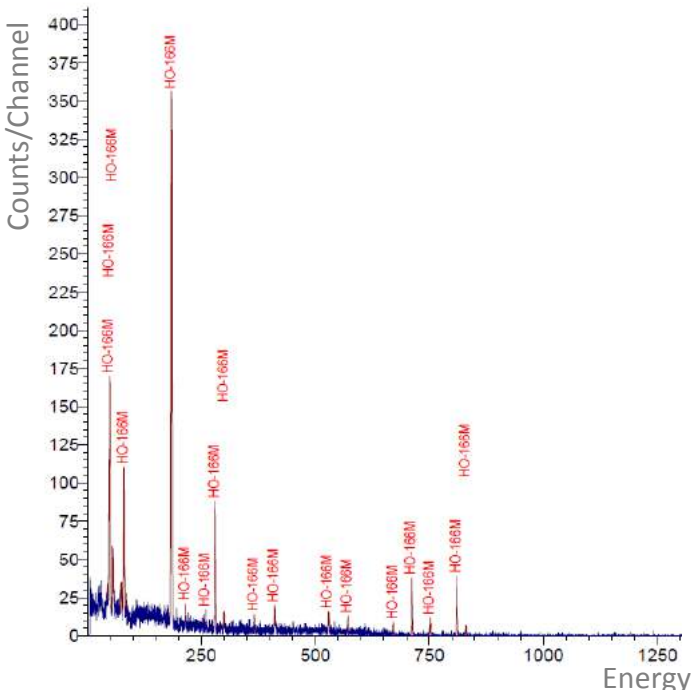
Background in ECHO

Background sources:

- **Radioactivity in the detector**
presence of ^{166m}Ho in Ho samples for implantation

RISIKO @ Physics Institute, Mainz University

$$\rightarrow {}^{166m}\text{Ho}/{}^{163}\text{Ho} < 10^{-8}$$



Accelerator Mass Spectrometry (AMS)
is a very powerful technique for measuring the corresponding very low isotopic ratio

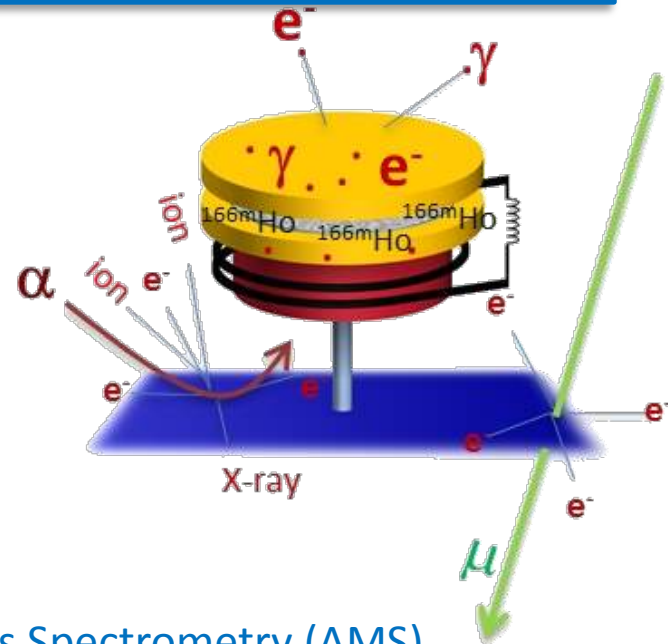
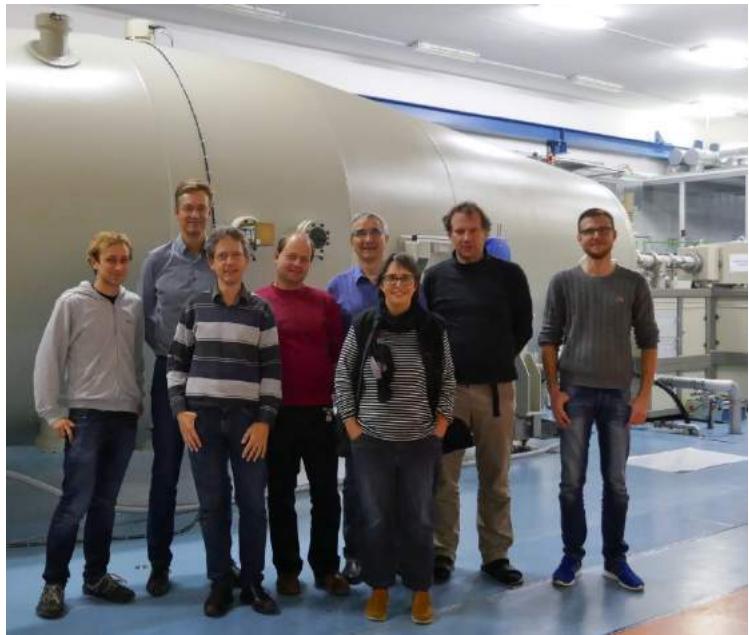
Background in ECHo

Background sources:

- **Radioactivity in the detector**
presence of ^{166m}Ho in Ho samples for implantation

RISIKO @ Physics Institute, Mainz University

$$\rightarrow {}^{166m}\text{Ho}/{}^{163}\text{Ho} < 10^{-8}$$



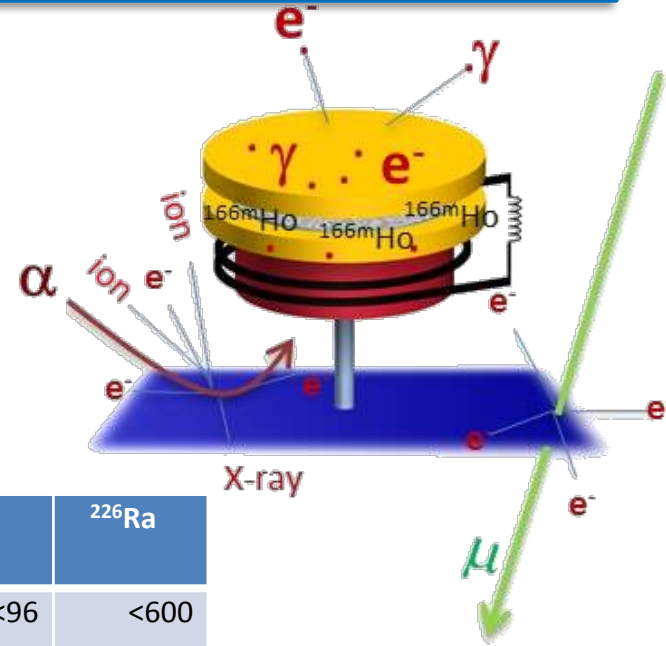
Accelerator Mass Spectrometry (AMS)
is a very powerful technique for measuring the
corresponding very low isotopic ratio

First tests at the [DREsdan AMS facility \(DREAMS\)](#)
at Helmholtz-Zentrum Dresden-Rossendorf
for experimental determination of the
ratio ${}^{163}\text{Ho}/{}^{166m}\text{Ho}$ in ECHo samples

Background in ECHO

Background sources:

- Radioactivity in the detector
- **Environmental radioactivity**
- Cosmic rays
Induced secondary radiation

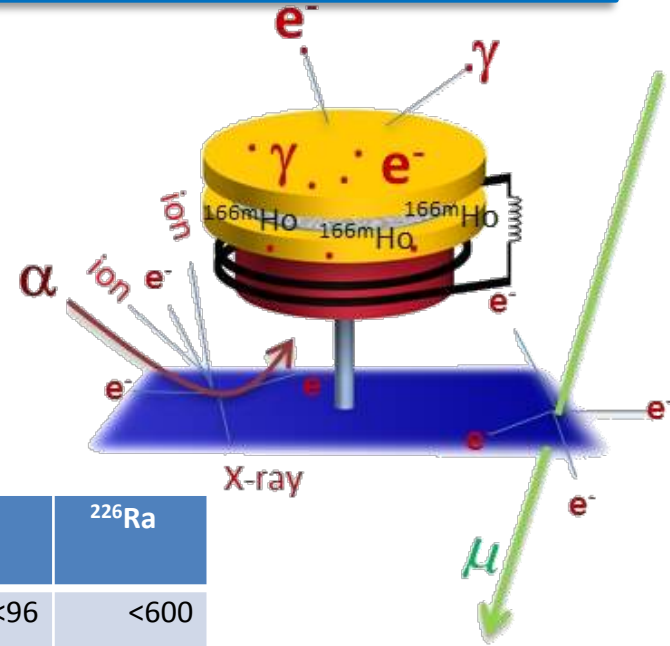


Sample	^{40}K	^{208}Tl	^{212}Pb	^{214}Bi	^{214}Pb	^{226}Ra
Cryostat copper [mBq/kg]	<480	<80	<190		<96	<600
Cryoperm [mBq/kg]	<335	<25	<45	<170	<40	<200
Connectors [mBq/kg]	5600	1600	10800	10800	10800	8000
Connectors [mBq] p.p.	3	1	6	6	6	4
Circuit board [mBq/kg]	625	4800	16300	8700	8000	5300
Circuit board [mBq/cm ²]	0.45	1.39	4.75	2.53	2.33	1.54
Cables [mBq/cm ²]	0.49					

Background in ECHO

Background sources:

- Radioactivity in the detector
- **Environmental radioactivity**
- Cosmic rays
Induced secondary radiation



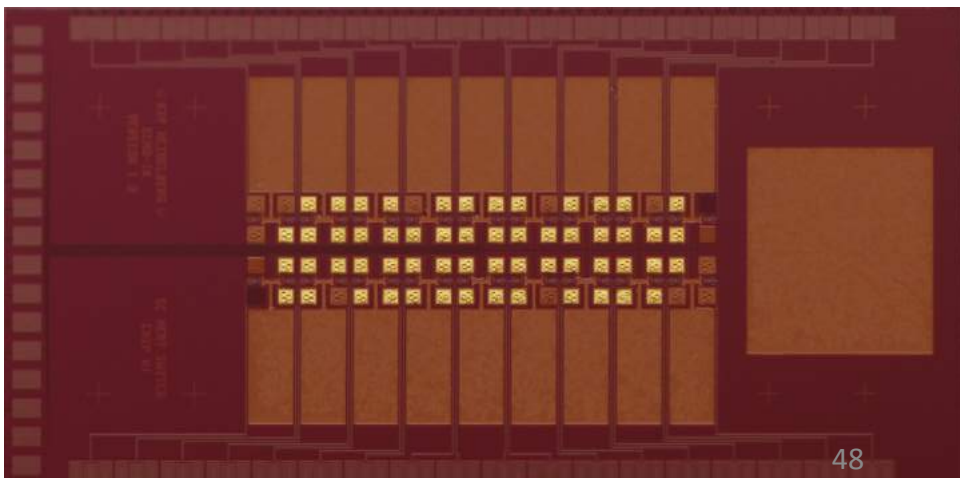
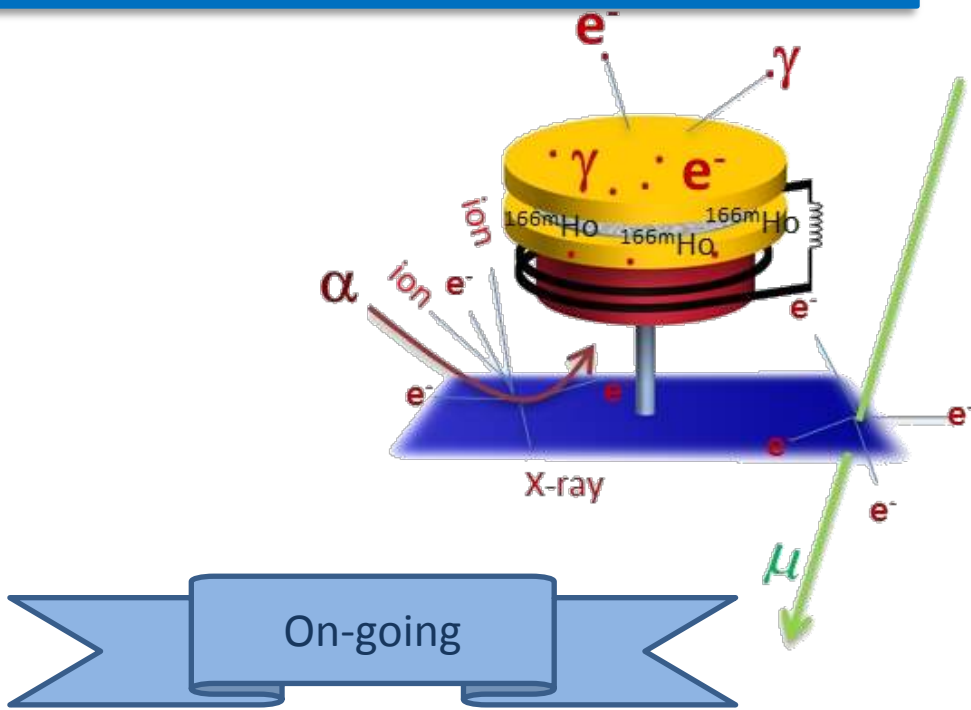
Sample	^{40}K	^{208}Tl	^{212}Pb	^{214}Bi	^{214}Pb	^{226}Ra
Cryostat copper [mBq/kg]	<480	<80	<190		<96	<600
Cryoperm [mBq/kg]	<335	<25	<45	<170	<40	<200
Connectors [mBq/kg]	5600	1600	10800	10800	10800	8000
Connectors [mBq] p.p.	2	1	6	6	6	4

After comparison with MC simulations
none of these item would lead to background
above the unresolved pile up limit

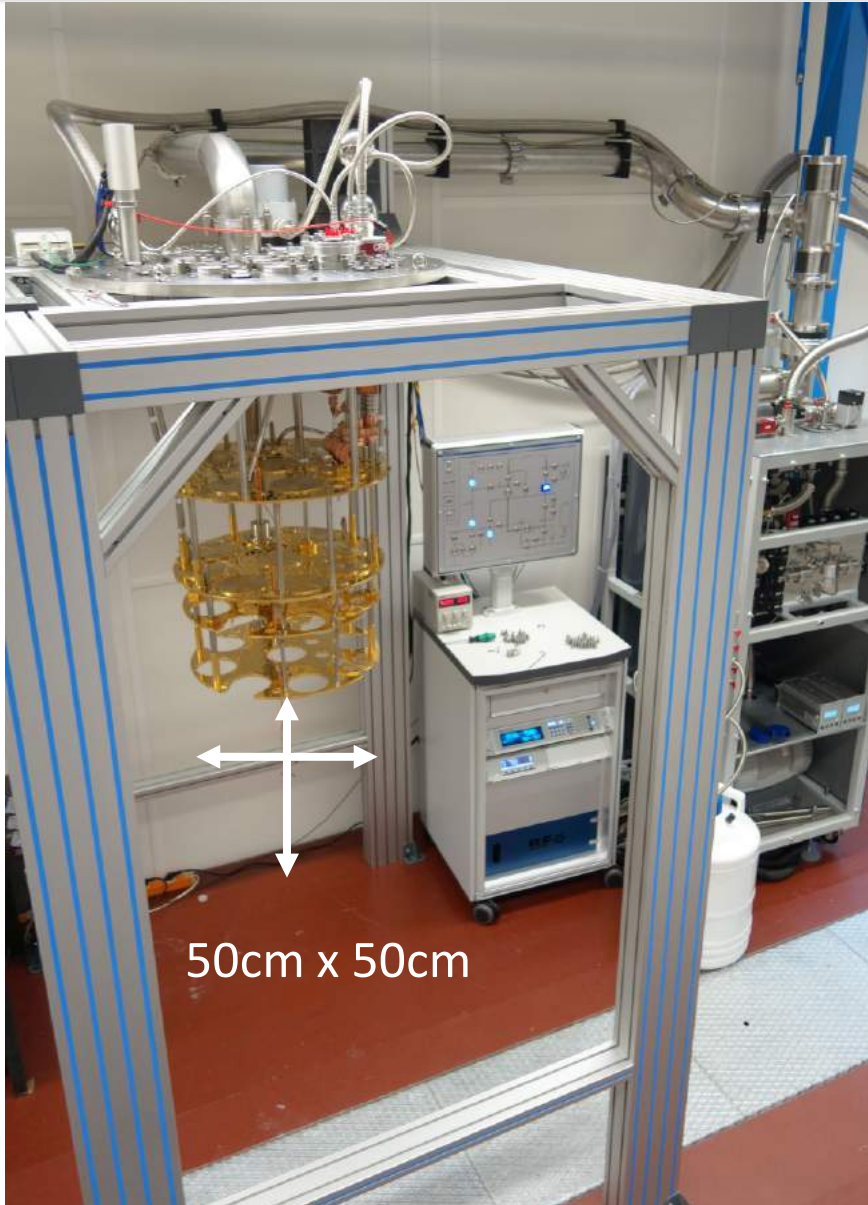
Background in ECHO

Background sources:

- Radioactivity in the detector
- Environmental radioactivity
- **Cosmic rays**
Induced secondary radiation



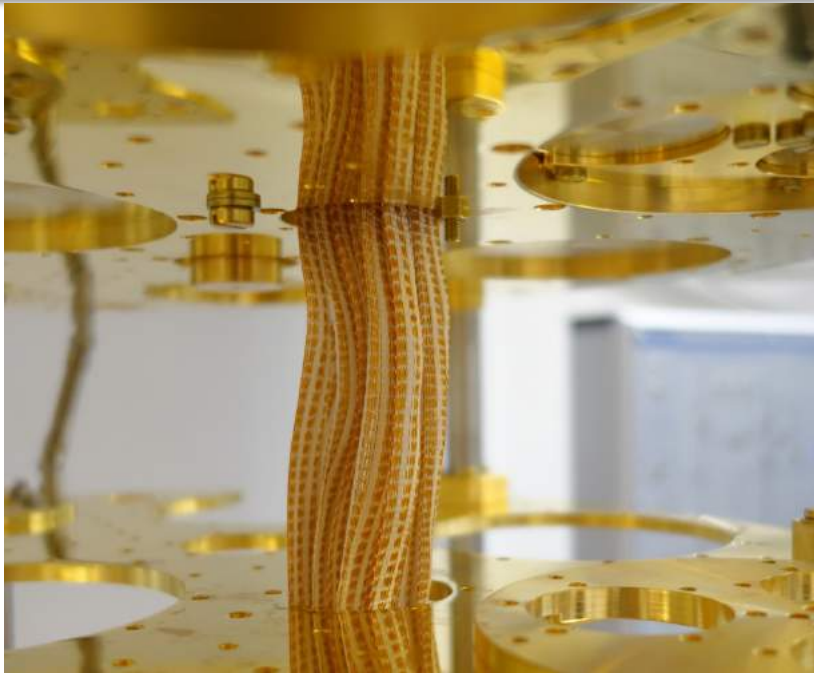
ECHo cryogenic platform



- Large space at MXC enough for several ECHo phases
- cooling power: **15µW @ 20 mK**
- Possibility to load 200kg for passive shielding

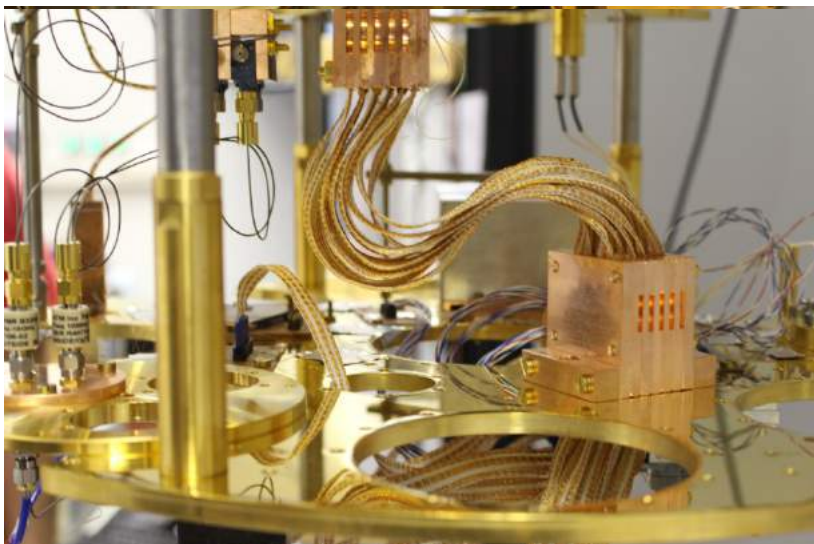


ECHo cryogenic platform



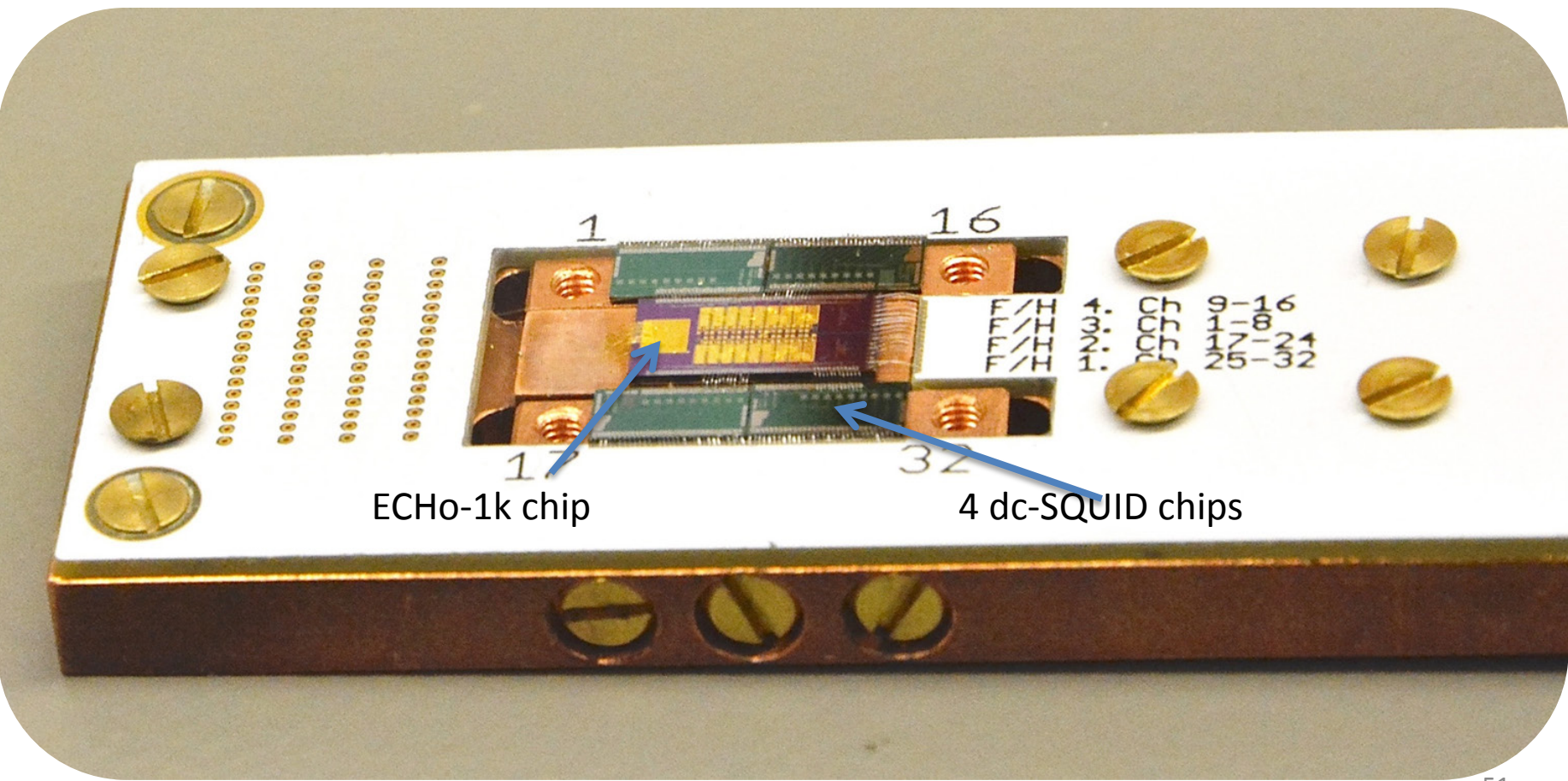
- Large space at MXC enough for several ECHo phases
- cooling power: **15 μ W @ 20 mK**
- Possibility to load 200kg for passive shielding
- Presently equipped with:
2 RF lines for microwave multiplexing readout of 2 MMC arrays

12 ribbons each with 30 Cu98Ni2 0.2 mm, 1.56 Ohm/m, cables from RT to mK
→ allows for parallel readout of
36 two-stage SQUID set-up



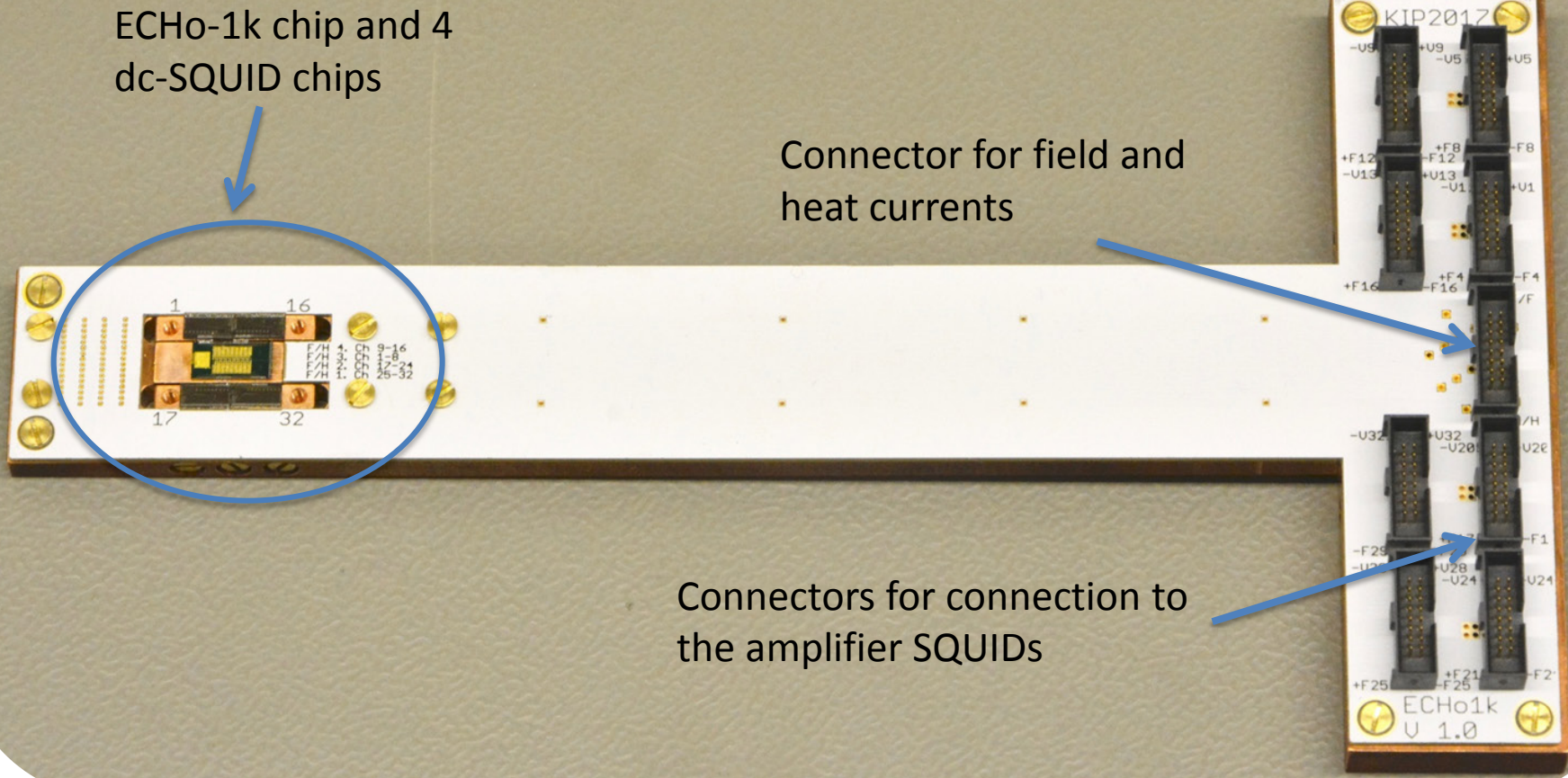
ECHO-1k set-up

- ECHO-1k chip implanted at RISIKO Uni-Mainz
→ ^{163}Ho activity $A = 2 \text{ Bq}$
- 4 Front-end chips each with 8 dc-SQUIDs



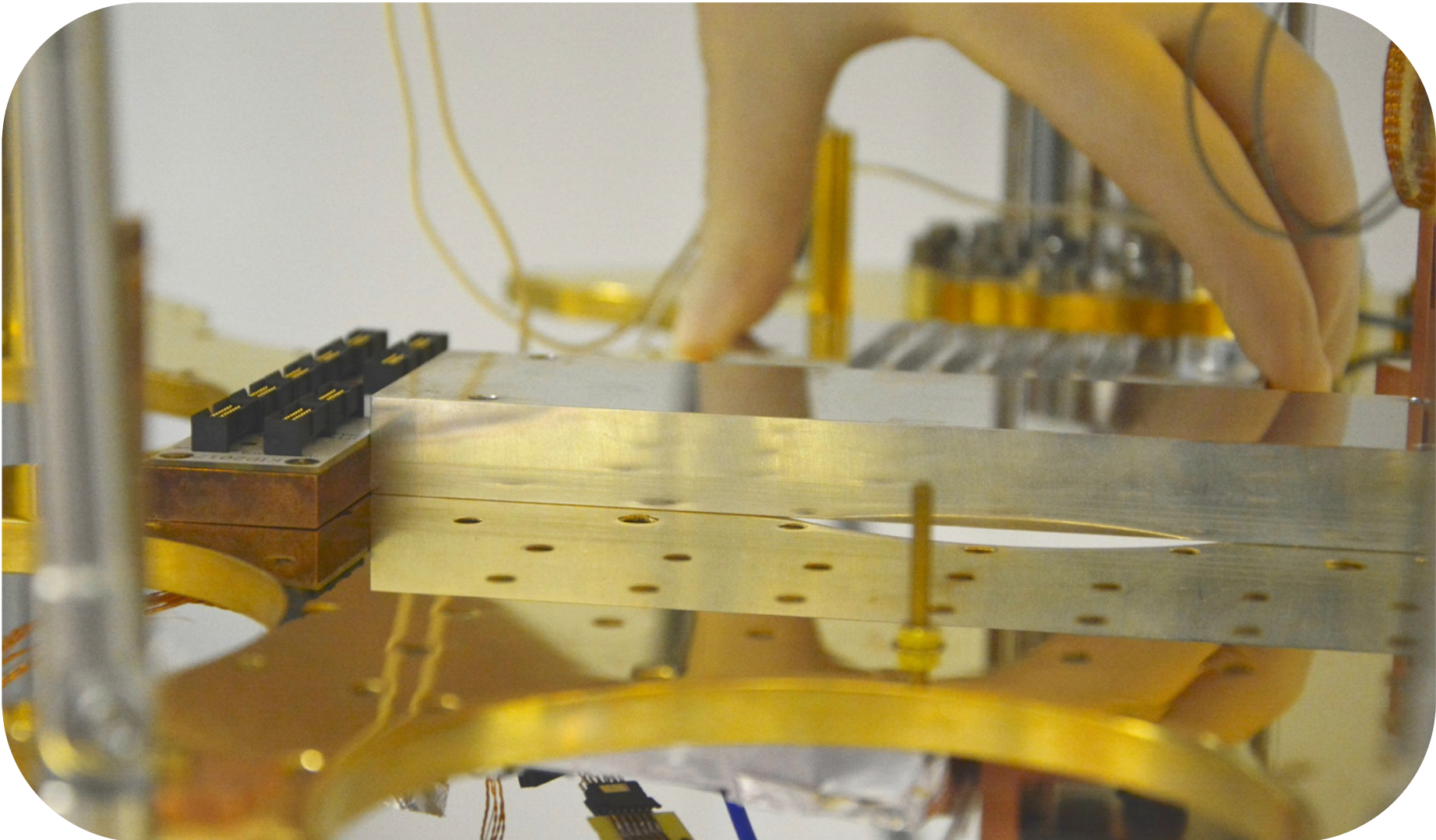
ECHO-1k set-up

- Circuit board designed for the ECHO-1k experiment
→ Parallel read-out of 64 pixels

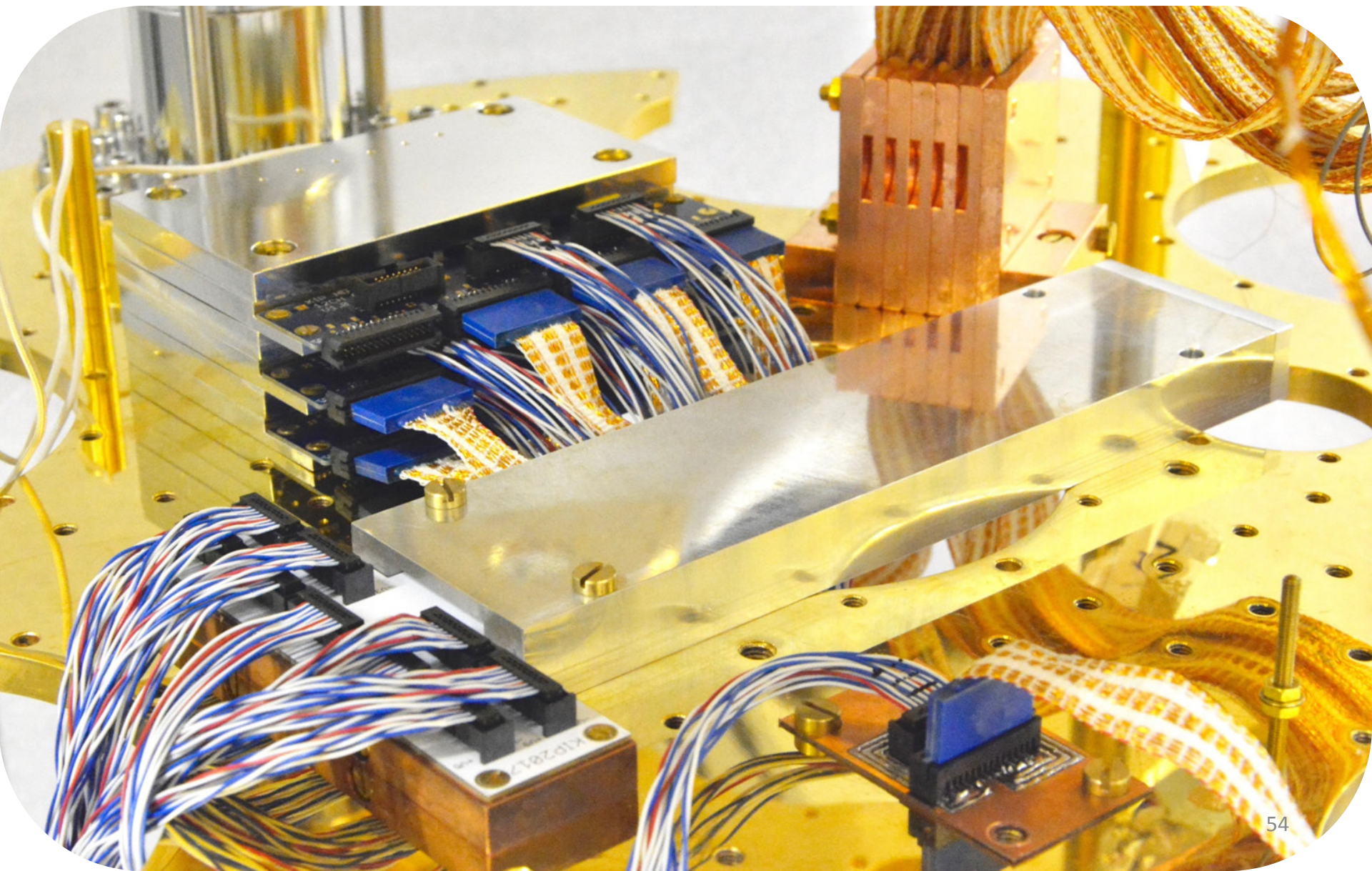


ECHO-1k set-up

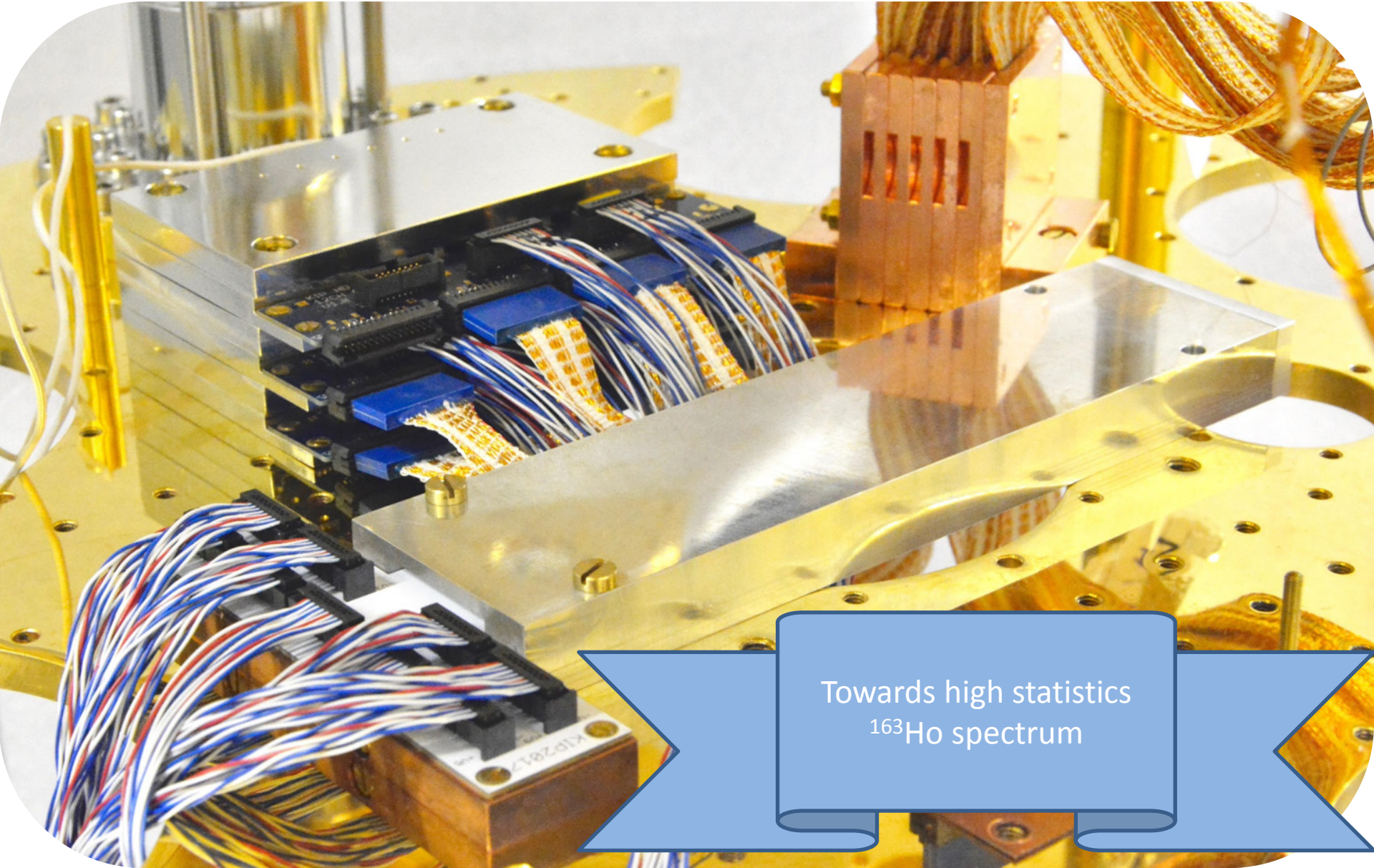
Aluminum superconducting shield



ECHO-1k set-up

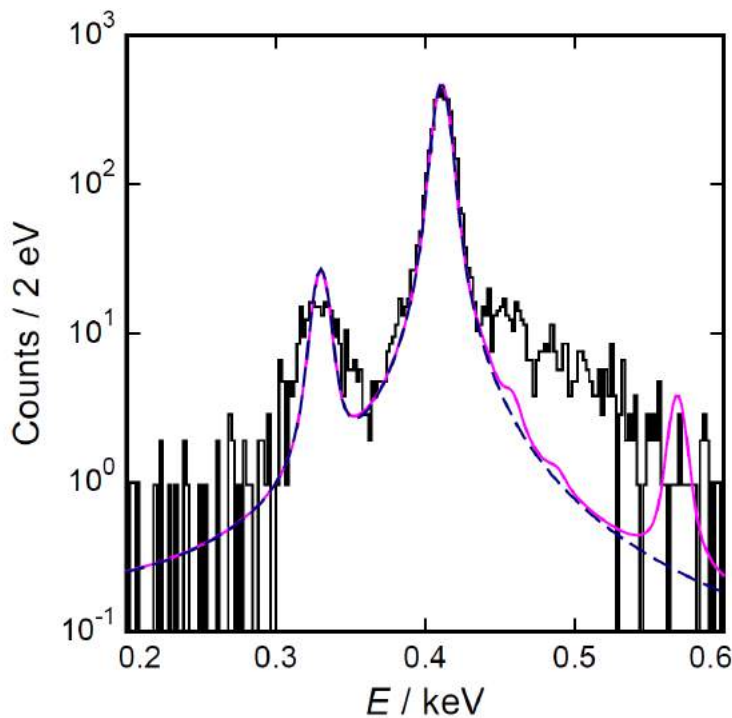


ECHo-1k set-up



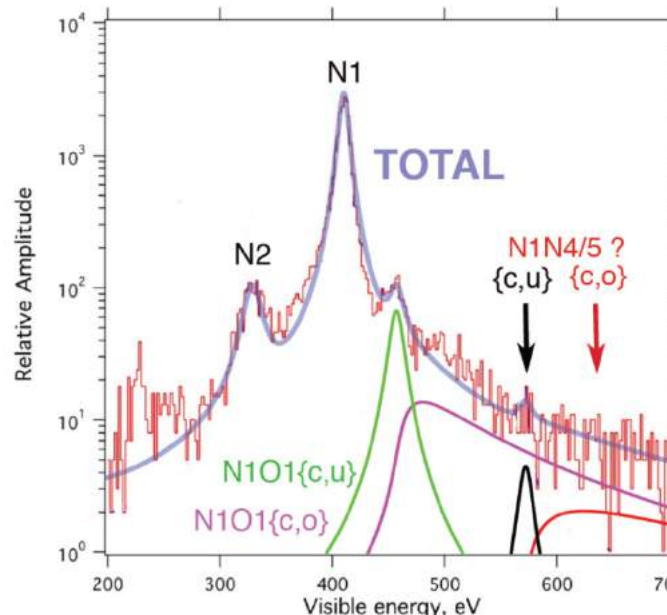
Towards high statistics
 ^{163}Ho spectrum

^{163}Ho spectral shape

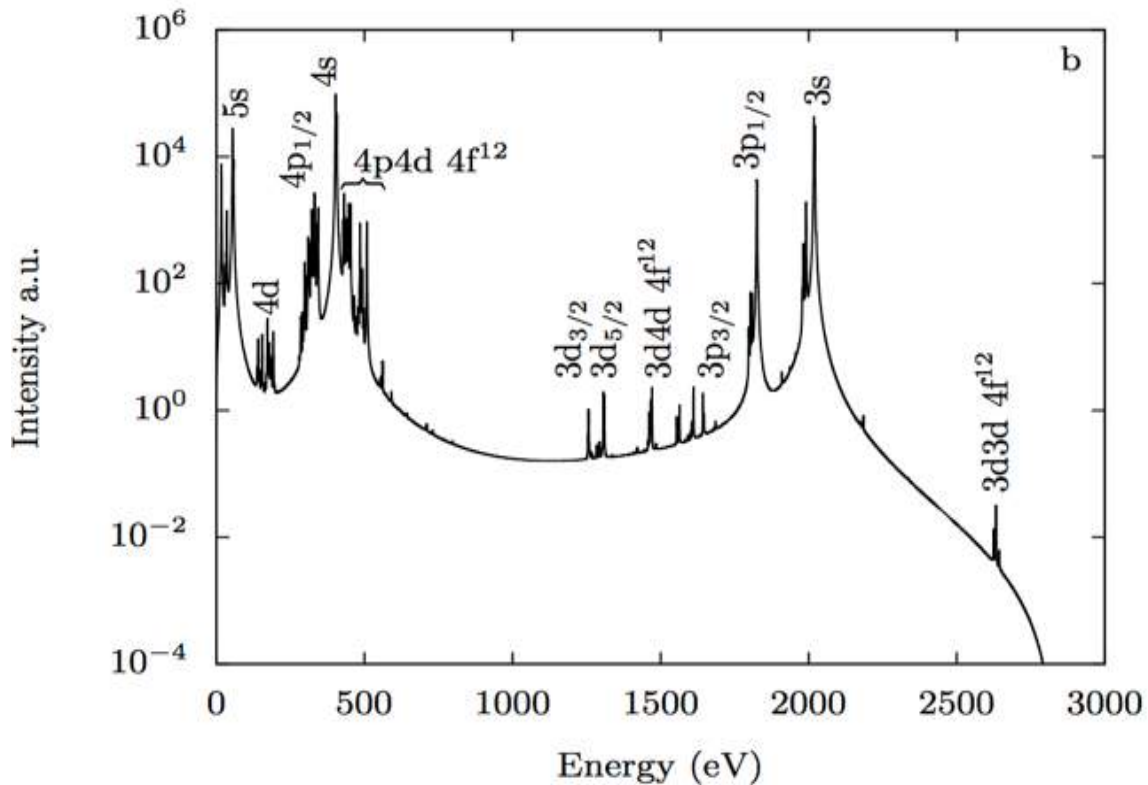


No good agreement between experimental spectrum and theory

- A. Faessler and F. Simkovic
Phys. Rev. C **91**, 045505 (2015)
- A. De Rujula and M. Lusignoli
JHEP 05 (2016) 015, arXiv:1601.04990v1
- A. Faessler et al.
J. Phys. G **42** (2015) 015108
- R. G. H. Robertson
Phys. Rev. C **91**, 035504 (2015)
- A. Faessler et al.
Phys. Rev. C **91**, 064302 (2015)
- A. Faessler et al.
Phys. Rev. C **95**, (2017) 045502



^{163}Ho spectral shape



New approach

Ab initio calculation of the ^{163}Ho electron capture spectrum

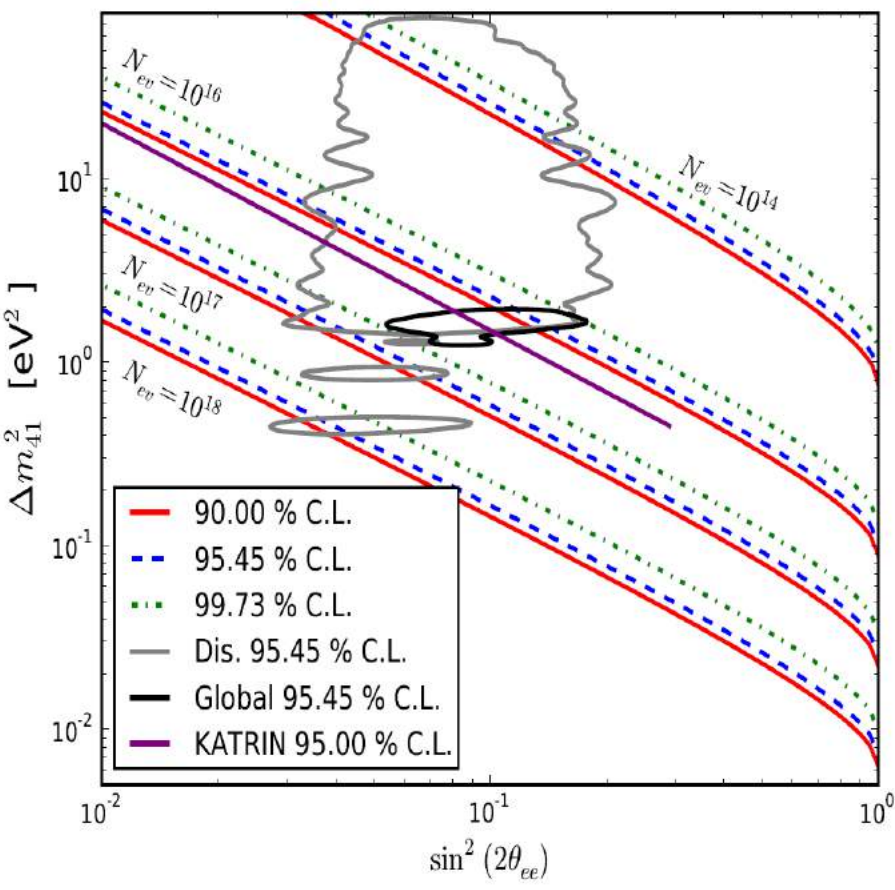
Brass et al., <https://arxiv.org/abs/1711.10309>

Restricted to **bound-states only**, i.e. the spectrum is given by a finite number of resonances

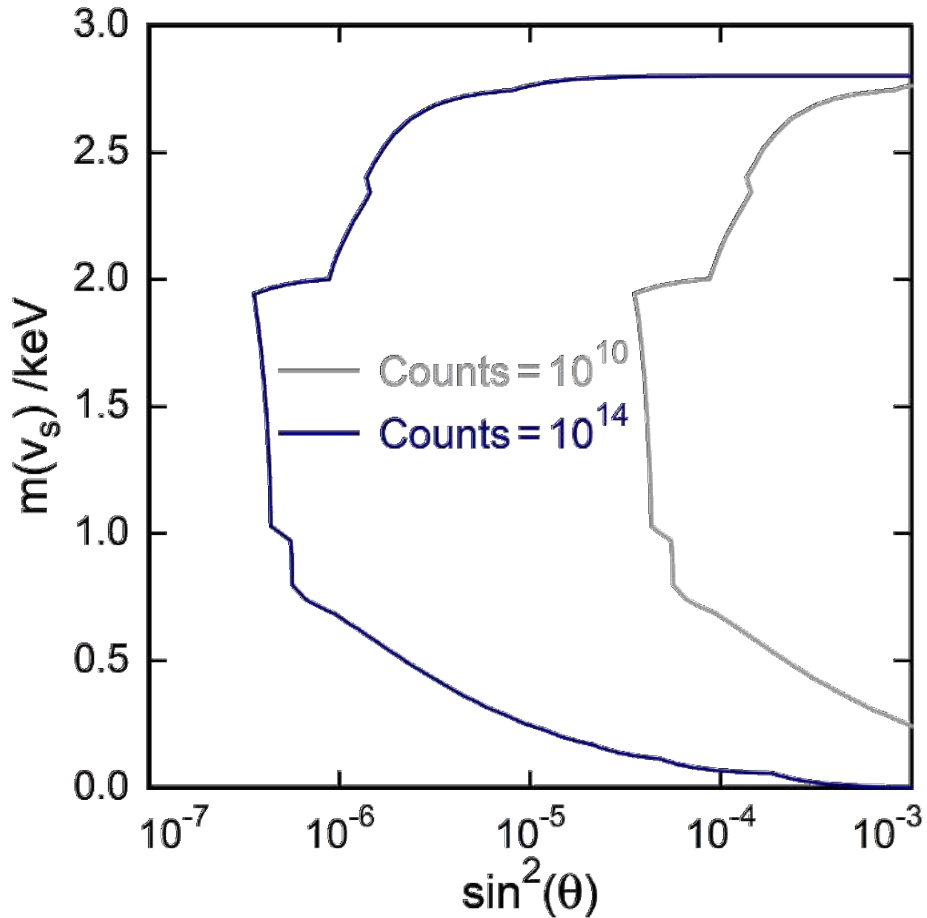
- Include decay to the continuum states
- Study the effect of metallic host

Sterile neutrinos search in ECHO

eV-scale sterile neutrinos



keV-scale serile neutrinos



L. Gastaldo, C. Giunti, E. Zavanin.,
High Energ. Phys. **06** (2016) 61.

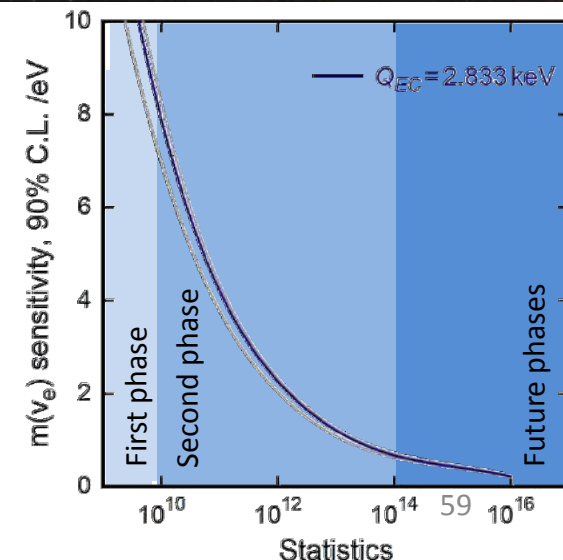
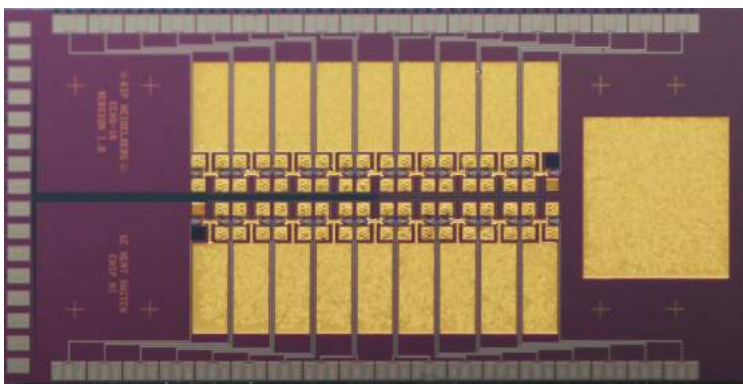
A White Paper on keV Sterile
Neutrino Dark Matter, *JCAP01*(2017)025

Conclusions and outlook

The ECHo collaboration aims to reach sub-eV sensitivity on the electron neutrino mass analysing high statistics and high resolution ^{163}Ho spectra

- Independent ^{163}Ho Q_{EC} measurement
 - $Q_{\text{EC}} = (2.833 \pm 0.030^{\text{stat}} \pm 0.015^{\text{syst}}) \text{ keV}$
 - $Q_{\text{EC}} = (2.858 \pm 0.010^{\text{stat}} \pm 0.05^{\text{syst}}) \text{ keV}$
- High purity ^{163}Ho sources have been produced
- ^{163}Ho ions can be successfully enclosed in microcalorimeter absorbers
- Large arrays have been tested and microwave SQUID multiplexing has been successfully proved
- A new limit on the electron neutrino mass is approaching

Er161 3.21 h 3/2-	Er162 0+ EC 0.14	Er163 75.0 m 5/2- EC	Er164 0+ EC 1.61	Er165 10.36 h 5/2- EC	Er166 0+ 33.6
Ho160 25.6 m 5+ EC *	Ho161 2.48 h 7/2- EC *	Ho162 15.0 m 1+ EC *	Ho163 4570 y 7/2- EC *	Ho164 29 m 1+ EC, β^- *	Ho165 7/2- 100



Department of Nuclear Physics, Comenius University, Bratislava, Slovakia

Fedor Simkovic

Department of Physics, Indian Institute of Technology Roorkee, India

Moumita Maiti

Goethe Universität Frankfurt am Main

Udo Kebschull, Panagiotis Neroutsos

Institute for Nuclear Chemistry, Johannes Gutenberg University Mainz

Christoph E. Düllmann, Klaus Eberhardt, Holger Dorrer, Fabian Schneider

Institute of Nuclear Research of the Hungarian Academy of Sciences

Zoltán Szűcs

Institute of Nuclear and Particle Physics, TU Dresden, Germany

Alexnder Domula, Kai Zuber

Institute for Physics, Humboldt-Universität zu Berlin

Alejandro Saenz

Institute for Physics, Johannes Gutenberg-Universität

Klaus Wendt, Sven Junck, Tom Kieck

Institute for Theoretical Physics, Heidelberg University

Martin Brass, Maurits Haverkort

Institute for Theoretical Physics, University of Tübingen, Germany

Amand Fäßler

Institut Laue-Langevin, Grenoble, France

Ulli Köster

ISOLDE-CERN

Marsh Bruce, Day Goodacre Tom, Johnston Karl, Rothe Sebastian,

Stora Thierry, Veinhard Matthieu

Kirchhoff-Institute for Physics, Heidelberg University, Germany

Christian Enss, Loredana Gastaldo, Andreas Fleischmann,
Clemens Hassel, Sebastian Kempf, Federica Mantegazzini, Mathias Wegner

Max-Planck Institute for Nuclear Physics Heidelberg, Germany

Klaus Blaum, Andreas Dörr, Sergey Eliseev, Mikhail Goncharov,
Yuri N. Novikov, Alexander Rischka, Rima Schüssler

Petersburg Nuclear Physics Institute, Russia

Yuri Novikov, Pavel Filianin

Physics Institute, University of Tübingen, Germany

Josef Jochum, Stephan Scholl

Saha Institute of Nuclear Physics, Kolkata, India

Susanta Lahiri



Thank you !